"Comparative Study of Flow Field around the Circular Pier placed in Rigid Bed"

A PROJECT

Submitted in partial fulfillment of the requirements for the award of the degree of

BACHELOR OF TECHNOLOGY

IN

CIVIL ENGINEERING

By

Mohd Ali 121613
Adarsh Pratap Singh 121655

Under the supervision of

Dr. Ashish Kumar

Associate Professor

JAYPEE UNIVERSITY OF INFORMATION TECHNOLOGY

WAKNAGHAT SOLAN – 173 234

HIMACHAL PRADESH INDIA

June, 2016

CERTIFICATE

This is to certify that the work which is being presented in the project title **"Comparative Study of Flow Field around the Circular Pier placed in Rigid Bed"** in partial fulfillment of the requirements for the award of the degree of Bachelor of technology and submitted in Civil Engineering Department, Jaypee University of Information Technology, Waknaghat is an authentic record of work carried out by **Mohd Ali (121613)** and **Adarsh Pratap Singh (121655)** during a period from July 2015 to June 2016 under the supervision of Dr. Ashish Kumar Associate Professor, Civil Engineering Department, Jaypee University of Information Technology, Waknaghat.

The above statement made is correct to the best of my knowledge.

Date: -

Dr. Ashok Kumar Gupta	Dr. Ashish Kumar	…………………
Professor & Head of Department	Associate Professor	External Examiner
Civil Engineering Department	Civil Engineering Department	
JUIT Waknaghat	JUIT Waknaghat	

ACKNOWLEDGEMENT

It is our proud privilege and duty to acknowledge the kind of help and guidance received from several people in preparation of this report. It would not have been possible to prepare this report in this form without their valuable help, cooperation and guidance.

The topic **"Comparative Study of Flow Field around the circular pier placed in rigid bed"** was very helpful to us in giving the necessary background information and inspiration in choosing this topic for the project. Our sincere thanks to our Project Guide **Dr.Ashish Kumar,** Associate Prof. for having supported the work related to this project. Their contributions and technical support in preparing this report are greatly acknowledged**.**

Mohd Ali **Adarsh Pratap Singh**

(121613) **(121655)**

ABSTRACT

In the present study experiments were carried out to measure the flow structure and turbulence characteristics around circular pier on rigid bed under clear water condition. The pier comprised of pier diameter 110 mm. Experimental run was conducted in which Acoustic Doppler Velocitimeter (ADV) was used to measure the instantaneous velocity components, turbulent intensity components and Reynolds' stresses at the central line of the pier in the upstream plane and downstream plane. The result of upstream and downstream are therefore presented herein.

Index

List of Figures

List of Table

List of symbols

Symbols

b = diameter or width of bridge pier

B = flume width

d = size of uniform sediment

d_{50} = median sediment grain diameter

F_r = Froude number

g = gravitational acceleration

h = depth of flow

k = turbulent kinetic energy

Q = discharge

r = distance in radial direction

R_{eb} = pier Reynolds number

S = energy slope

u, v, w = Cartesian velocity components in x, y and z directions respectively

u', v', w' = fluctuation of u, v, and w components of velocity respectively

u = bed shear velocity of approach flow

U_∞ = velocity of approach flow

U_c= velocity of approach flow corresponding to incipient motion of sediment

$\sqrt{u'u'}, \sqrt{v'v'}$= longitudinal and transverse components of turbulence intensity

$\sqrt{w'w'}$ = vertical component of turbulence intensity

$u'w', v'w'$= components of Reynolds' Stress

INTRODUCTION

1.1 General

The estimate of the maximum possible scour around a bridge pier is necessary for the safe design of bridges. A large number of studies have been conducted to predict the scour depth around piers. Based on these studies, semi-empirical equations are available for the maximum scour depth. A lingering concern is that most of these equations are over-predicting the maximum scour depth for field, or even for laboratory conditions. Understanding of the Complex flow field and erosion mechanisms can provide a way out this problem. A comprehensive understanding of the turbulent flow structure can provide more insight into the scouring process and aid to predict scour depth precisely. For a better understanding of the flow pattern and turbulent flow around piers, many researchers have focused on the flow around piers with and without a scour hole. Most of these studies are related to single piers and provide detailed information on the flow around them. Due to geotechnical and economical reasons, pile groups and complex piers have become popular in bridge design. However, the direct application of the results derived for a single pier may be problematic. Despite a large number of investigations around single piers, a comprehensive understanding of flow around pile groups and complex piers is still lacking.

A main cause of bridge failure mostly is scour around its piers and abutments. The process of scour around bridge pier involves the complexities of both the three dimensional flow patterns and the sediment transport. The estimation of scour extent and its depth at bridge sites therefore continues to be a major concern for the hydraulic engineers. In the present study flow pattern and turbulence characteristics around a circular bridge pier have been investigated experimentally in the rigid bed.

Bridges are required in order to cross the waterways by transport carriers. Thus bridges provide a smooth way to the transportation system. A main cause of bridge failure is scour by the flow around its pier and abutment. The estimation of scour extent and its depth at bridge sites therefore continues to be a major concern for the hydraulic engineers. Extensive research work has been carried out on the topic of scour. Less work however is reported on study of flow pattern around the pier in the rigid bed. In the present study flow patterns and turbulence characteristics in the vertical planes, upstream downstream and at various angles of the pier have been investigated experimentally in rigid bed.

1.2 Mechanism of scour

The boundary layer in the flow past a bridge element undergoes a three-dimensional separation. This separated shear layer rolls up along the obstruction to form a vortex system in front of the element which is swept downstream by the river flow. Viewed from the top, this vortex system has the characteristic shape of a horseshoe and thus called a horseshoe vortex. The formation of the horseshoe vortex and the associated down flow around the bridge element results in increased shear stress and hence a local increase in sediment transport capacity of the flow. This leads to the development of a deep hole (scour hole) around the bridge element, which in turn, changes the flow pattern causing a reduction in shear stress by the flow thus reducing its sediment transport capacity. The temporal variation of scour and the maximum depth of scour at bridge elements therefore mainly depend on the characteristics of flow, pier and river-bed material. The formation of the horseshoe vortex and the associated down flow cause scour at different elements of a bridge such as pier, abutment and spur dike. The mechanism of scour around bridge piers has been studied by Kothyari *et al* (1992a & b) whereas studies on the mechanism of scour around abutments and spur dikes are available in Kothyari & RangaRaju (2001). Vittal *et. al*(1994) and Kumar *et.al*(1999) investigated the effectiveness of several appurtenances for reduction of scour around bridge piers.

1.3 Objectives

The main objective of the present study is to carry out a detailed experimental investigation of the flow pattern around a single pier and double pier in a moderately rough flat bed in order to provide a better understanding of the three-dimensional flow. The experiments were conducted under clear water conditions. All the measurements were taken by an Acoustic Doppler Velocimeter (ADV). The contours of the time-averaged velocity components, turbulence intensities, and Reynolds's shear stresses at different horizontal and vertical planes are presented. Streamlines and velocity vectors obtained from the velocity fields are used to study the details of flow features. Besides providing insight into the flow anatomy, the experimental data of this study can also be used for validation of numerical models.

In the present study, an ADV is used to study and compare velocity, turbulence, and Reynolds's stresses with the available experimental data. The objectives are therefore to:

- To study the flow and the turbulence characteristics around the circular uniform pier founded in the rigid bed.

- To compare flow pattern around uniform circular pier in the rigid bed placed at a distance of three times of pier diameter in the direction of flow .

1.4 Limitation of study

- Study is confined to circular piers only
- Flow characteristic has been measured in the rigid bed placed at a distance of three times of pier diameter in the direction of flow only

LITERATURE REVIEW

2.1 Introduction

The process of scour around bridge piers is complex due to three-dimensional flow distribution and sediment transport around the pier. A lot of have been carried out in the past mainly with the objective of developing relationships for maximum scour depth. As a result, a large amount of literature is available on the topic of bridge scour and also its control. A handful of studies only are however available on the flow field around the bridge piers in rigid bed.

2.2 Flow pattern around the circular uniform pier in rigid bed condition.

Ahmed and Rajaratnam (1998) conducted detailed experiments on the flow past circular uniform piers placed on smooth, rough and mobile beds. The experiments were conducted in a flume 20m long and 1.22m wide, with a sediment recess 0.2m deep, 0.78m long , which was long enough to accommodate the scoured bed around the circular pier. The velocity vectors and bed shear stress vector were measured with two 3-tube yaw probes. The flow was noticed to pass through the scour hole which was reflected by a stronger down flow. The bed roughness was observed to induce a steeper pressure gradient and thus a stronger down flow in front of the pier. Based on experiments these concluded that in the presence of scour hole, the upstream flow accelerates into the scour hole rather than separating from the bed. They further reported that down flow velocity in front of the pier reached as much as 95 percent of the approach velocity inside the scour hole before diminishing again. From the limited amount of data for rigid bed experiments, they reported that the maximum down flow in the absence of scour hole was about 35% of the approach velocity. The velocity profiles in the upstream plane of symmetry were represented by Clauser type defect scheme.

Muzammil and Gangadhariah (2003) experimentally investigated the dynamics of scour hole development around the circular uniform pier. The experiments were conducted in a glass walled flume of length 5.0m and width 0.5m with sediment of median size 0.16mm and 0.6 mm. Circular hollow glass cylinders were used as piers with diameter varying from 31.0mm to 78.5mm. The mudflow visualization technique developed by them was used to visualize the horseshoe vortex in a plane of symmetry in front of piers they characterized the horseshoe vortex in terms of vortex dimensions, tangential velocity and strength for flows as rigid bed, on solidified scour bed and on mobile sediment bed. They also developed an expression for estimation of equilibrium scour depth based on the vortex velocity variation in scour hole and validated it by sing some experimental data. They concluded that:

(a) In the rigid bed, the mean size of the primary vortex of the horseshoe vortex is about 20% of the pier diameter in size, while the vortex tangential velocity is approximately 50% of the mean velocity of the approach flow for 10000<R_{e_b}< 14000.

(b) As the scour hole develops, the horseshoe vortex sinks into the scour hole and its mean size increases linearly with the depth of scour .the variation of vortex velocity and strength with scour hole development shows increasing trends in the initial stages of scour whereas it indicates the decreasing trend in the later scouring stages.

Kumar and Samaiya (2011) carried out experiment on rigid bed. They used ADV to get the instantaneous velocity components at the upstream of pier at different vertical planes .in the plane at α=0° no significant change was noticed in the values of u, v,and w components of the velocity between these two experiments runs over the entire depth of flow and over the entire region of measurement. Similarly no significant changes is observed in the profiles of $\sqrt{u'u'}$ and $\sqrt{w'w'}$ over entire region of measurement. However close to the pier while r< 200 mm, the component $\sqrt{v'v'}$ is noticed to be higher in magnitude for the experimental run UPRB. The reynold's stress components show no appreciable change in their values due to the presence of top of the foundation.

Dey and Raikar (2007) conducted the experimental study on the turbulent horseshoe vortex in an equilibrium scour hole and intermediate stage of scour hole around a circular uniform pier of diameter 0.12 under clear-water scour condition. The experiment were carried out in a 15m long, 0.9 m wide and 0.7 m deep rectangular channel having uniform sediment bed .the measurement of the flow field and turbulence intensities were taken by an Acoustic Doppler Velocitimeter (ADV) within the intermediate (having depth of 0.25, 0.5, 0.75 times of the equilibrium scour depth) and equilibrium scour depth at the upstream of pier. The flow measurement were also taken in a equilibrium scour hole around the square pierwith side facing the approach flow for the purpose of comparison with uniform circular pier. They presented contours of time averaged velocities, turbulence intensities and Reynolds stresses at different vertical planes for developing and established equilibrium scour hole. On the basis of study they concluded that,

(a) There exist a core of higher magnitude of turbulence intensities and Reynolds stresses that increases with the development of the scour hole .

(b) The magnitude of bed shear stress at the upstream of the pier are generally greater and lower (almost equal) than the critical bed shear stress in the intermediate and equilibrium scour hole.

(c) For the square pier the flow, turbulence and stress parameters are greater than those for a circular pier in an equilibrium scour hole.

2.3 Concluding remarks

The following conclusions are drawn on the basis of the review of literature made above.

(a) The flow field around a pier presents the picture of a complex phenomenon. A detailed description of the flow modified by the presence of pier in the flow is essential to control and make realistic estimation of the scour depth around the piers. Several empirical and semi empirical relations are available for computation of scour depth around the uniform and the non-uniform piers. But many times predictions by these are not realistic. A lack of understanding of the flow pattern around the bridge piers is the main reason of this problem. Correct understanding of flow pattern around the bridge piers is the main reason of this problem. A vast amount of literature is available on the topic of scour around circular piers, where less number of studies are were conducted to investigate the flow pattern around such piers. The flow pattern around circular compound piers is not yet investigated. Such geometries of bridge foundations are however, mostly used in bridge structures in the Indian-subcontinent.

(b) Only a few investigators have studied the process of scour involving circular compound piers. No effort has been made as yet for investigating the temporal evolution of scour around circular compound piers; a geometry frequently adopted by the practitioners for bridge design in India.

EXPERIMENTAL SET-UP AND PROCEDURE

3.1 General

Extensive data are available in literature on depth of scour around circular uniform piers. A little information however, is available on flow structure around circular piers with rigid bed. Sufficient data are also not available on variation of flow field around the circular pier in rigid bed. Therefore, it is intended to study the flow pattern and variation of velocity around rigid bed during the present investigation. Keeping this in view experiments were planned and conducted in the Hydraulics Laboratory of the Department of Civil Engineering, Jaypee University of Information and Technology, Waknaghat. The present Chapter contains the description of the material, equipment used and the experimental procedure adopted for the investigation.

3.2 Details of Experimental Setup

3.2.1 Flume

A fixed bed masonry flume of 10.0 m length, 0.75 m width and 0.60 m depth was used in the experiments. The flume receives its water supply from a constant head overhead tank. The water supply in the flume was regulated with the help of a valve provided at the inlet of the flume. A working section in the flume is 3.0 m long, 0.75 m wide and 0.3 m deep, which is located 2 m downstream of the flume entrance.

An adjustable steel gate was provided at the downstream end of the flume to enable adjustment of the depth of the flow in the flume. Adjustable rails and trolleys were mounted on the two walls of the flume to carry the pointer gauge and other equipment used for measurements of flow pattern, water surface. The working section was filled with the desired sediment to the level of the flume bed. The piers were placed at the centre of the working section of the flume. Rigid bed was made by sprinkling a mixture of cement and water on the sand and allowing it to get hard. The photographic view of the flume is given in Fig. 3.1.

3.2.2 Sediment

River sediment retained and passed between two successive sieves was used in all the experiments as the sediment. Two such uniform size non-cohesive river bed sediment having size = 0.5 mm, was used in all the experiments as the sediment. Both of these sediments had a relative density of 2.65.

3.2.3 Acoustic Doppler Velocimeter (ADV)

The ADV is an instrument for measuring the point velocity of water flow. With the use of appropriate software, the values of the velocity are gathered and stored in a computer. The probe head includes one transmitter and three receivers. The remote sampling volume is located typically 5 cm from the tip of the transmitter, but some studies showed that the distance might change slightly. The sampling volume size is determined by the sampling conditions and manual setup. In a standard conFiguration, the sampling volume is about a cylinder of water with a diameter of 6 mm and a height of 9 mm, although newer laboratory ADVs may have smaller sampling volume (e.g. Sontek micro ADV, Nortek Vectrino+). The signal strength, SNR and correlation values are used primarily to determine the quality and accuracy of the velocity data, although the signal strength (acoustic backscatter intensity) may related to the instantaneous suspended sediment concentration with proper calibration. The velocity component is measured along the line connecting the sampling volume to the receiver. Acoustic Doppler Velocitimeter is shown in Fig. 3.2 .

3.2.4 Piers

The models of circular uniform piers and circular compound piers were prepared using reinforced concrete. Two circular cylinders of uniform section having diameters of 110 mm were used. The photographic view of pier models used in the present study is shown in Fig. 3.3

Fig 3.1 Photographic view of the flume

Fig. 3.2 Acoustic Doppler Velocitimeter

Fig 3.3 Piers at a stream wise spacing equal to three times of pier size

3.2.5 Pitot Tube

Pitot tube is a pressure measurement instrument used to measure fluid flow velocity. The Pitot tube was invented by the French engineer Henri Pitot in the early 18th century and was modified to its modern form in the mid-19th century by French scientist Henry Darcy. It is widely used to determine the airspeed of an aircraft, water speed of a boat, and to measure liquid, air and gas flow velocities in industrial applications. The Pitot tube is used to measure the local flow velocity at a given point in the flow stream and not the average flow velocity in the pipe or conduit.

3.3 Procedure

Two experiments were conducted. In the first experiment a circular pier having diameter b= 110 mm was installed vertically in the middle of the test section and the flow condition described in Table 3.1 was established. The bed was made rigid by spraying light solution of cement on the channel bed working section so that no scour activity takes place during the flow. Thus run was performed on rigid bed. In the second experiment another pier was installed at a distance three times pier diameter and its effect on the flow parameters on the upstream piers in five different radial direction i.e. $\alpha =$ 0°, 45°, 90°, 135°, 180° is compared.

In each experiment, before start of experimentation, a preliminary run was performed without the pier in place. A discharge Q of 0.0154 m^3/s and flow depth h of 110 mm was determined such that sediment particles in the test section were subjected to the condition of threshold of their motion. The vertical distributions of the time-averaged velocity were measured in the test section much upstream of the pier. This yielded the average approach velocity U_∞ of flow equal to 0.187 m/s. The shear velocity u_* of the approach flow was obtained through the law of the wall. The critical shear velocity u_{*c} for the corresponding grain size was determined by Shield's diagram. The clear water condition prevailed during the experiment as u_*/u_{*c} value was ≤ 1.

Table 3.1 Hydraulic parameters for the experiment run

B (m)	S_0	h (m)	Q (m^3/s)	B/h	U_∞(m/s)	F_r	Re_h	d_{50} (mm)	b (m)
0.75	0.000128	0.11	0.0154	6.82	0.187	0.18	25420	0.5	0.11

B - Width of flume, S_0 - energy slope , Re_h – Reynolds number , b – diameter of pier,

F_r - Froude Number

3.4 Velocity Measurements

In the first experiment, measurement for the flow velocity components, turbulence intensities and Reynolds stresses were made in a vertical plane of symmetry ahead of pier at α = 0° , and just behind of pier at α = 180° using an Acoustic Doppler Velocimeter (ADV) . Here α is the angular direction of the plane with α = 0° corresponding to upstream central line of the channel. Velocity distributions were measured in vertical planes at different radial distances (r) from the centre of pier *i.e.* r = 75, 85, 95, 105, 135, 155, 205 mm at α = 0° and at r = 185, 205, 225, 235, 245, 255, 535 mm for α = 180°. The coordinates of each point is defined by (r, α, z) with z being vertical distance above the general bed level of the channel.

In the second experiment another pier was installed at a distance three times pier diameter and its effect on the flow parameters on the upstream piers in five different radial direction i.e. α = 0°, 45°, 90°, 135°, 180° is compared.

The three-dimensional velocity measurements were made using the ADV. An ADV can instantaneously measure all the three components of velocity at a given point in the flow domain. The measurements were taken at any particular point for long durations in order to ensure that observations become stationary. The measurements were made at a frequency of 25 Hz over duration of 4 minutes at each location. Each time series on velocity components was edited for a minimum signal to noise ratio of 17 and minimum correlation coefficient of 70%.

ANALYSIS OF DATA AND DISCUSSION OF RESULTS

4.1 General

Detailed analysis of the data collected on flow structure around the circular uniform pier is presented in this chapter. The experiments were conducted in two series; in the first experiment the study of flow parameters at upstream and downstream of isolated pier is done. In the second experiment another pier was installed at a distance three times pier diameter and its effect on the flow parameters on the upstream piers in five different radial direction i.e. α = 0°, 45°, 90°, 135°, 180° is compared. A detailed discussion on how flow structure alters due to installation of second pier is presented here.

4.2 Flow Field Around Isolated Pier

The measurements were made at two different vertical planes in radial directions α = 0° and 180° from the flow. The variation in time averaged components of velocities (longitudinal *u*; transverse *v* and vertical *w*) in the plane at α =0° is shown in Fig. . The velocity components were normalized using upstream flow velocity U_∞ while the vertical distance *z* is normalized using depth of flow *h.* Approaching to the pier *i.e.* while *r* is small the u component is small as the distance from pier increases on upstream side of pier the u component increases this happens because disturbance decreases as the distance increases. The *v* component of the velocity is mostly negligibly small in this plane. Approaching to the pier, the *w* component of velocity has larger values in downward direction which is being considered as negative. This means there is dominancy of strong down flow in this region with maximum value of downward velocity being equal to about half of the approach flow velocity.

Figure shows the measured time averaged velocity components *viz.u, v* and *w* over the vertical plane in the downstream of the pier *i.e.* at α = 180°. In the plane at α = 180°, close to the pier *i.e.* while *r* is small, the *u* component shows a reversal of flow near the water surface also far away from the pier *i.e.* while *r* is larger, the *u* component albeit is larger as compared to its value near the pier but it still has a decreasing tendency nearer the surface of the flow. In the wake region *i.e.* when α = 180°, the *v* component is seen to fluctuate about its mean value. The normalized value of *v* component is seen to vary between –0.2 and 0.2 over this plane. On the contrary to the observations at α = 0° the value of *w* component is always positive at α = 180° revealing that upward flow in the wake region.

4.3 Effect on Flow Field Due To Installation of Second Pier

The measurements were made at five different vertical planes in radial directions and in each direction a set of three readings at a distance of 105mm, 155mm and 205mm are compared before and after installation of second pier.

4.3.1 Vertical distribution of velocity

(i) Figures 5.7-5.9 shows the comparison of u, v and w component of velocity in the plane at α =0 degree. The variation of time averaged components of velocities (longitudinal *u;* transverse *v;* and vertical *w*) at upstream of first pier and distance of *r* = 105 mm, 155 mm and 205 mm, the velocity component of *u* and *v* decreases slightly after installation of second pier while it remains almost constant for *w* component. This variation is more prominent as the distance *r* is decreased.

(ii) Figures 5.16-5.18 shows the comparison of u, v and w component of velocity in the plane at α =45 degree.

(a) At *r* = 105 mm, the velocity components in *u* and *v* direction significantly increases. The *w* component decreases from its initial value.

(b) At *r* = 155 mm, the velocity components in *u* and *v* direction significantly increases. The *w* component remains constant.

(c) At *r* = 205 mm, the velocity components in *u* and *v* direction increases. The *w* component remains constant.

(iii) Figures 5.25-5.27 shows the comparison of u, v and w component of velocity in the plane at α =90 degree.

(a) At *r* = 105 mm, the velocity components in *w*and *v* direction is almost equivalent in magnitude but in *u* component the velocity significantly increases. The *u* component increases almost twice of its initial value.

(b) At *r* = 155 mm, the velocity components in *u* direction is almost equivalent in magnitude but in *v* component the velocity significantly increases. In *w* component the magnitude decreases.

(c) At *r* = 205 mm, the velocity components in *u* and *v* direction is almost equivalent in magnitude. In *w* component the magnitude decreases.

(iv) Figures 5.34-5.36 shows the comparison of u, v and w component of velocity in the plane at α =135 degree.

(a) At *r*= 105 mm, the velocity components in *u* and *w* direction are almost equivalent in magnitude but in *v* component the velocity significantly increases.

(b) At r= 155 mm, the velocity component in w direction is almost equivalent in magnitude but in u and v component the velocity significantly increases, the v component changes its orientation from negative to positive.

(c) At r= 205 mm, the velocity components in w direction is almost equivalent in magnitude but in u and v component the velocity significantly increases. The v component increases five times of its initial value, whereas change in magnitude of u is also major.

(v) Figures 5.43-5.45 shows the comparison of u, v and w component of velocity in the plane at α =180 degree.

(a) At r= 105 mm, the velocity components in u and v direction are almost equivalent in magnitude but in w component the velocity slightly increases.

(b) At r = 155 mm, the velocity components in w and v direction are almost equivalent in magnitude of previous reading but in u component the velocity slightly increases in negative direction indicating increase in flow reversal.

(c) At r = 205 mm, no major changes are observed in any component of velocity. αα

(vi) Downstream of second pier. Figures 5.52-5.54 shows the comparison of u, v and w component of velocity in the plane at α =180 degree.

(a) At r = 105 mm, the velocity components in u direction significantly increases. The $w$and v component remains constant.

(b) At r = 155 mm, the velocity components in u direction increases. The w and v component remains constant.

(c) At r = 205 mm, the velocity components in u direction decreases. The v component increases and w component remains constant.

4.3.2 Vertical distribution of turbulence characteristics

(i), Figures 5.10-5.15 shows the comparison of u, v and w component of velocity in the plane at α =0 degree.

(a) At r = 105 mm, no major changes are observed in any turbulence characteristics.

(b) At r = 205 mm, no major changes are observed in any turbulence characteristics except decrease in magnitude of longitudinal component of Reynolds's stress.

(c) At r = 205 mm, no major changes are observed in any turbulence characteristics.

(ii) Figures 5.19-5.24 shows the comparison of u, v and w component of velocity in the plane at α =45 degree.

(a) At r = 105 mm, slight increase in magnitude of turbulence intensities and no major changes are observed in any Reynolds's stresses.

(b) At r = 155 mm, slight increase in magnitude of turbulence intensities and slight decrease in magnitude of Reynolds's stresses are observed.

(c) At r = 205 mm, slight increase in magnitude of turbulence intensities and slight decrease in magnitude of Reynolds's stresses are observed.

(iii) Radial direction of 90°,(Refer Fig. 5.35. 5.36, 5.38, 5.39, 5.41, 5.42) Figures 5.28-5.33 shows the comparison of u, v and w component of velocity in the plane at α =90 degree.

(a) At r = 105 mm, no major changes are observed in any turbulence characteristics.

(b) At r = 155 mm, no major changes are observed in any turbulence characteristics.

(c) At r = 205 mm, slight increase in magnitude of turbulence intensities and no major changes are observed in any Reynolds's stresses.

(iv) Figures 5.37-5.42 shows the comparison of u, v and w component of velocity in the plane at α =135 degree.

(a) At r = 105 mm, no major changes are observed in any turbulence characteristics except increase in magnitude of vertical and longitudinal components of turbulence intensity.

(b) At r = 155 mm, no major changes are observed in any turbulence characteristics except slight decrease in Reynolds's stresses.

(c) At r = 205 mm, all turbulence characteristics show a major increase in their magnitude except longitudinal component of Reynolds's stress.

(v) Figures 5.46-5.51 shows the comparison of u, v and w component of velocity in the plane at α =180 degree.

(a) At r = 105 mm, all the turbulence characteristics shows a decrease after the installation of second pier, this can attributed to back water flow which decreases the turbulence as it also decreases the velocity.

(b) At r = 155 mm, no major changes are observed in any turbulence characteristics except decrease in magnitude of transverse component of turbulence intensity.

(c) At r = 205 mm, no major changes are observed in any turbulence characteristics except decrease in magnitude of transverse and longitudinal components of turbulence intensity.

(iv) Radial direction of 90°,(Refer Fig. 5.35. 5.36, 5.38, 5.39, 5.41, 5.42) Figures 5.28-5.33 shows the comparison of u, v and w component of velocity in the plane at α =90 degree.

(a) At r = 105 mm, no major changes are observed in any turbulence characteristics.

(b) At r = 155 mm, no major changes are observed in any turbulence characteristics.

(c) At r = 205 mm, slight increase in magnitude of turbulence intensities and no major changes are observed in any Reynolds's stresses.

(vi) Downstream of second pier. Figures 5.55-5.60 shows the comparison of u, v and w component of velocity in the plane at α =180 degree.

(a) At r = 105 mm, major increase in magnitude of turbulence characteristics are observed.

(b) At r = 155 mm, major increase in magnitude of turbulence intensities are observed, but Reynolds's stresses remains almost the same.

(c) At r = 205 mm, major increase in magnitude of turbulence characteristics are observed, except in longitudinal component of Reynolds's stress.

CONCLUSIONS

5.1 General

The main objective of the present study is to carry out a detailed experimental investigation of the flow pattern around a single pier and double pier in a moderately rough flat bed in order to provide a better understanding of the three-dimensional flow. The experiments were conducted under clear water conditions

The objectives are therefore (i) to study the flow and the turbulence characteristics around the circular uniform pier founded in the rigid bed, (ii) to compare flow pattern around uniform circular pier in the rigid bed placed at a distance of three times of pier diameter in the direction of flow .

5.2 Flow field around Circular Pier

The experiments were conducted in two series; in the first experiment the study of flow parameters at upstream and downstream of isolated pier is done. In the second experiment another pier was installed at a distance three times pier diameter and its effect on the flow parameters on the upstream piers in five different radial direction i.e. $\alpha =$ 0°, 45°, 90°, 135°, 180° is compared at a distance of 105, 155 and 205 mm from centre of pier .

The variation of time averaged components of velocities (longitudinal *u;* transverse *v;* and vertical *w*) at upstream of first pier and distance of *r* = 105 mm, 155 mm and 205 mm, while in downstream at *r*= 105 mm, the velocity components in *u* and *v* direction are almost equivalent in magnitude but in *w* component the velocity slightly increases. At *r* = 155 mm, the velocity components in *w* and *v* direction are almost equivalent in magnitude of previous reading but in *u* component the velocity slightly increases in negative direction indicating increase in flow reversal, at *r* = 205 mm, no major changes are observed in any component of velocity. At *r* = 105 mm, no major changes are observed in any turbulence characteristics, *r* = 205 mm, no major changes are observed in any turbulence characteristics except decrease in magnitude of longitudinal component of Reynolds's stress, at *r* = 205 mm, no major changes are observed in any turbulence characteristics.

Observations at radial direction of 45° shows when *r* = 105 mm, the velocity components in *u* and *v* direction significantly increases. The *w* component decreases from its initial value. When *r* = 155 mm, the velocity components in *u* and *v* direction significantly increases. The *w* component remains constant. When r = 205 mm, the velocity components in *u* and *v* direction increases. The w component remains constant, r = 105 mm, slight increase in magnitude of turbulence intensities and no major changes are observed in any Reynolds's stresses, r = 155 mm, slight increase in magnitude of turbulence intensities and slight decrease in magnitude of Reynolds's stresses are observed, r = 205 mm, slight increase in magnitude of turbulence intensities and slight decrease in magnitude of Reynolds's stresses are observed.

Observations at radial direction of 90° shows when r = 105 mm, the velocity components in $w$and v direction is almost equivalent in magnitude but in u component the velocity significantly increases. The u component increases almost twice of its initial value, r = 155 mm, the velocity components in u direction is almost equivalent in magnitude but in v component the velocity significantly increases. In w component the magnitude decreases, r = 205 mm, the velocity components in u and v direction is almost equivalent in magnitude. In w component the magnitude decreases, at r = 105 mm, no major changes are observed in any turbulence characteristics, at r = 155 mm, no major changes are observed in any turbulence characteristics, at r = 205 mm, slight increase in magnitude of turbulence intensities and no major changes are observed in any Reynolds's stresses.

Observations at radial direction of 135° shows when r = 105 mm, the velocity components in u and w direction are almost equivalent in magnitude but in v component the velocity significantly increases. At r= 155 mm, the velocity component in w direction is almost equivalent in magnitude but in u and v component the velocity significantly increases, the v component changes its orientation from negative to positive, r= 205 mm, the velocity components in w direction is almost equivalent in magnitude but in u and v component the velocity significantly increases. The v component increases five times of its initial value, whereas change in magnitude of u is also major, r = 105 mm, no major changes are observed in any turbulence characteristics except increase in magnitude of vertical and longitudinal components of turbulence intensity, r = 155 mm, no major changes are observed in any turbulence characteristics except slight decrease in Reynolds's stresses, r = 205 mm, all turbulence characteristics show a major increase in their magnitude except longitudinal component of Reynolds's stress.

Downstream of first pier, r = 105 mm, all the turbulence characteristics shows a decrease after the installation of second pier, this can attributed to back water flow which decreases the turbulence as it also decreases the velocity. r = 155 mm, no major changes are observed in any turbulence characteristics except decrease in magnitude of transverse component of turbulence intensity, r = 205 mm, no major changes are observed in any turbulence characteristics except decrease in magnitude of transverse and longitudinal components of turbulence intensity.

Observations at radial direction of 180° shows when r = 105 mm, the velocity components in u direction significantly increases. The $w$and v component remains constant, at r = 155 mm, the velocity components in u direction increases. The w and v component remains constant, at r = 205 mm, the velocity components in u direction decreases. The v component increases and w component remains constant, at r = 105 mm, major increase in magnitude of turbulence characteristics are observed, at r = 155 mm, major increase in magnitude of turbulence intensities are observed, but Reynolds's stresses remains almost the same, at r = 205 mm, major increase in magnitude of turbulence characteristics are observed, except in longitudinal component of Reynolds's stress.

REFERENCES

1. Ahmed, F., and Rajaratnam N. (1998). “Flow around bridge piers” J. Hydr Engr., 12(3), 288-300.

2. A. Kumar and U.C. Kothyari (2005). “Flow characteristics within the scour hole around a circular bridge pier”. Hydro 2005, 599-608.

3. A. Kumar and N. K. Samaiya (2011).“Comparative study of flow characteristics around circular compound piers in rigid bed condition”.H63-H70.

4. B. A. Ashtiani and A. A. Kordkandi (2012). “Flow field around single and tandem piers.” Flow Turbulence Combust (2013) 90:471–490.

Part I

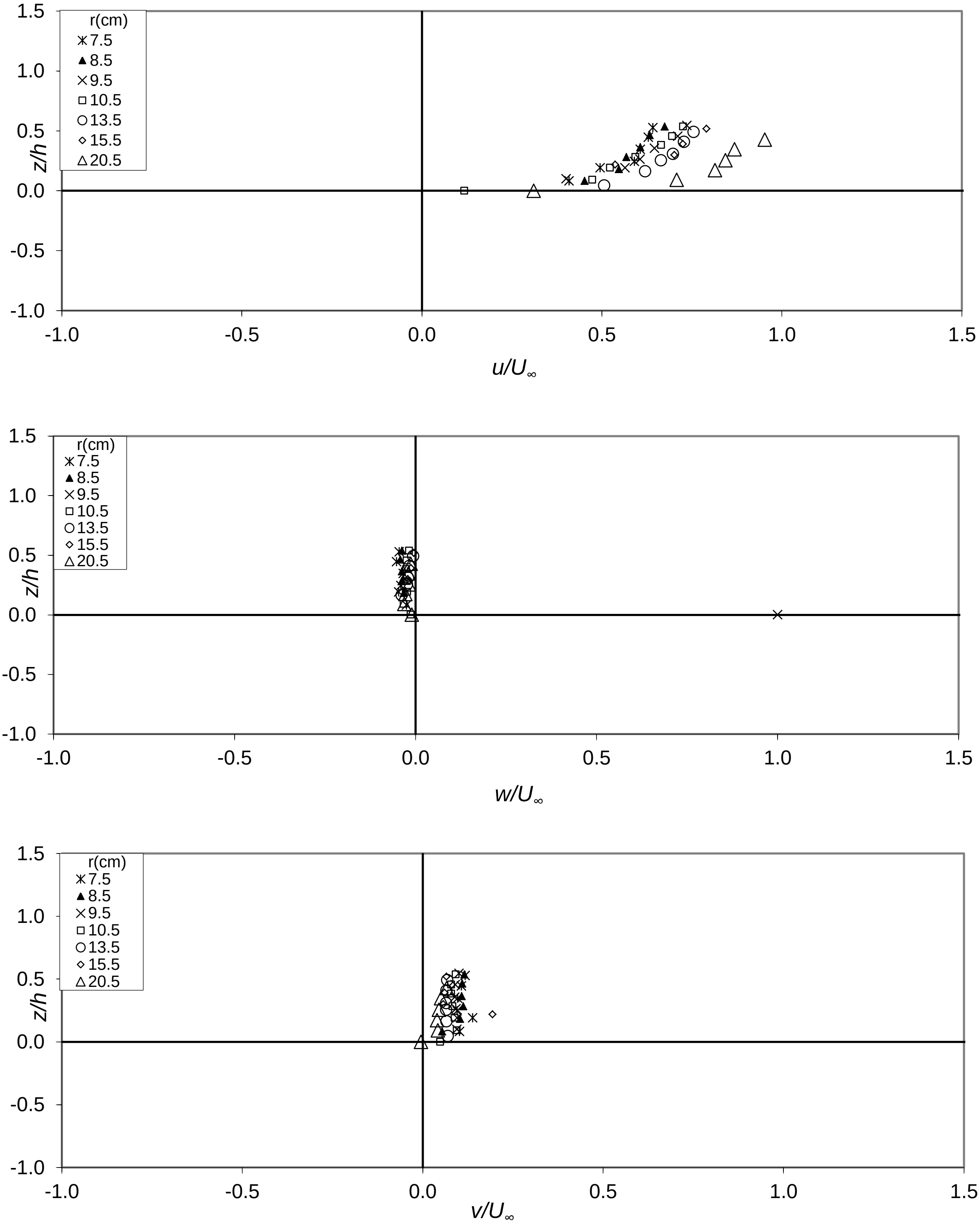

Fig 5.1 Normalized profiles of u, v and w measured upstream of pier (α = 0°)

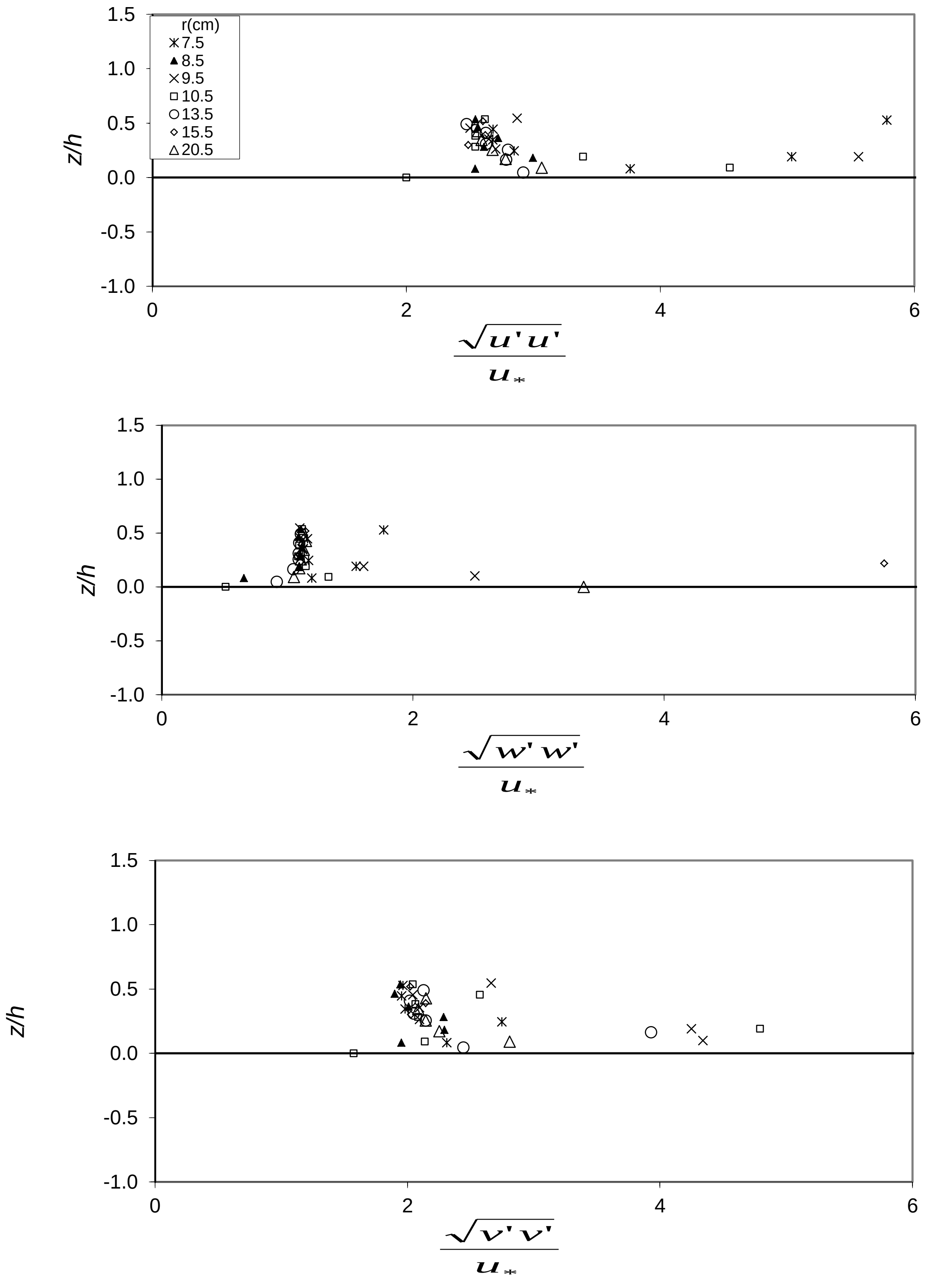

Fig 5.2 Distribution of normalized turbulence intensities (α = 0°)

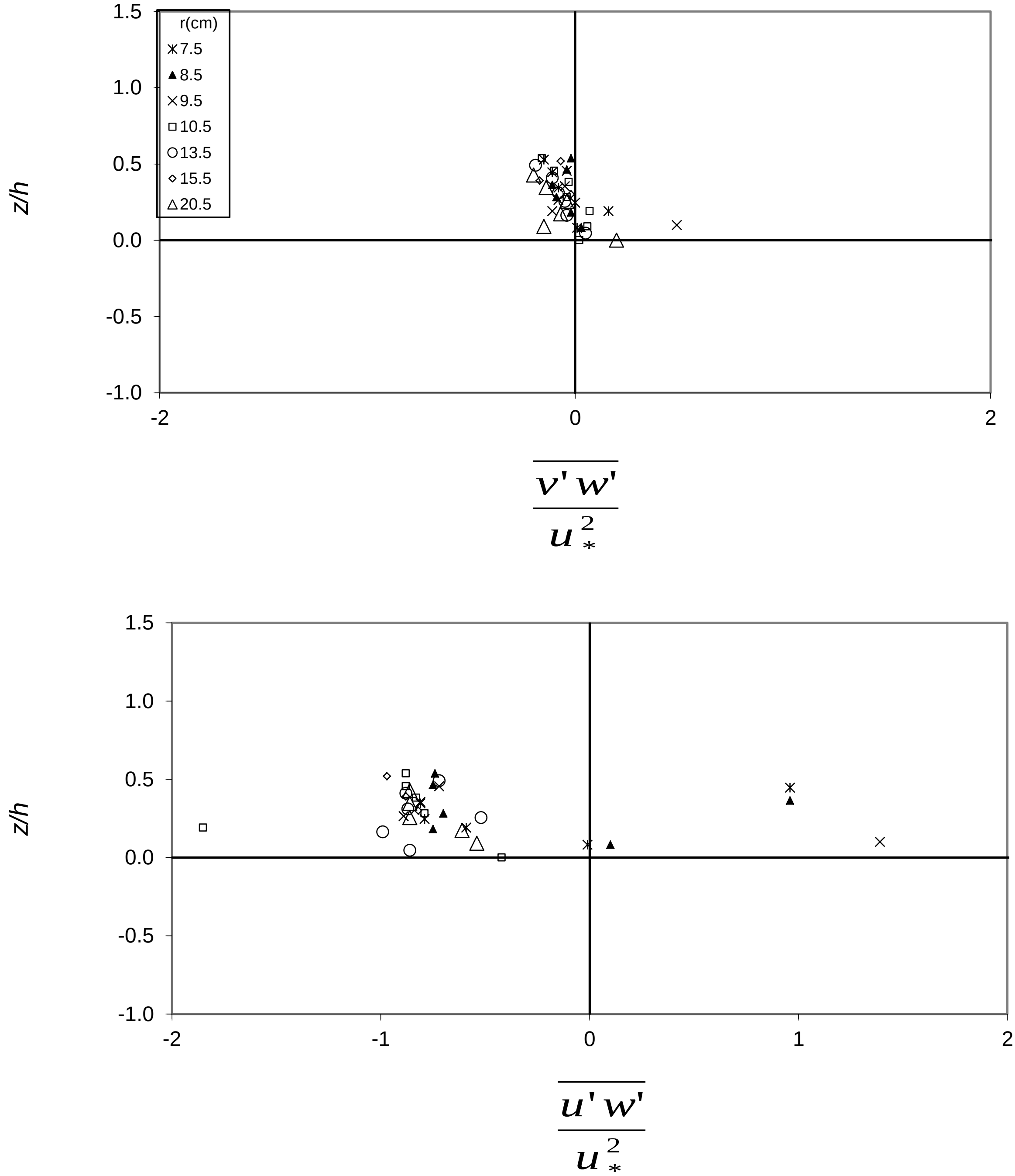

Fig 5.3 Distribution of normalized Reynolds stresses upstream plane (α = 0°)

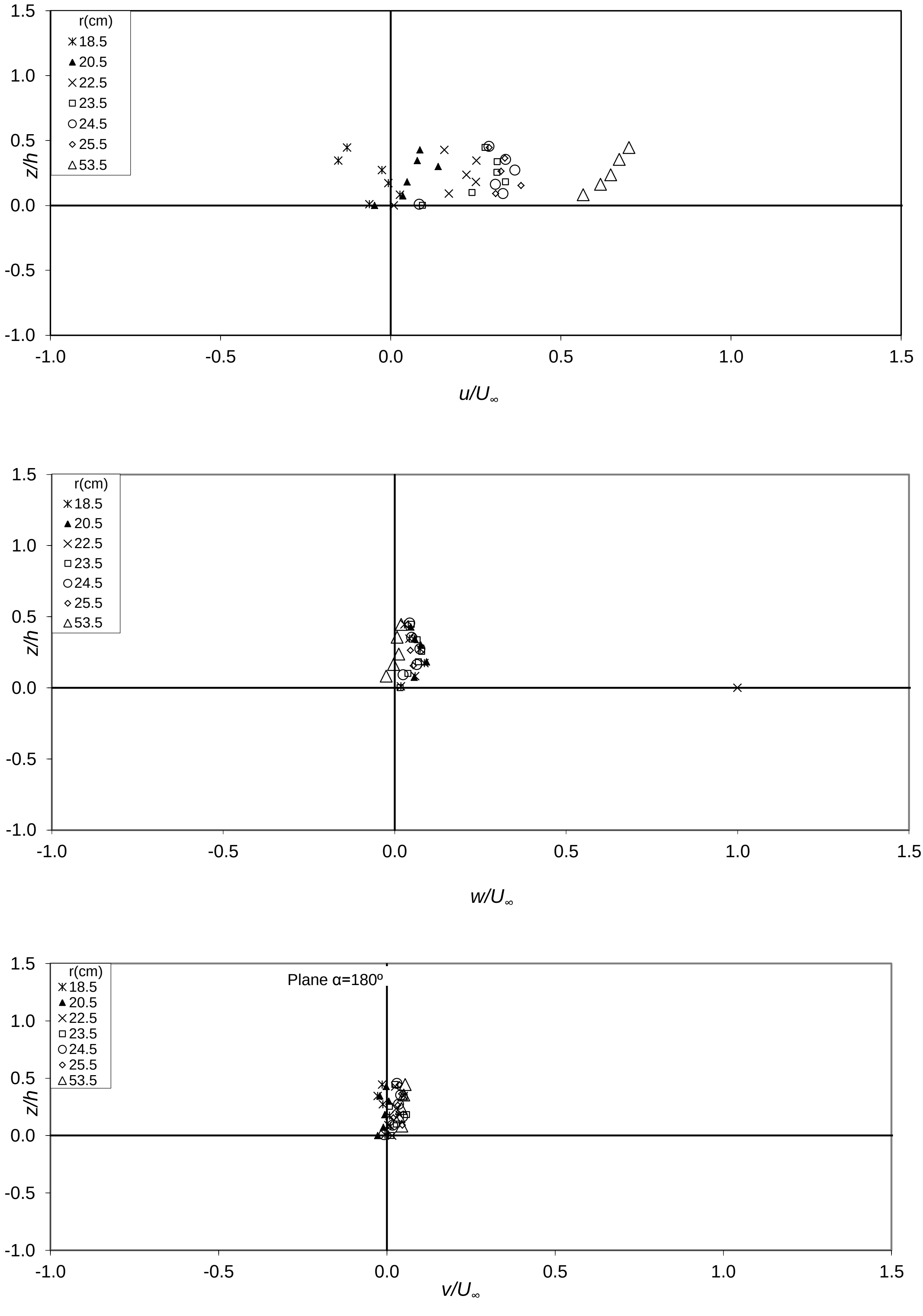

Fig 5.4 Normalized profiles of u, v and w measured downstream of pier (α = 180°)

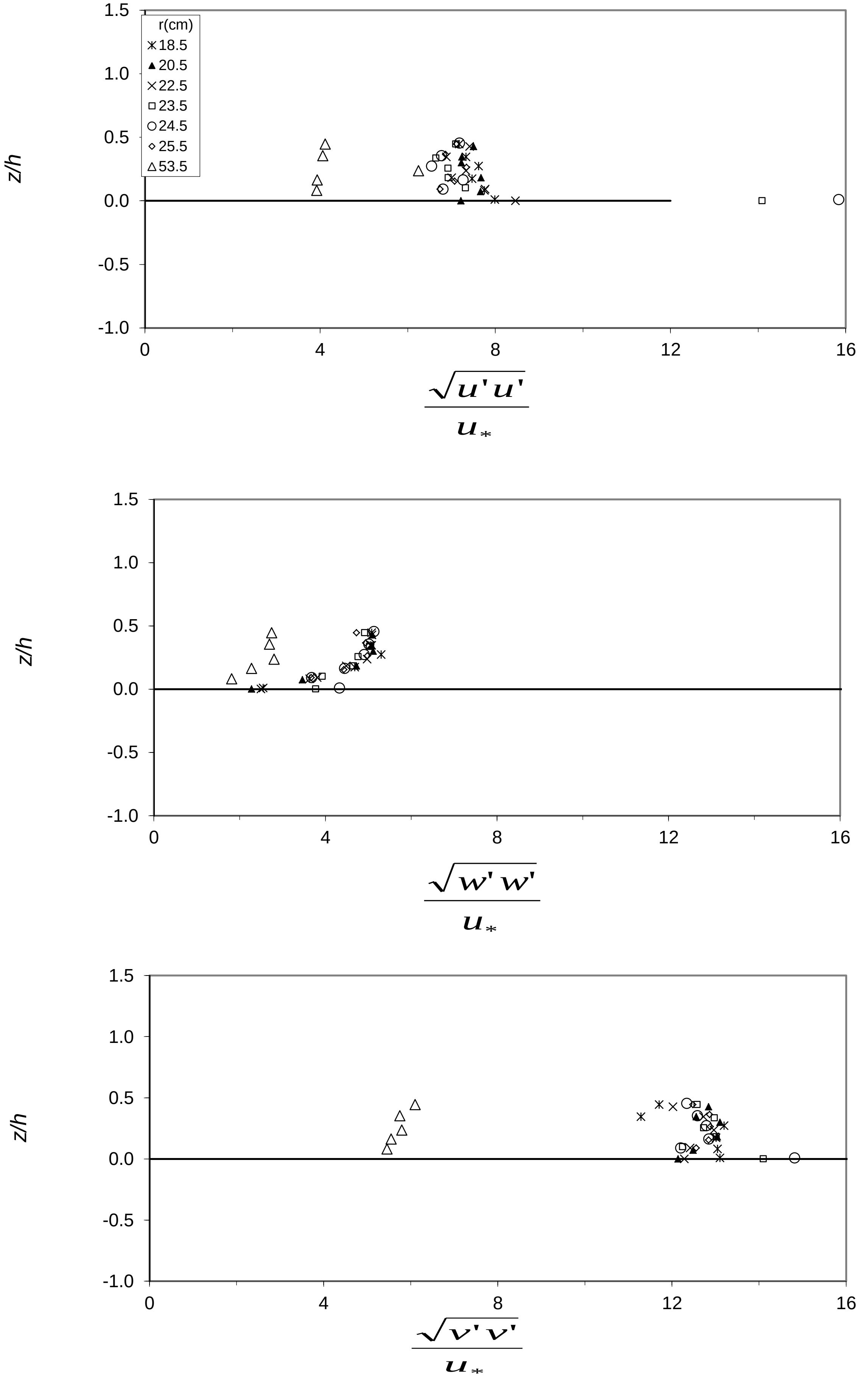

Fig 5.5 Distribution of normalized turbulence intensities (α = 180°)

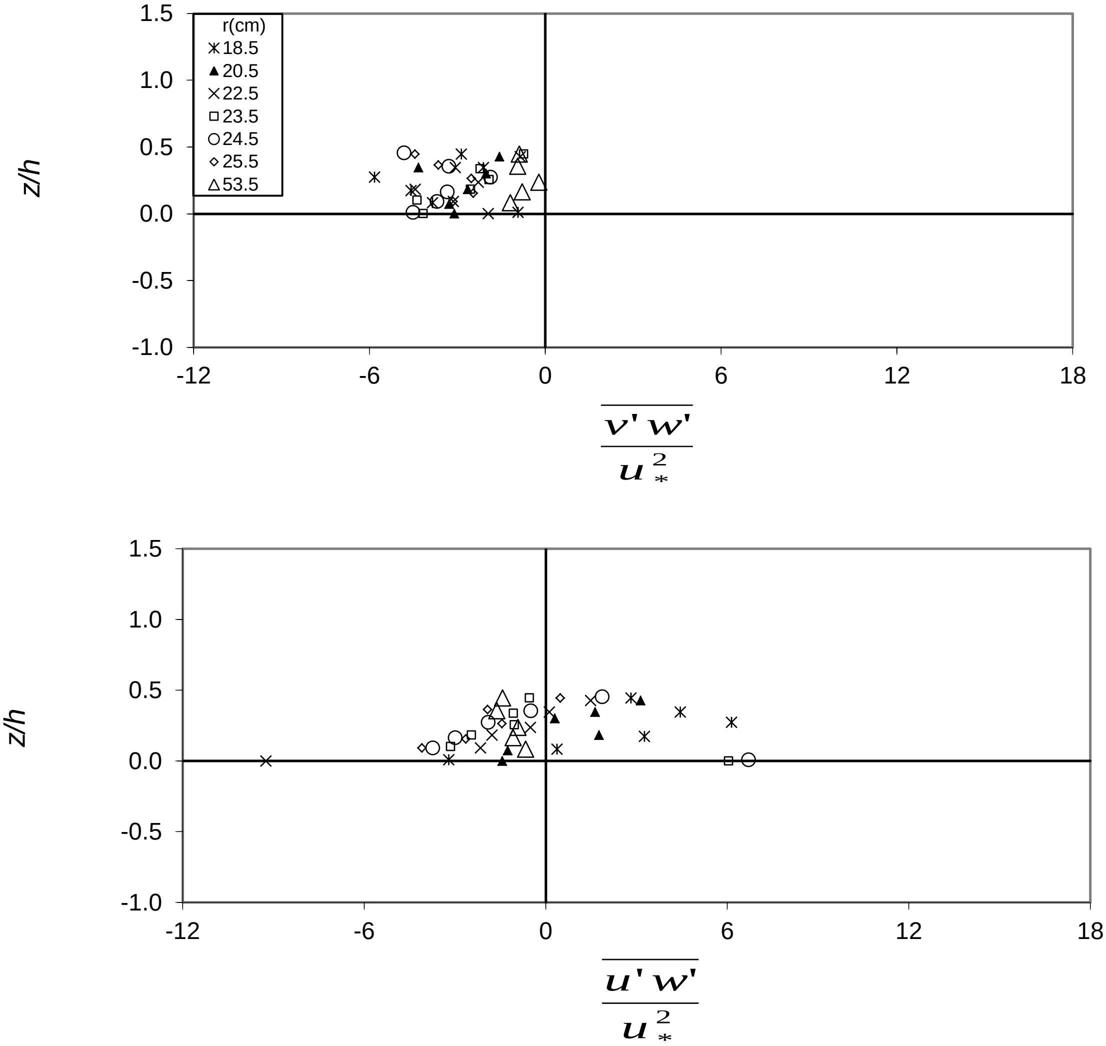

Fig 5.6 Distribution of normalized Reynolds stresses downstream plane (α = 180°)

PART 2

First pier upstream

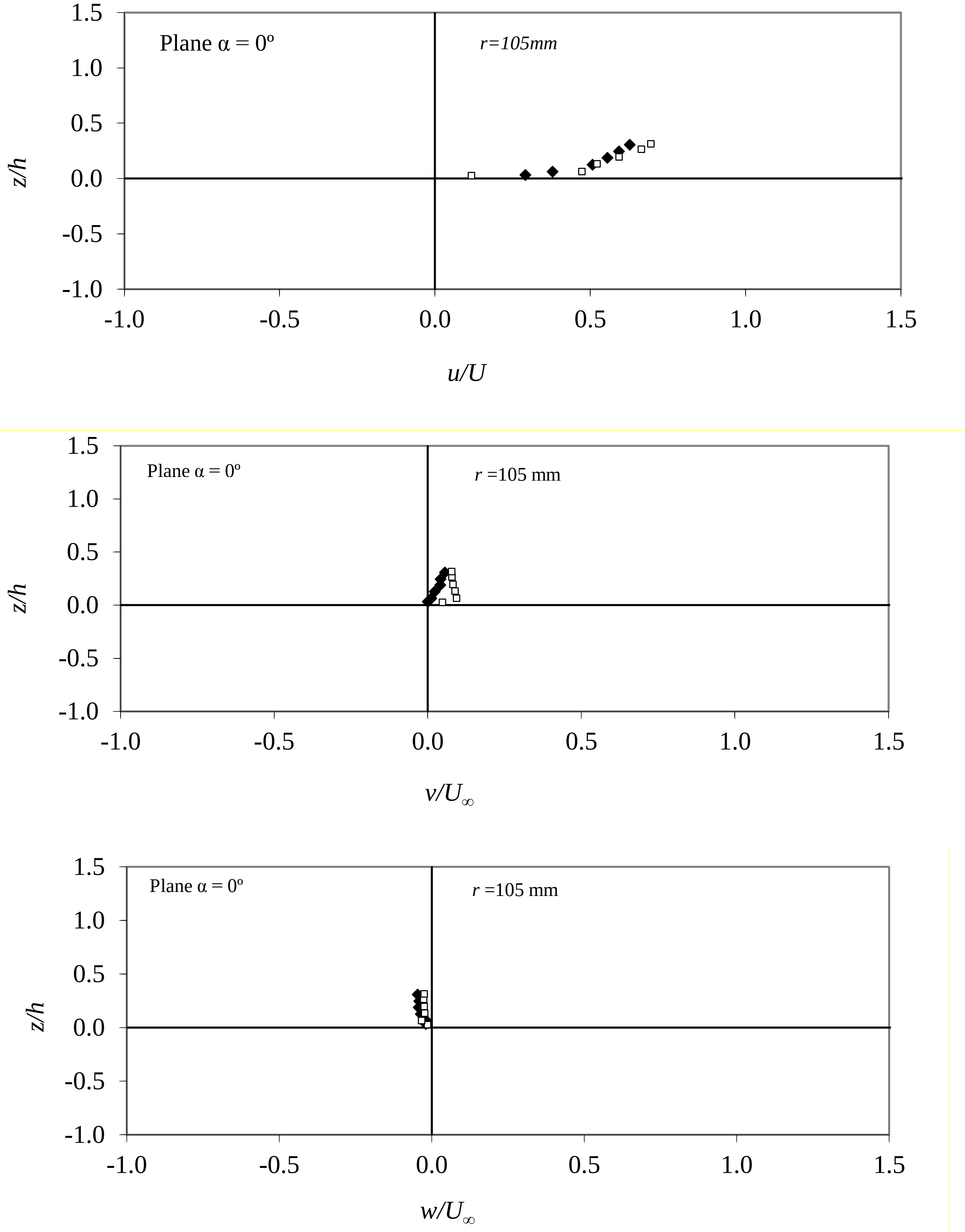

□: Isolated Pier, ♦: Effect of Second Pier at 3d Spacing

Fig. 5.7 Effect of downstream pier on the velocity of upstream pier for comparison of normalized velocity components (α = 0° and r = 105 mm)

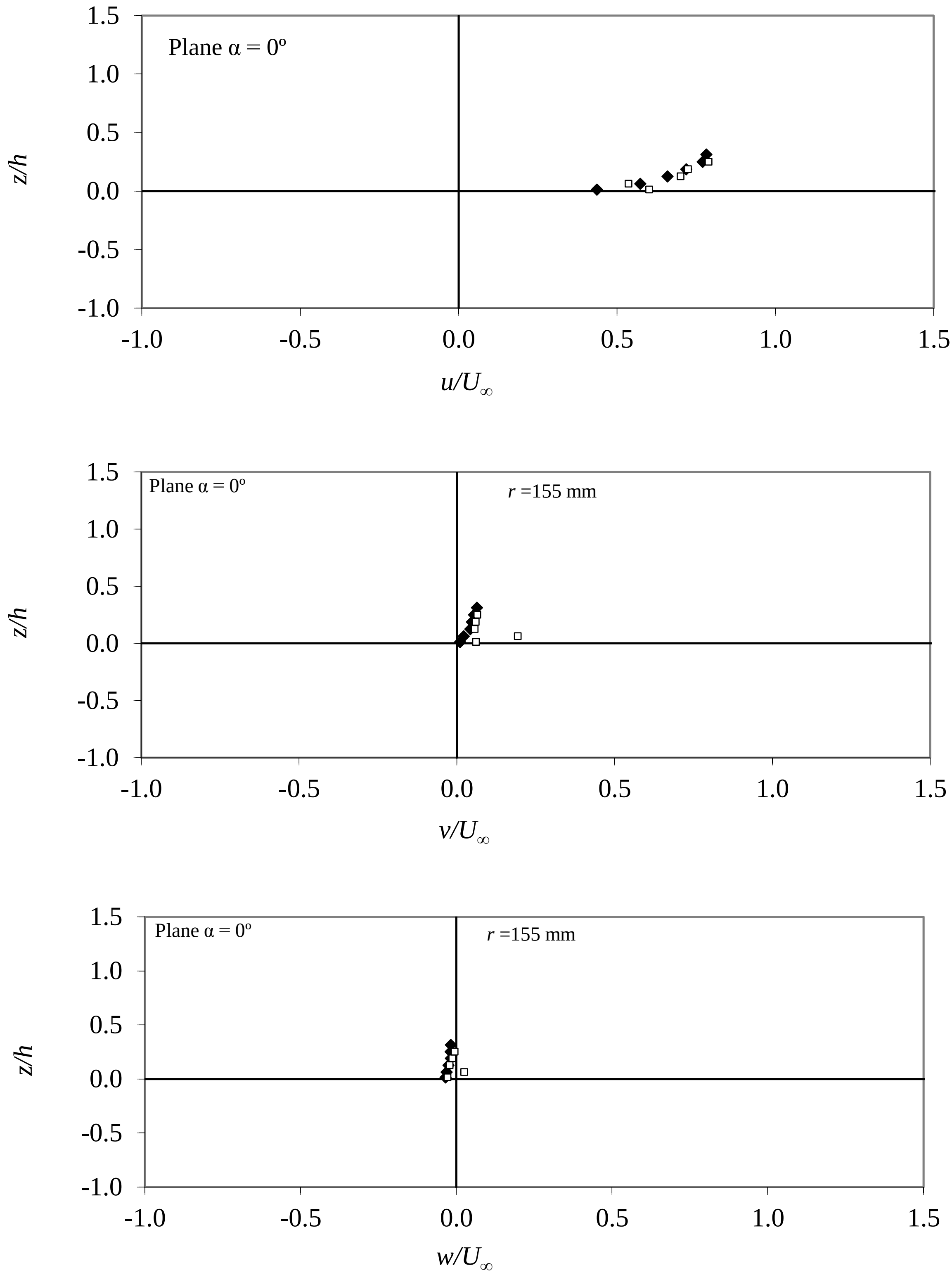

□: Isolated Pier, ♦: Effect of Second Pier at 3d Spacing

Fig. 5.8 Effect of downstream pier on the velocity of upstream pier for comparison of normalized velocity components (α = 0° and r = 155 mm)

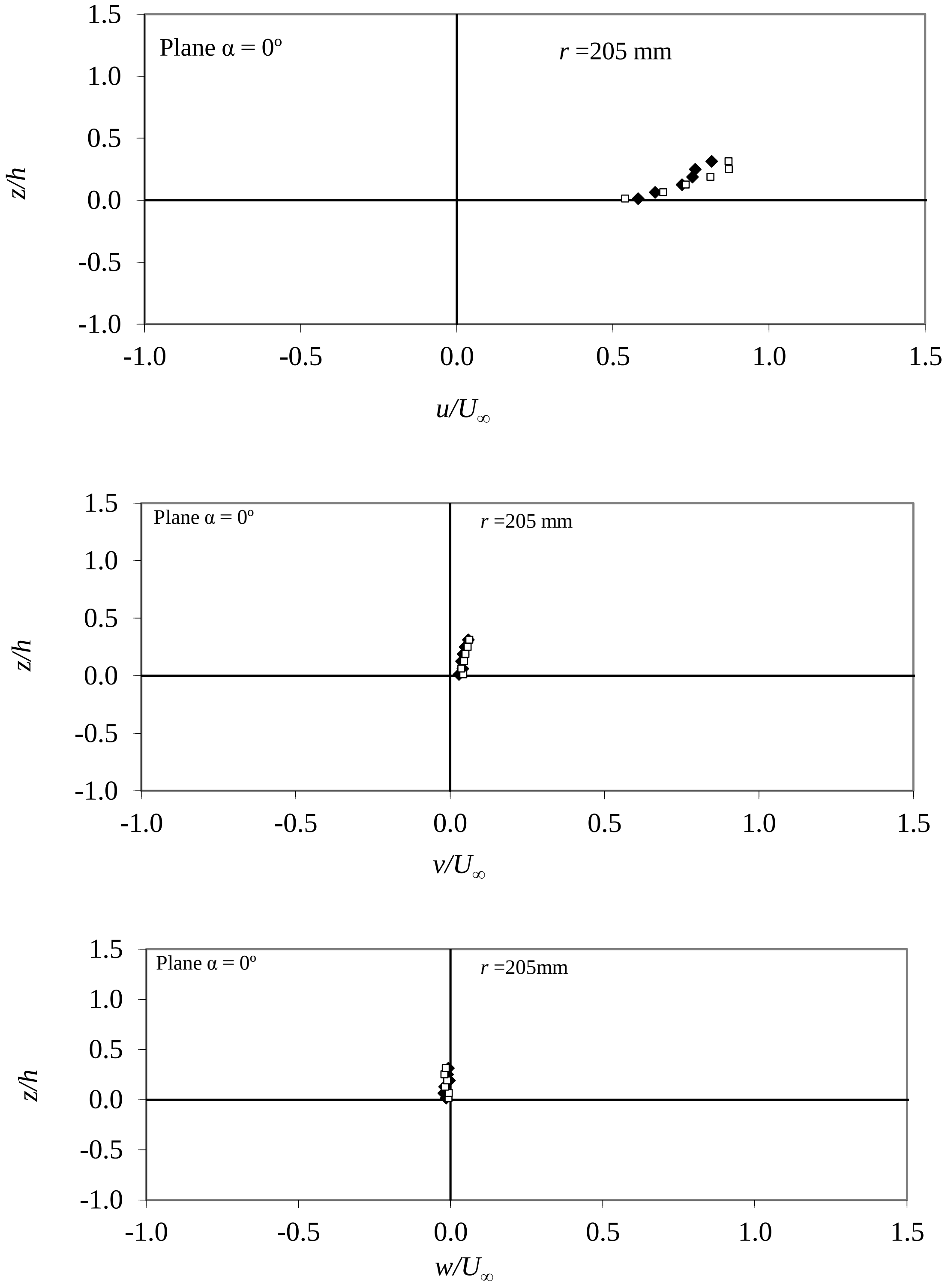

□: Isolated Pier, ♦: Effect of Second Pier at 3d Spacing

Fig.5.9 Effect of downstream pier on the velocity of upstream pier for comparison of normalised velocity components (α = 0° and r = 205 mm)

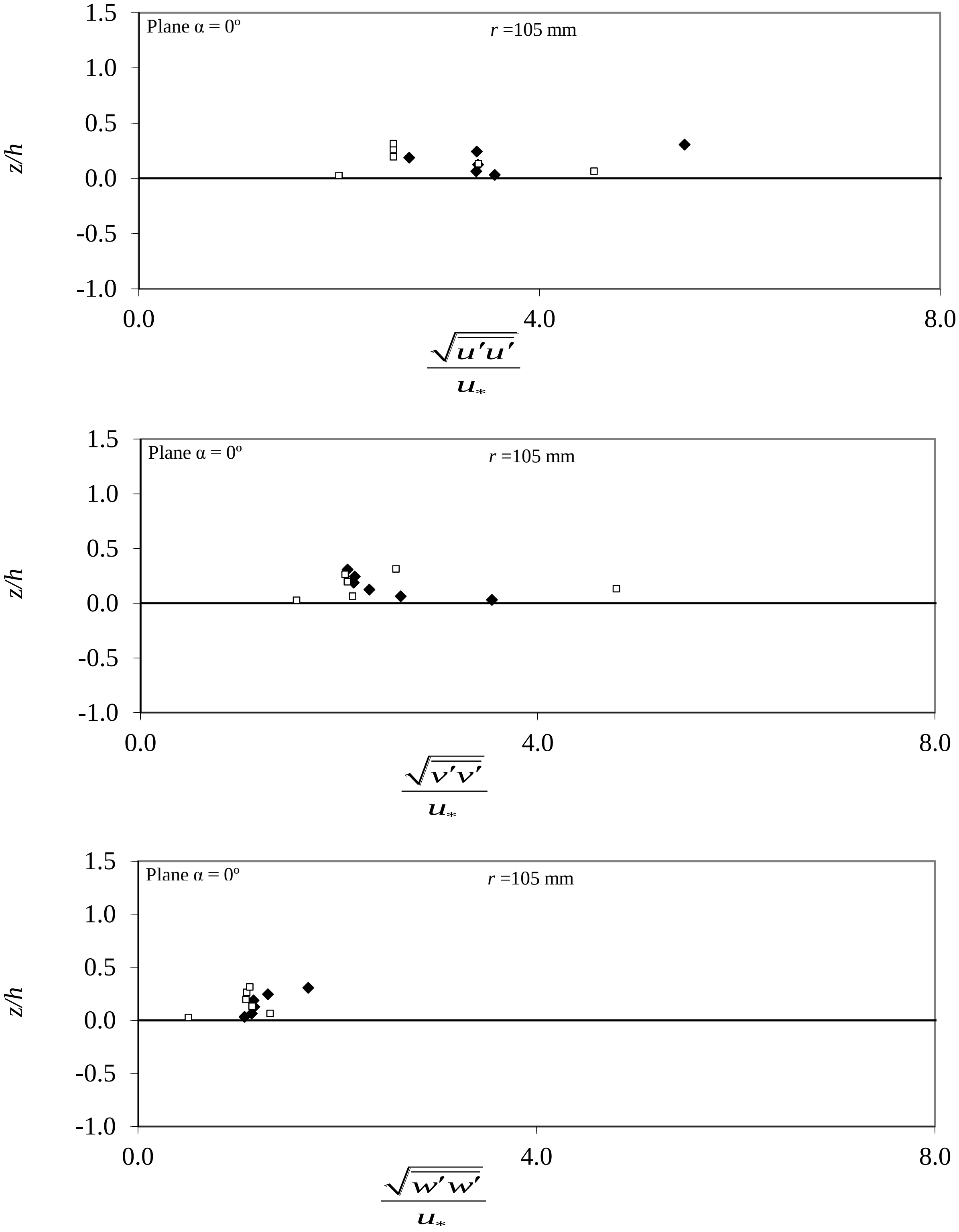

□: Isolated Pier, ♦: Effect of Second Pier at 3d Spacing

Fig. 5.10 Effect of downstream pier on the velocity of upstream pier for comparison of normalised turbulent intensities (α = 0° and r = 105 mm)

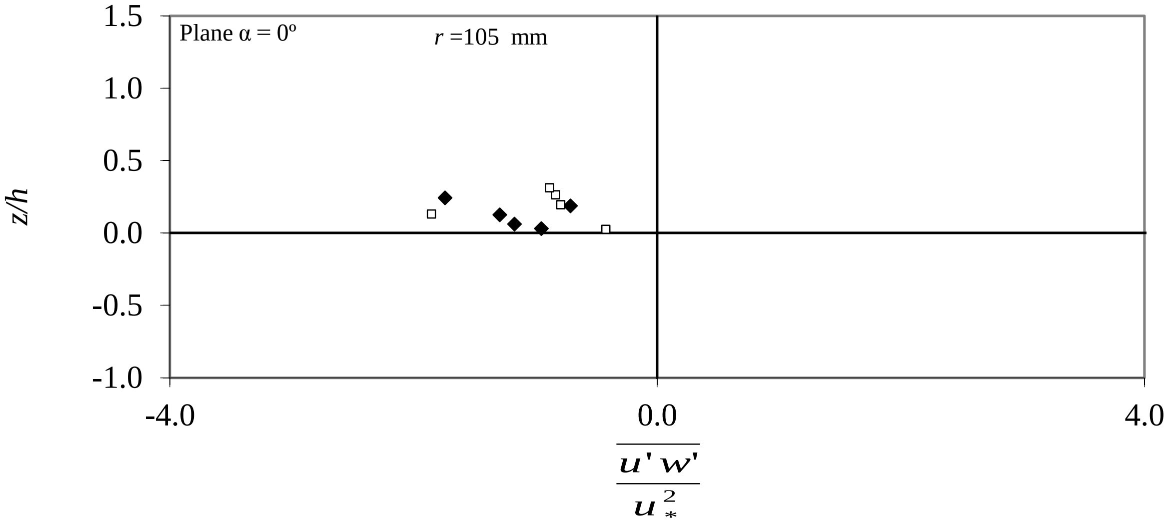

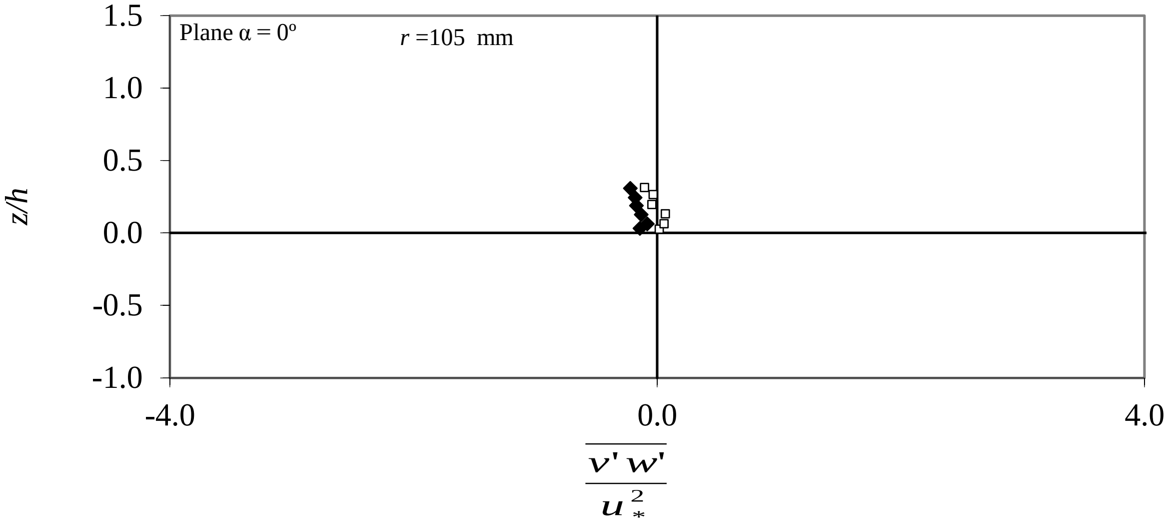

□: Isolated Pier, ♦: Effect of Second Pier at 3d Spacing

Fig 5.11 Effect of downstream pier on the velocity of upstream pier for comparison of normalised Reynolds's stresses (α = 0° and r = 105 mm)

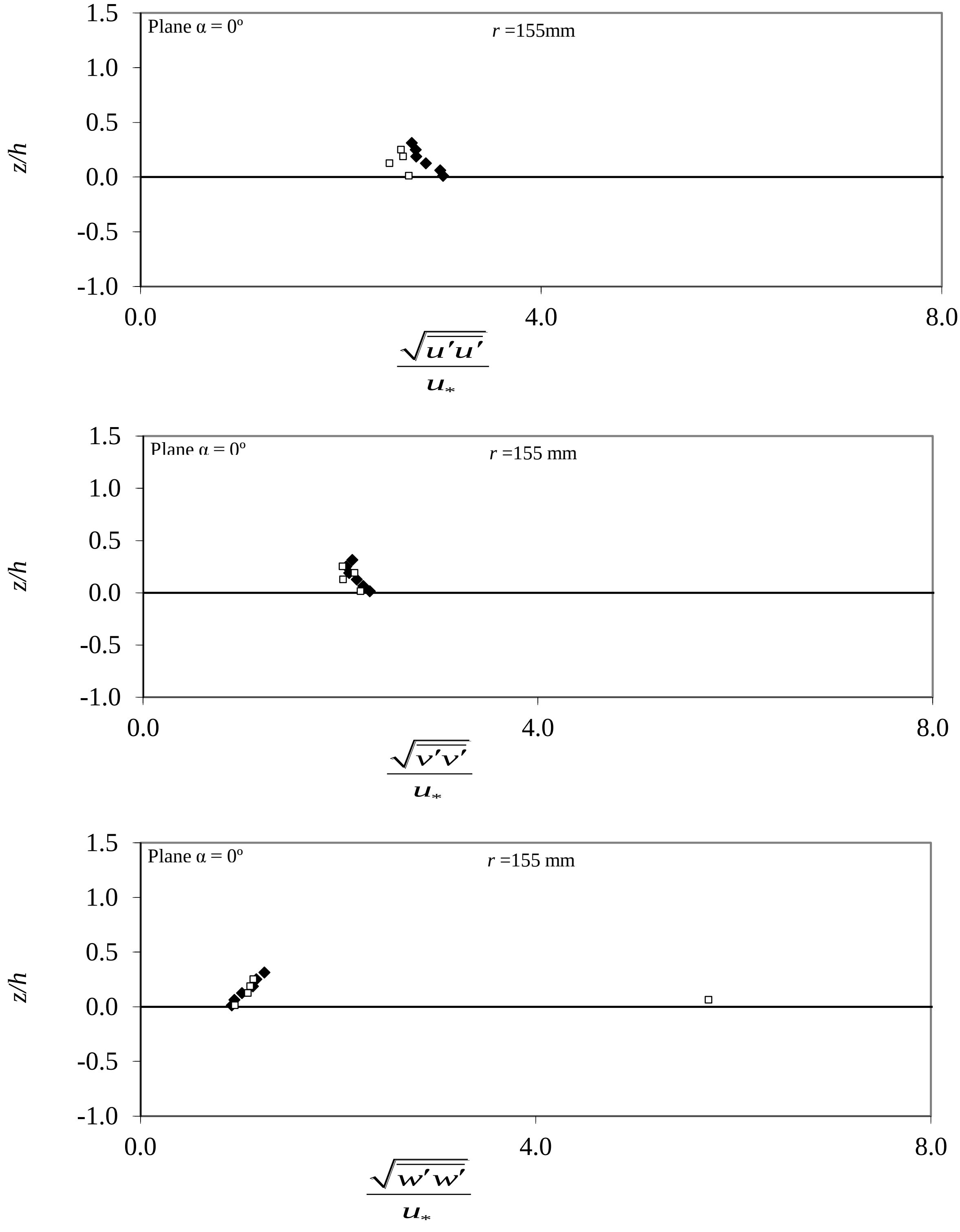

□: Isolated Pier, ♦: Effect of Second Pier at 3d Spacing

Fig. 5.12 Effect of downstream pier on the velocity of upstream pier for comparison of normalised turbulent intensities (α = 0° and r = 155 mm)

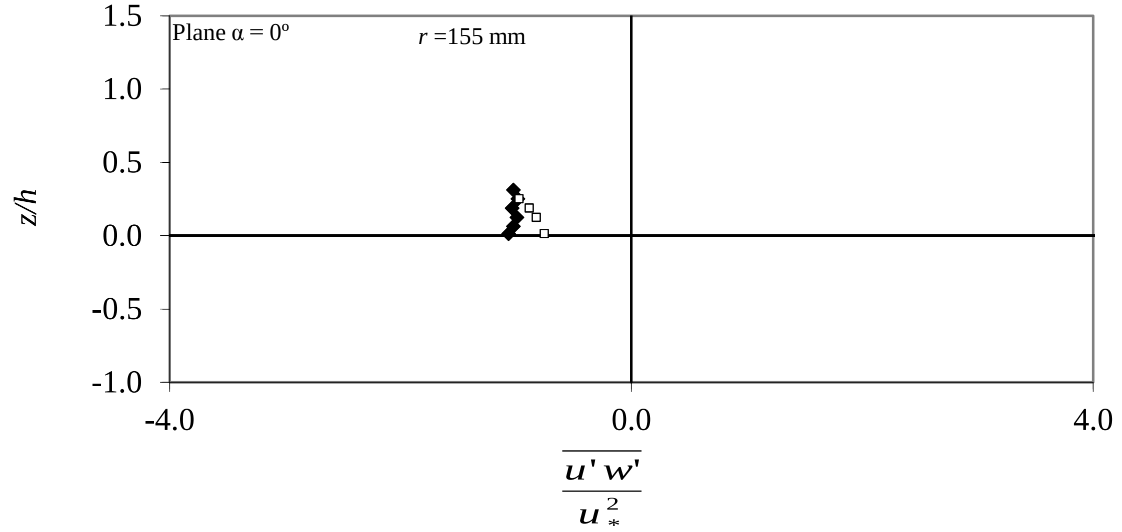

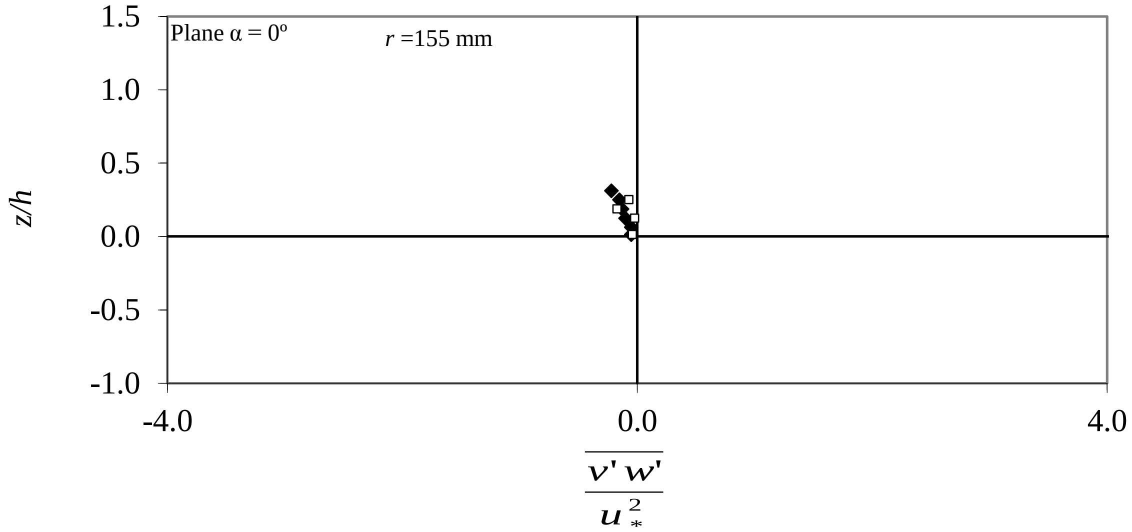

□: Isolated Pier, ♦: Effect of Second Pier at 3d Spacing

Fig 5.13 Effect of downstream pier on the velocity of upstream pier for comparison of normalised Reynolds's stresses (α = 0° and r = 155 mm)

‘

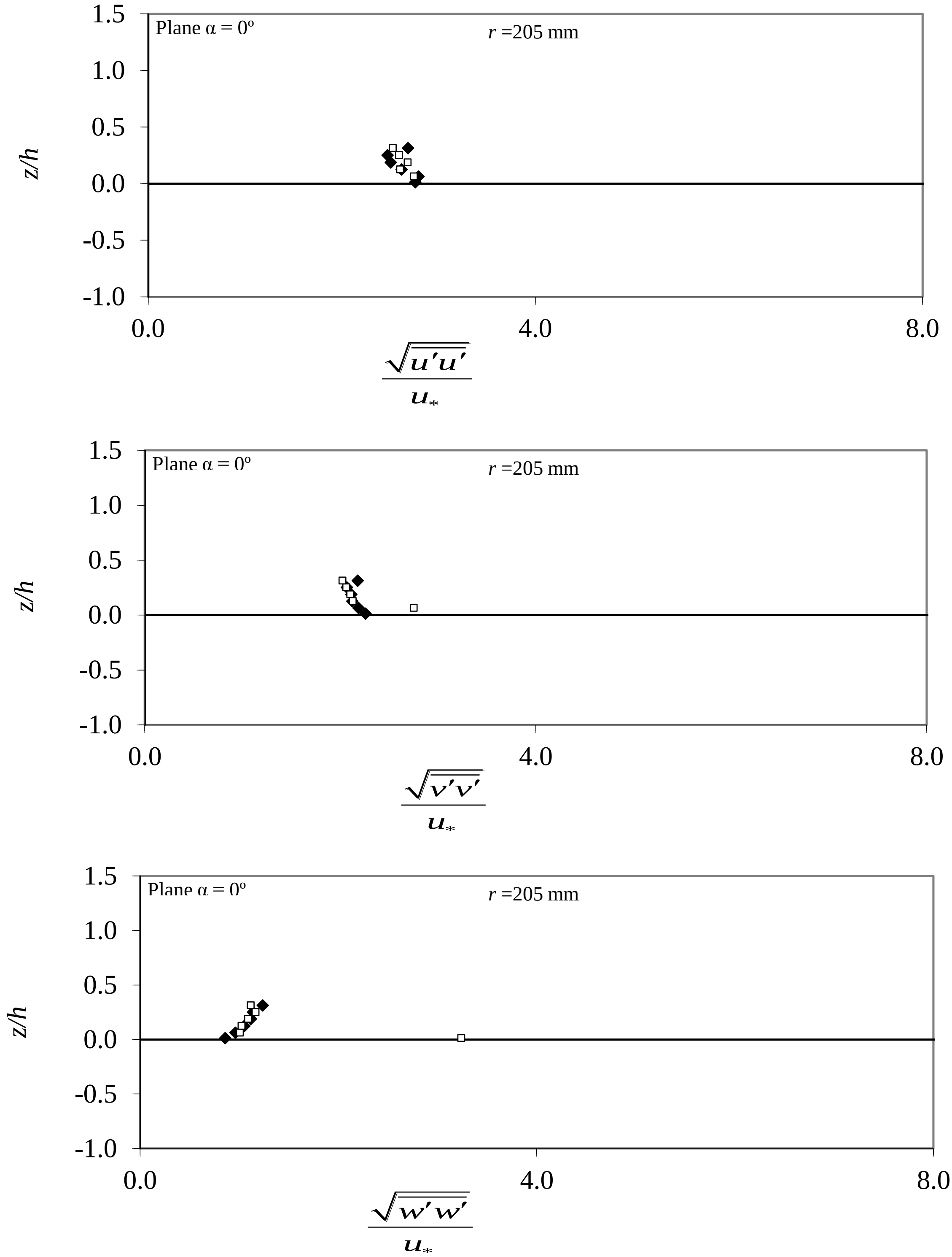

□: Isolated Pier, ♦: Effect of Second Pier at 3d Spacing

Fig 5.14 Effect of downstream pier on the velocity of upstream pier for comparison of normalised turbulence intensities (α = 0° and r = 205 mm)

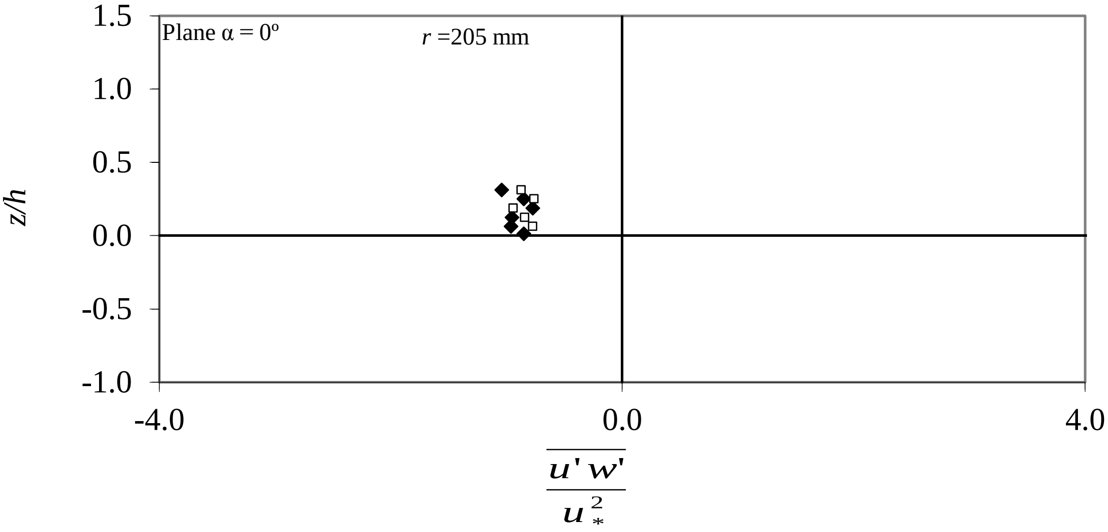

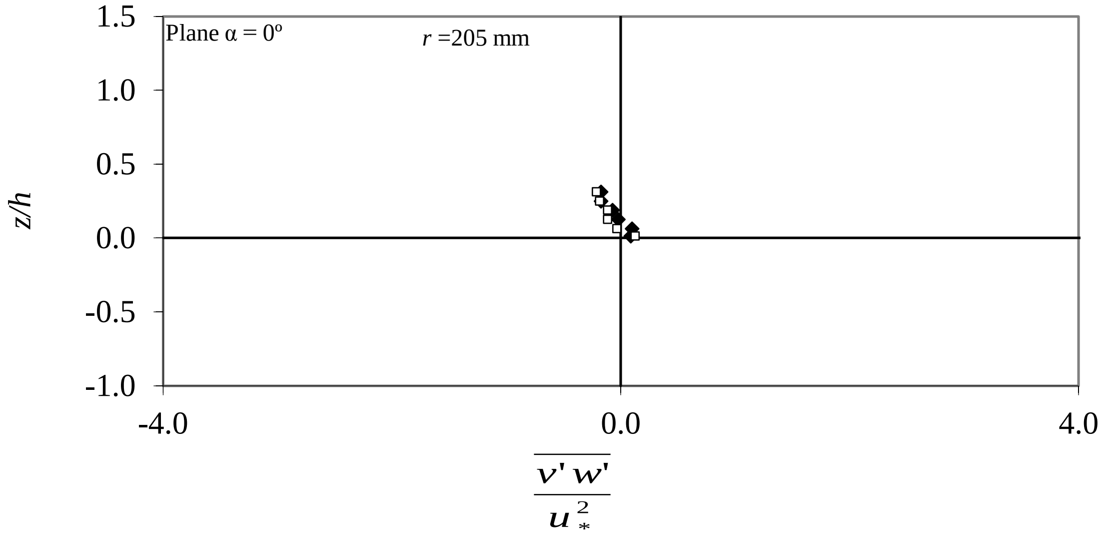

□: Isolated Pier, ♦: Effect of Second Pier at 3d Spacing

Fig 5.15 Effect of downstream pier on the velocity of upstream pier for comparison of normalised Reynolds's stresses (α = 0° and r = 205 mm)

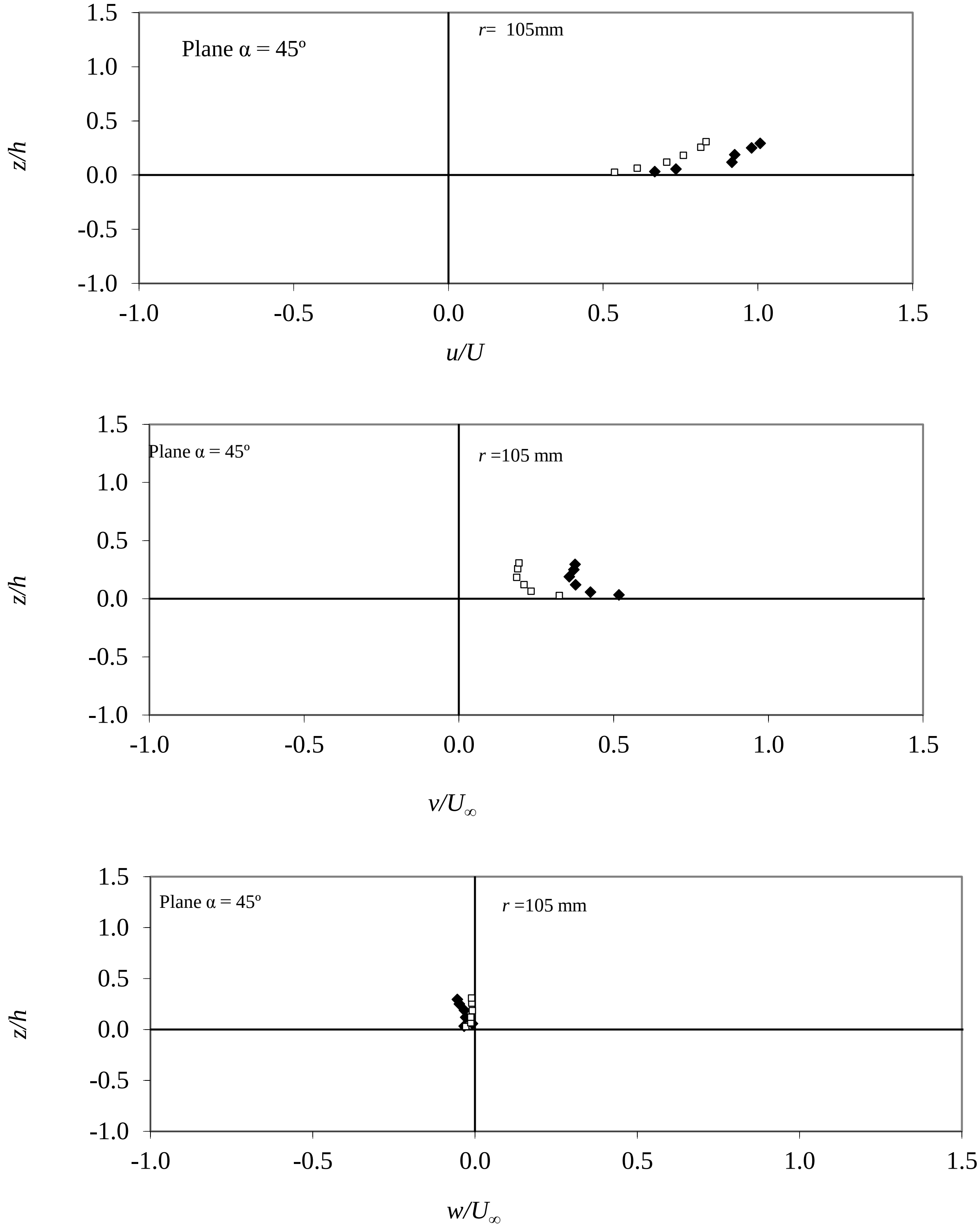

□: Isolated Pier, ♦: Effect of Second Pier at 3d Spacing

Fig 5.16 Effect of downstream pier on the velocity of upstream pier for comparison of normalised velocity components (α = 45° and r = 105 mm)

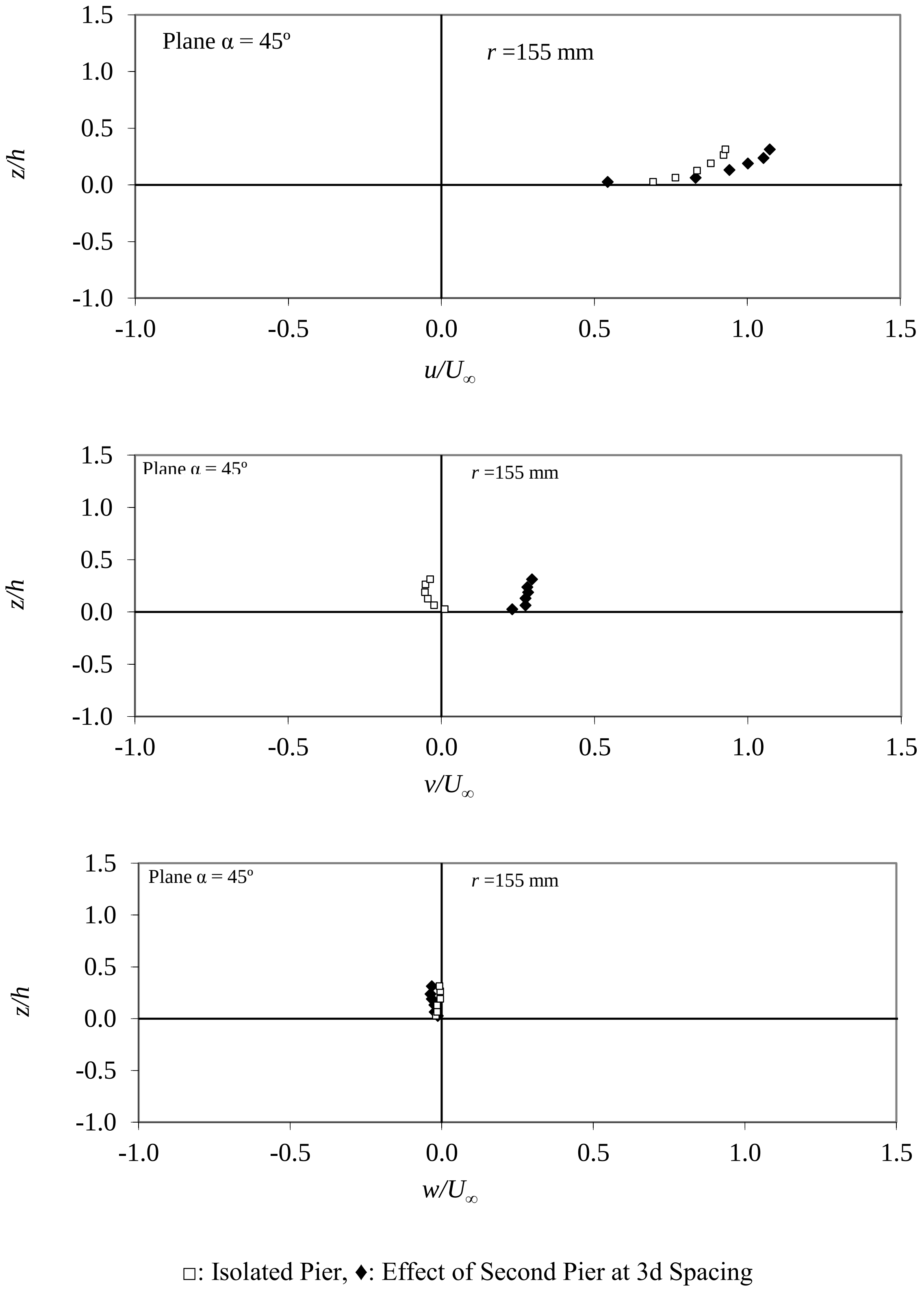

Fig 5.17 Effect of downstream pier on the velocity of upstream pier for comparison of normalised velocity components (α = 45° and r = 155 mm)

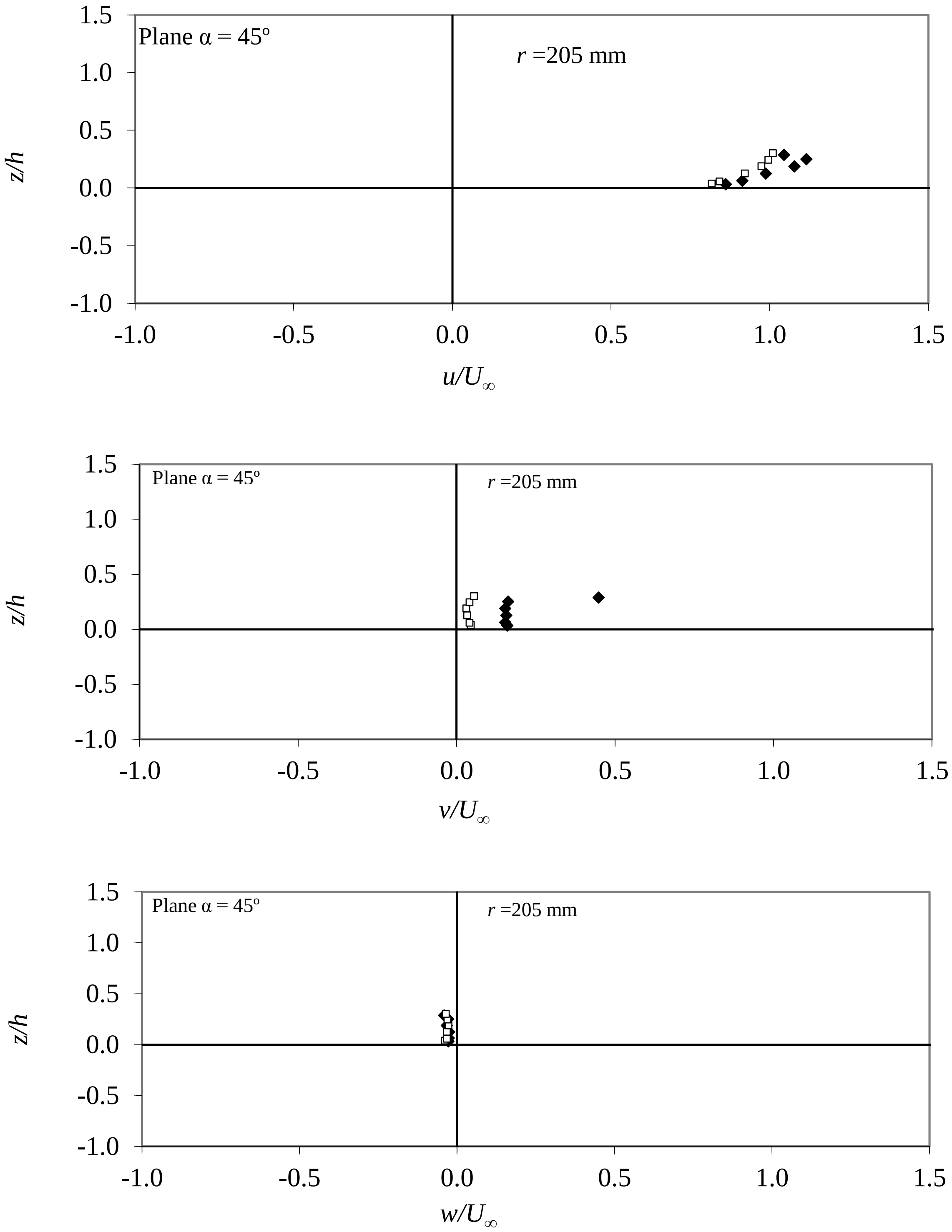

□: Isolated Pier, ♦: Effect of Second Pier at 3d Spacing

Fig 5.18 Effect of downstream pier on the velocity of upstream pier for comparison of normalised velocity components (α = 45° and r = 205 mm)

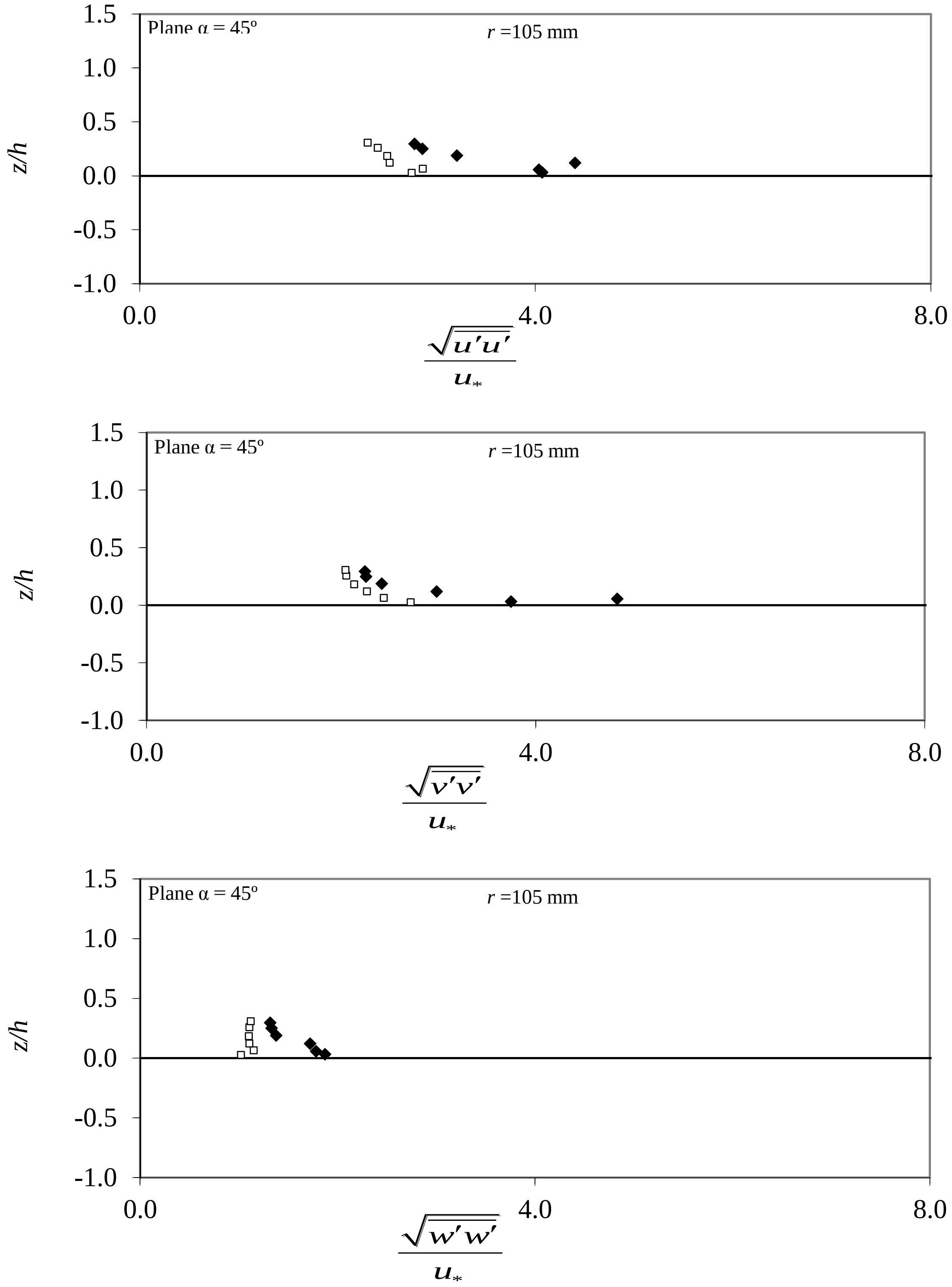

□: Isolated Pier, ♦: Effect of Second Pier at 3d Spacing

Fig 5.19 Effect of downstream pier on the velocity of upstream pier for comparison of normalised turbulence intensities (α = 45° and r = 105 mm)

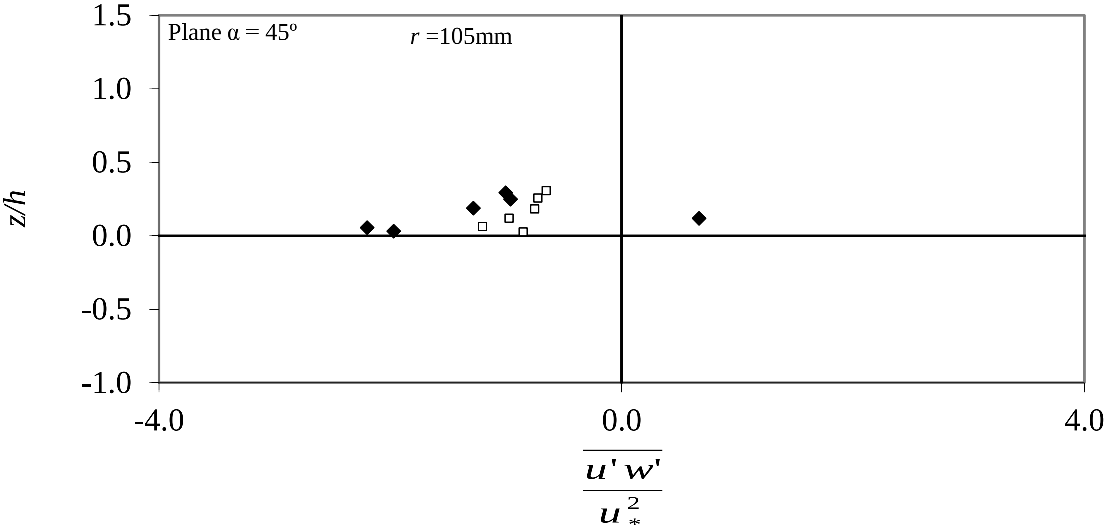

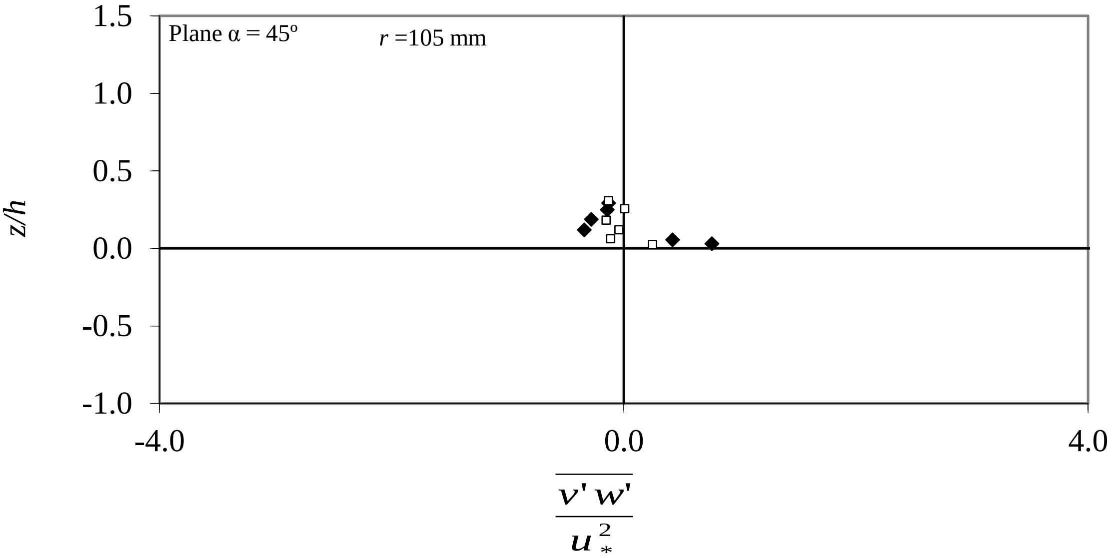

□: Isolated Pier, ♦: Effect of Second Pier at 3d Spacing

Fig 5.20 Effect of downstream pier on the velocity of upstream pier for comparison of normalised Reynolds's stresses (α = 45° and r = 105 mm)

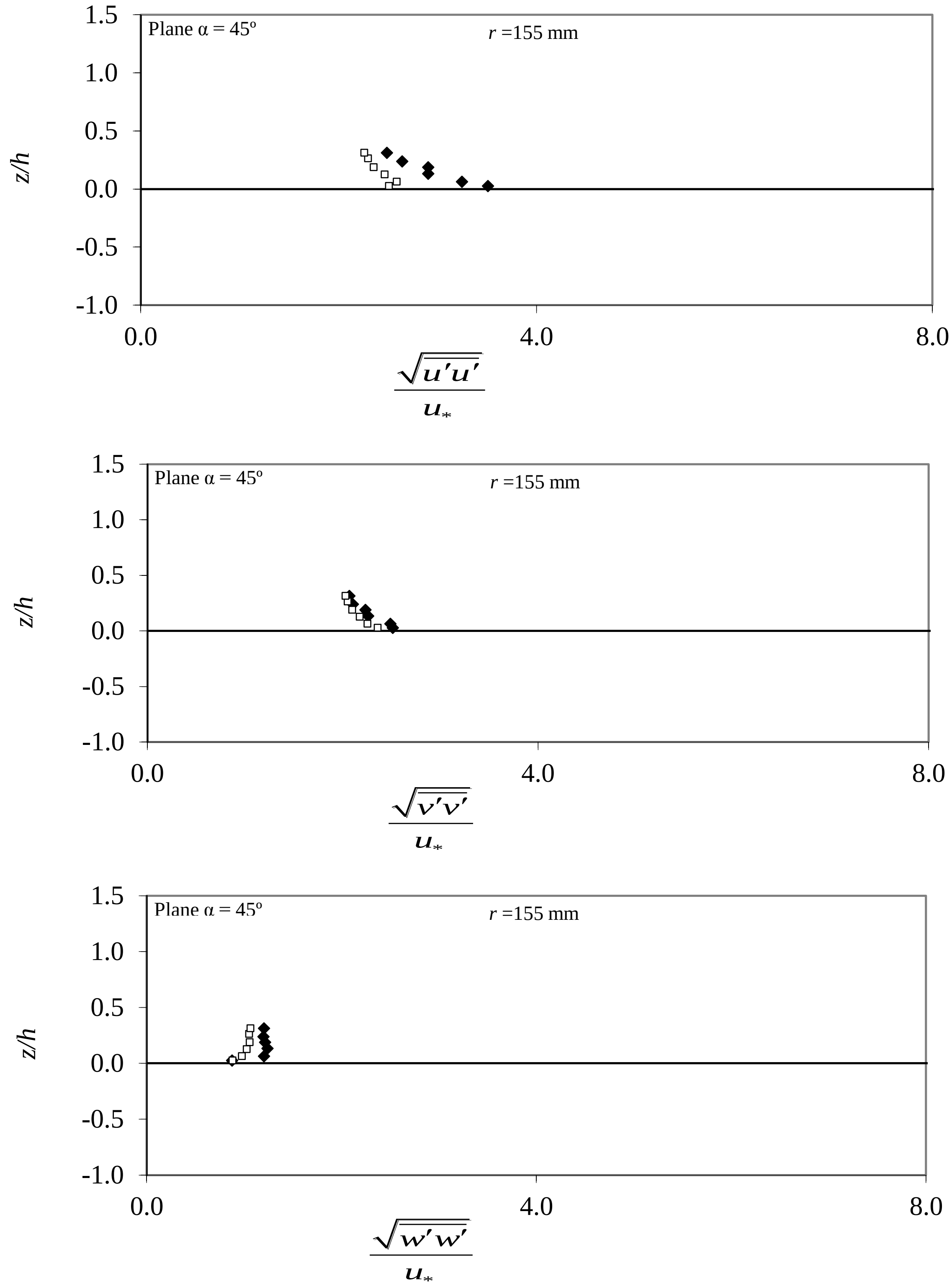

□: Isolated Pier, ♦: Effect of Second Pier at 3d Spacing

Fig 5.21 Effect of downstream pier on the velocity of upstream pier for comparison of normalised turbulence intensities (α = 45° and r = 155 mm)

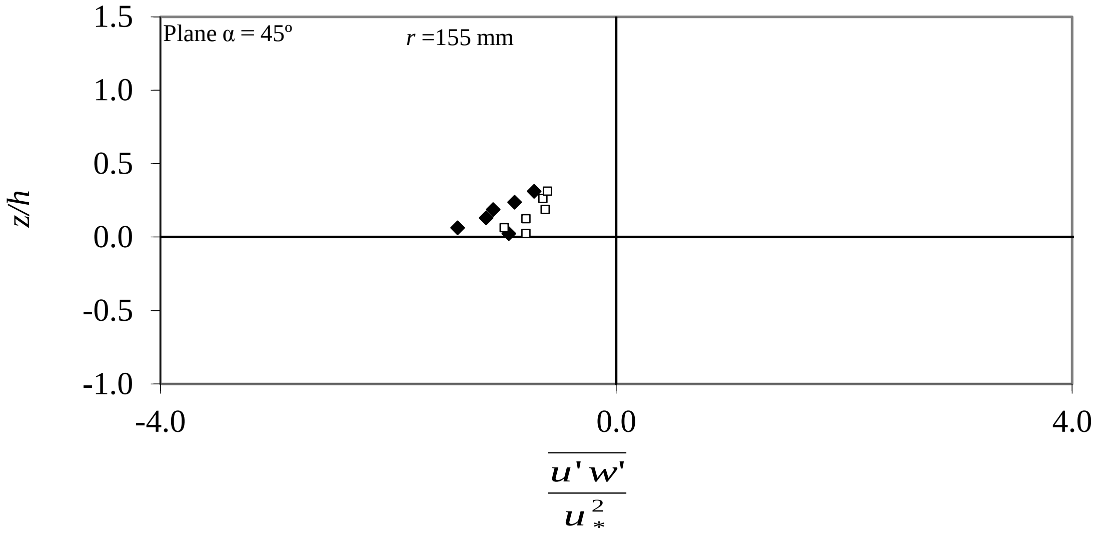

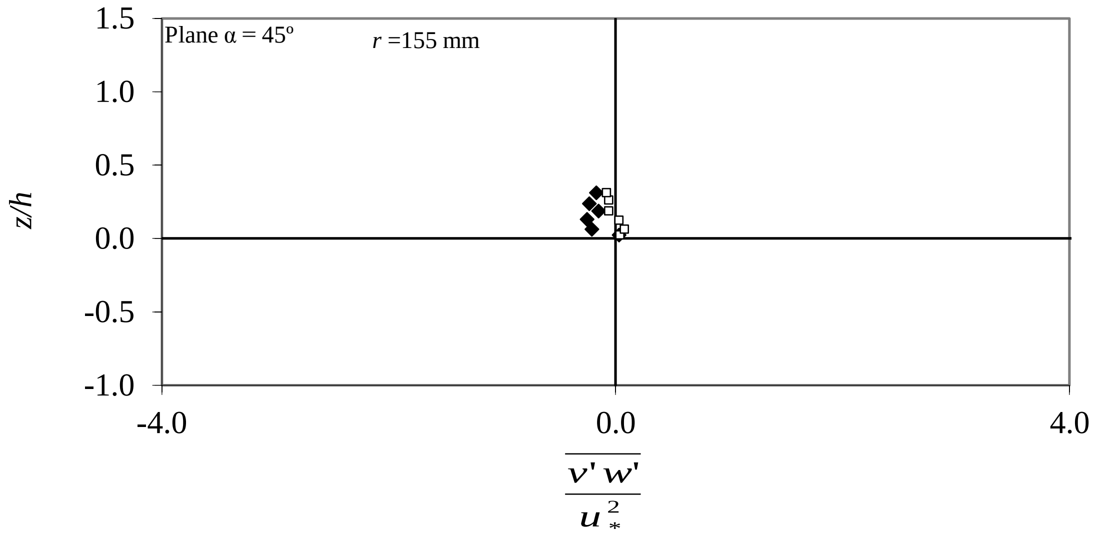

□: Isolated Pier, ♦: Effect of Second Pier at 3d Spacing

Fig 5.22 Effect of downstream pier on the velocity of upstream pier for comparison of normalised Reynolds's stresses (α = 45° and r = 155 mm)

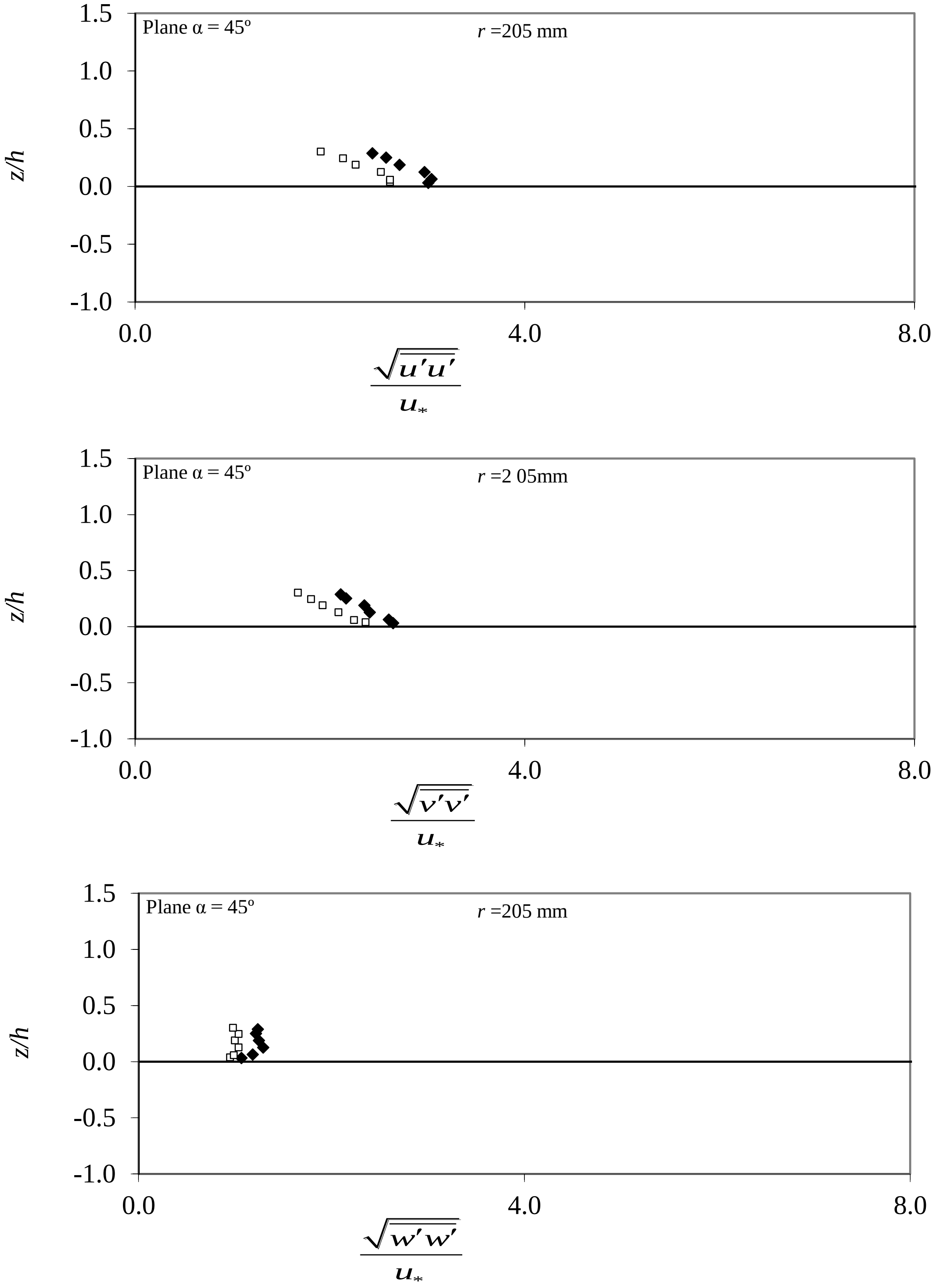

□: Isolated Pier, ♦: Effect of Second Pier at 3d Spacing

Fig 5.23 Effect of downstream pier on the velocity of upstream pier for comparison of normalised turbulence intensities (α = 45° and r = 205 mm)

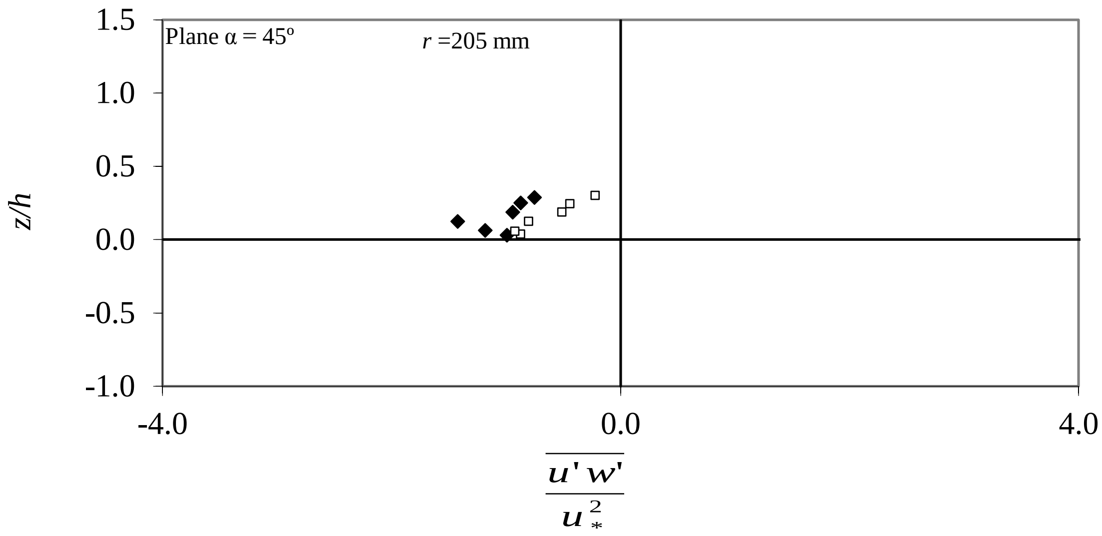

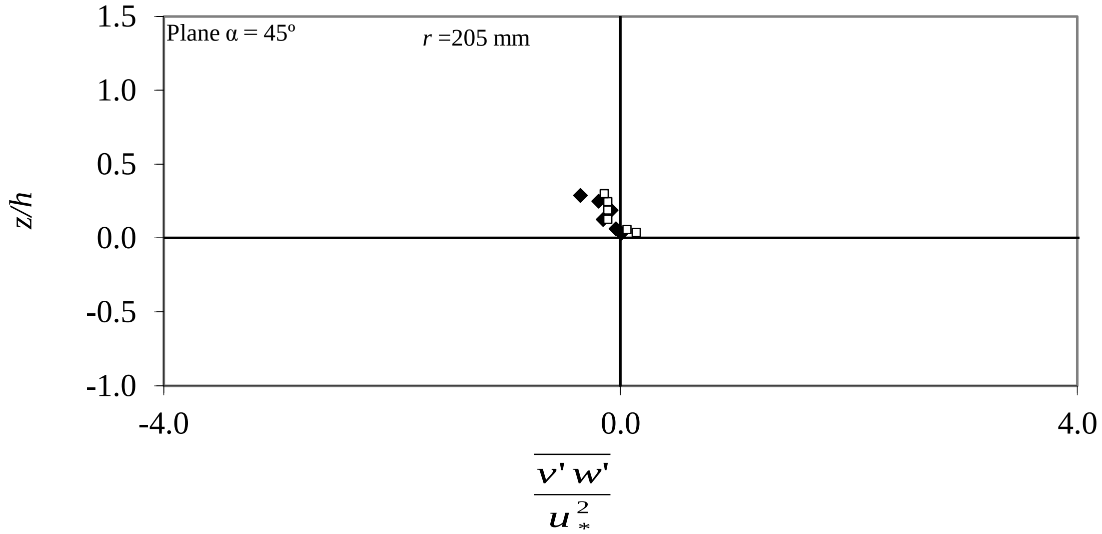

□: Isolated Pier, ♦: Effect of Second Pier at 3d Spacing

Fig 5.24 Effect of downstream pier on the velocity of upstream pier for comparison of normalised Reynolds's stresses (α = 45° and r = 205 mm)

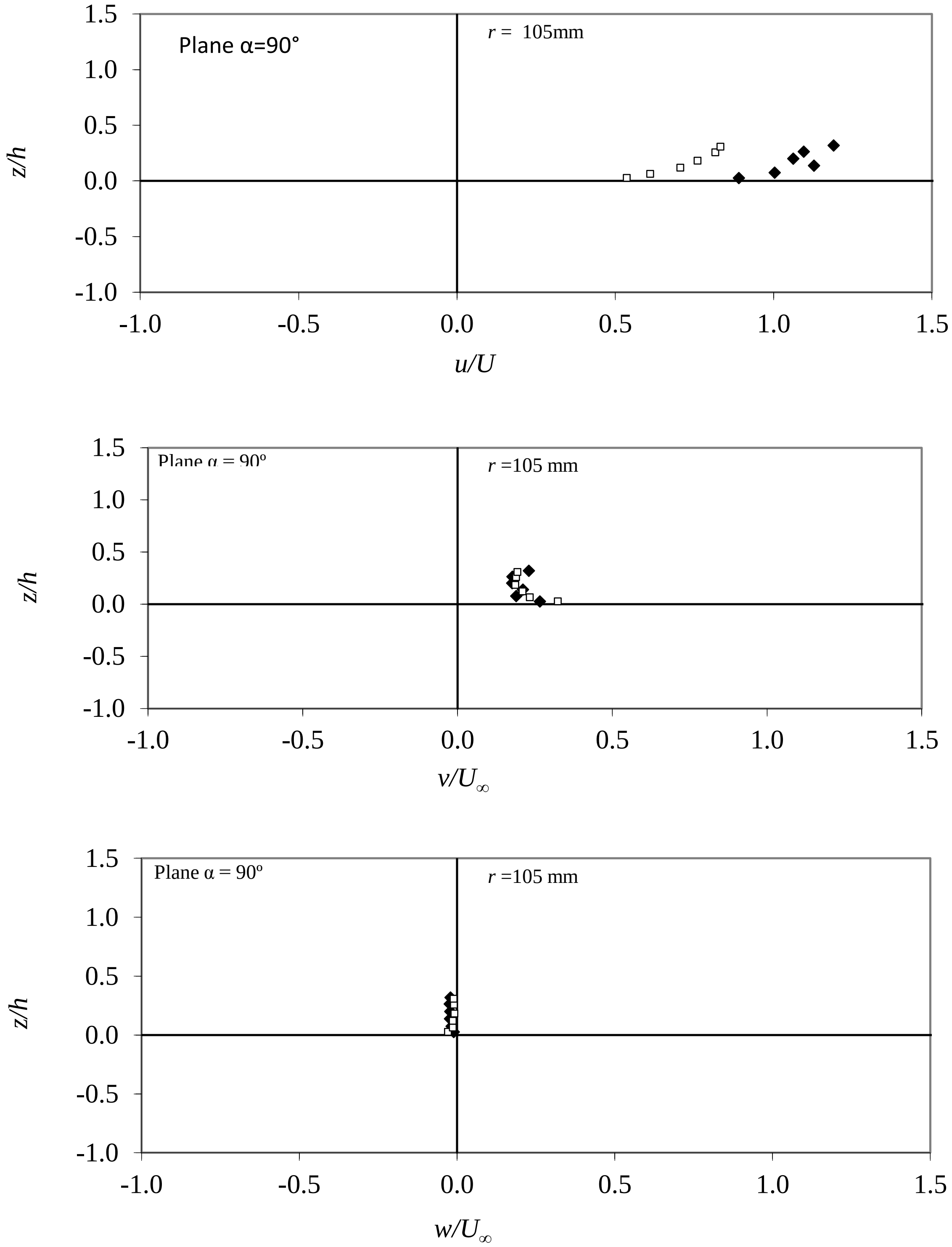

□: Isolated Pier, ♦: Effect of Second Pier at 3d Spacing

Fig 5.25 Effect of downstream pier on the velocity of upstream pier for comparison of normalised velocity components (α = 90° and r = 105 mm)

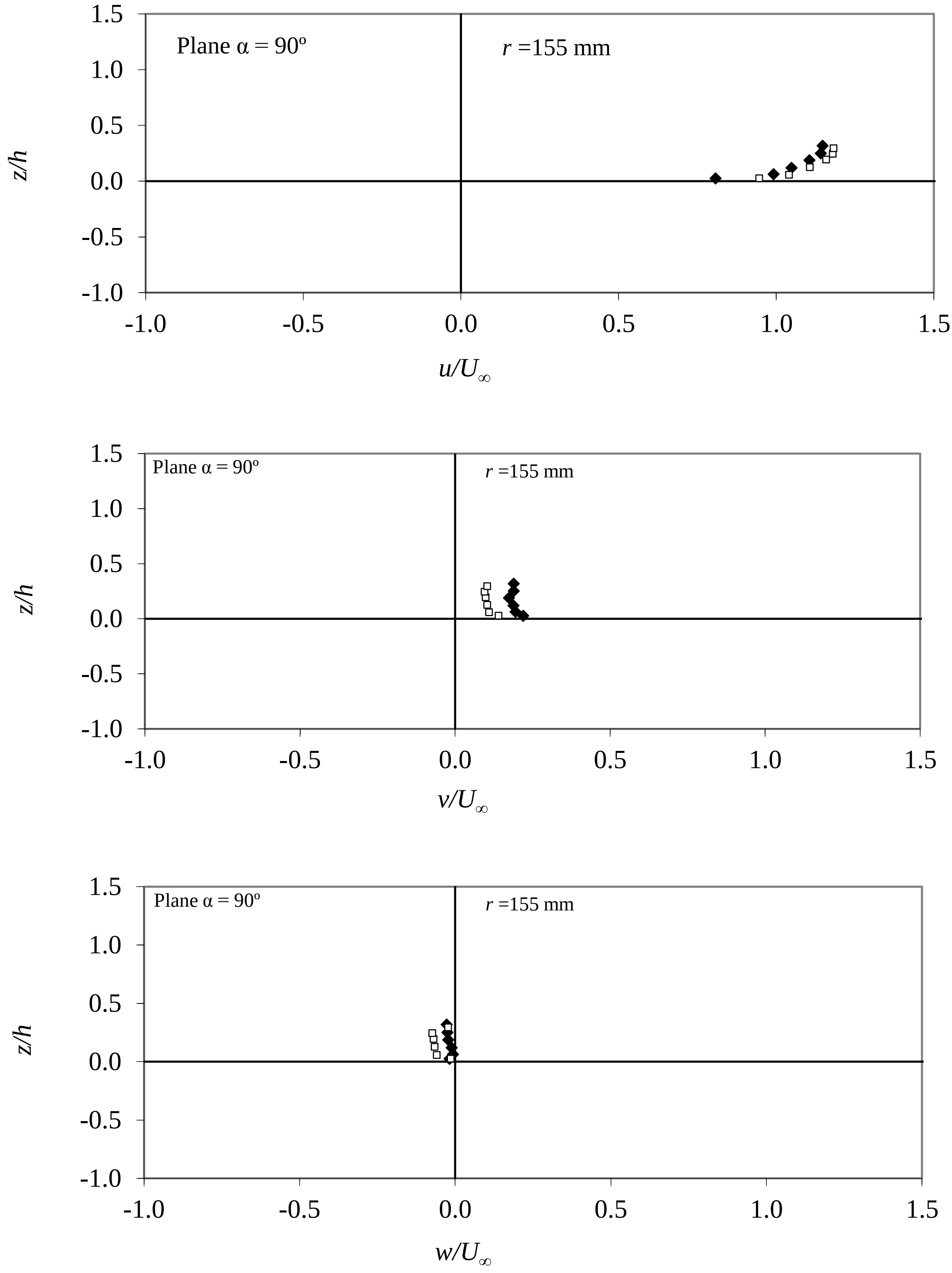

□: Isolated Pier, ♦: Effect of Second Pier at 3d Spacing

Fig 5.26 Effect of downstream pier on the velocity of upstream pier for comparison of normalised velocity components (α = 90° and r = 155 mm)

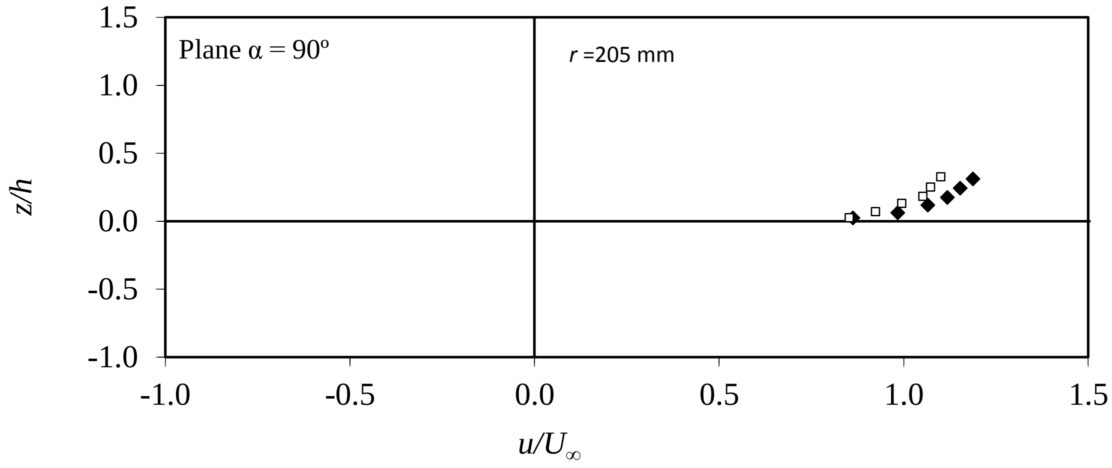

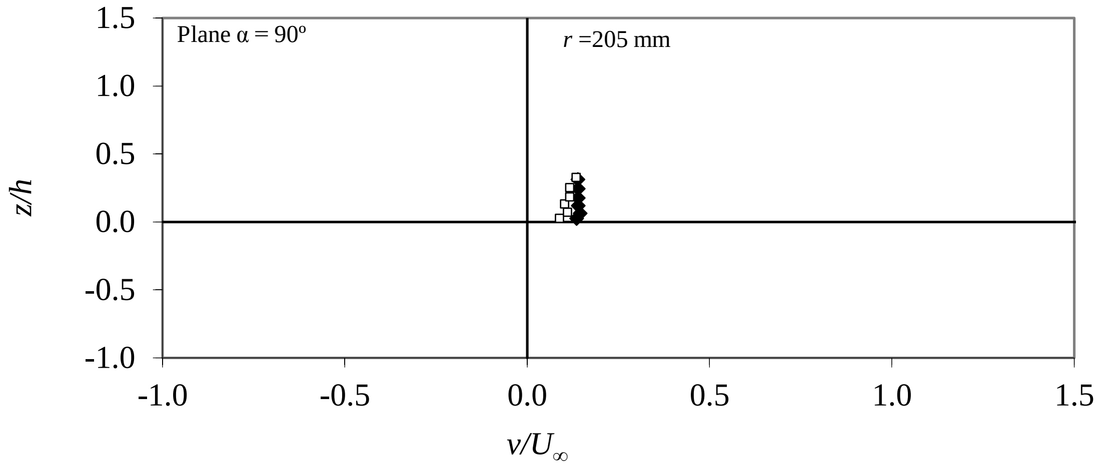

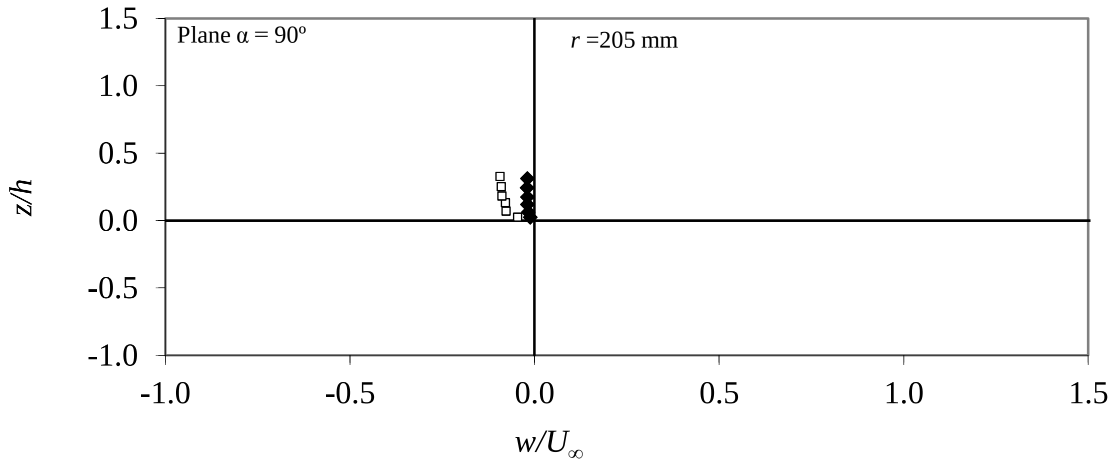

□: Isolated Pier, ♦: Effect of Second Pier at 3d Spacing

Fig 5.27 Effect of downstream pier on the velocity of upstream pier for comparison of normalised velocity component(α = 90° and r = 205 mm)

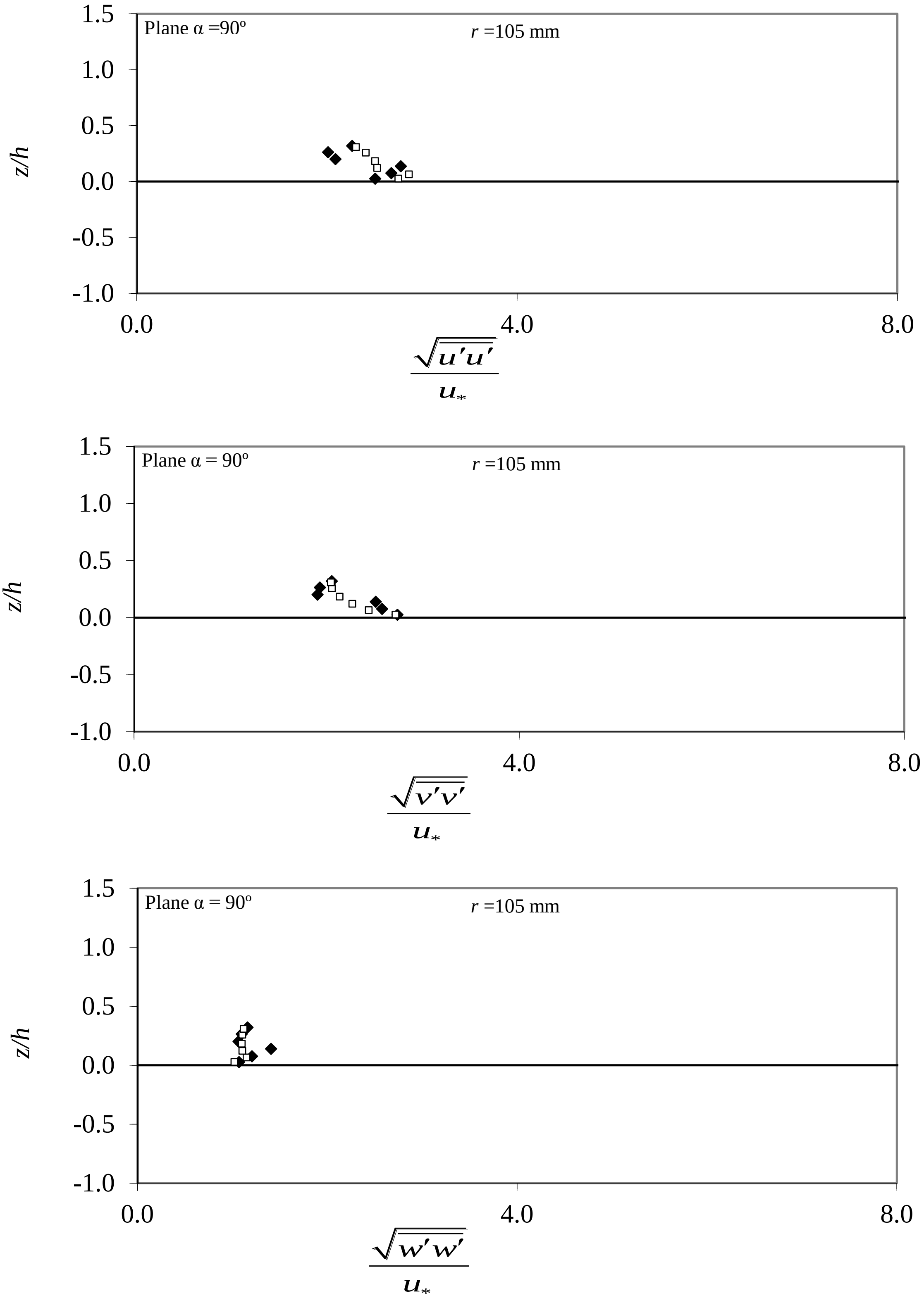

□: Isolated Pier, ♦: Effect of Second Pier at 3d Spacing

Fig 5.28 Effect of downstream pier on the velocity of upstream pier for comparison of normalised turbulence intensities (α = 90° and r = 105 mm)

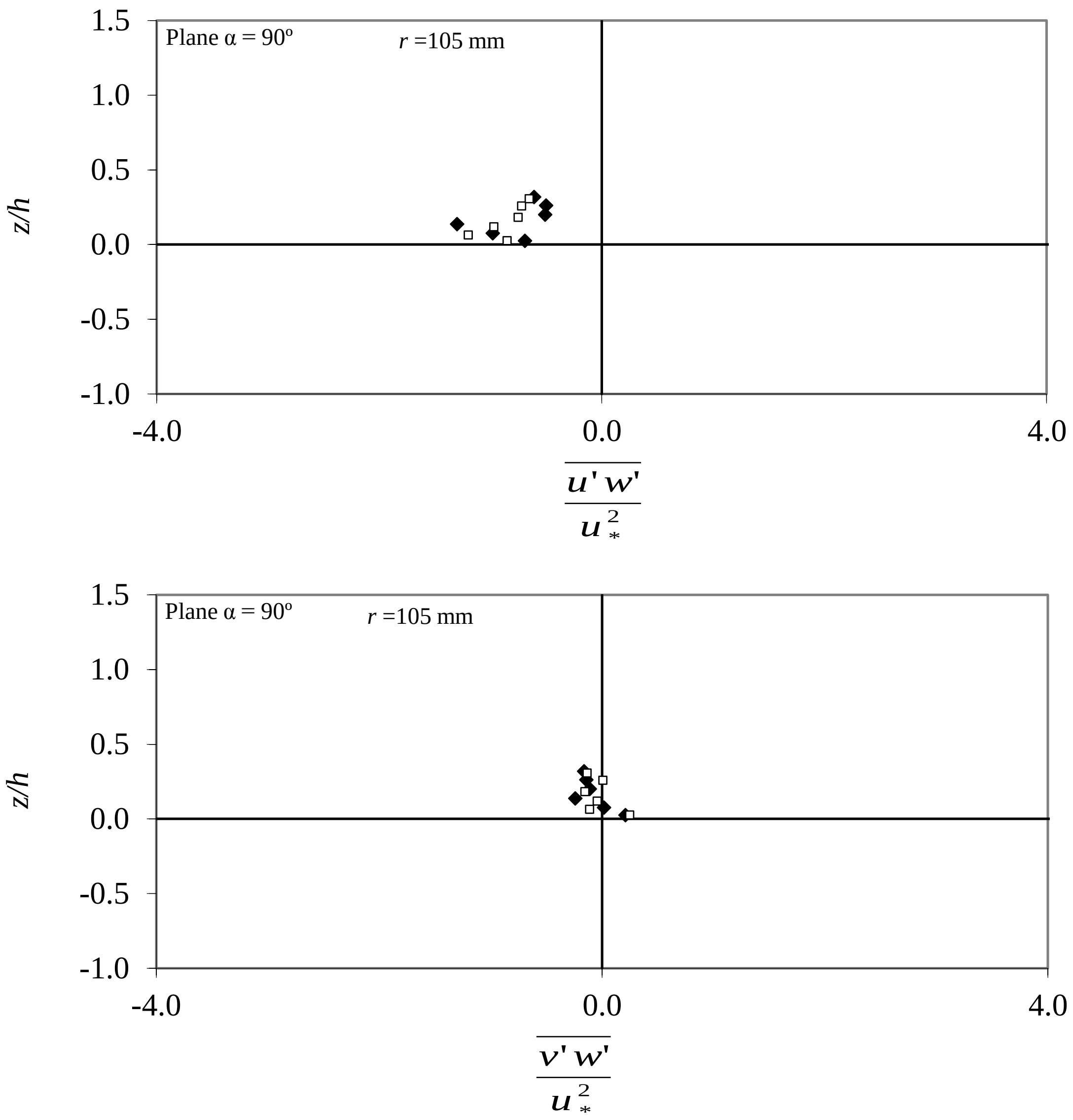

□: Isolated Pier, ♦: Effect of Second Pier at 3d Spacing

Fig 5.29 Effect of downstream pier on the velocity of upstream pier for comparison of normalised Reynolds's stresses (α = 90° and r = 105 mm)

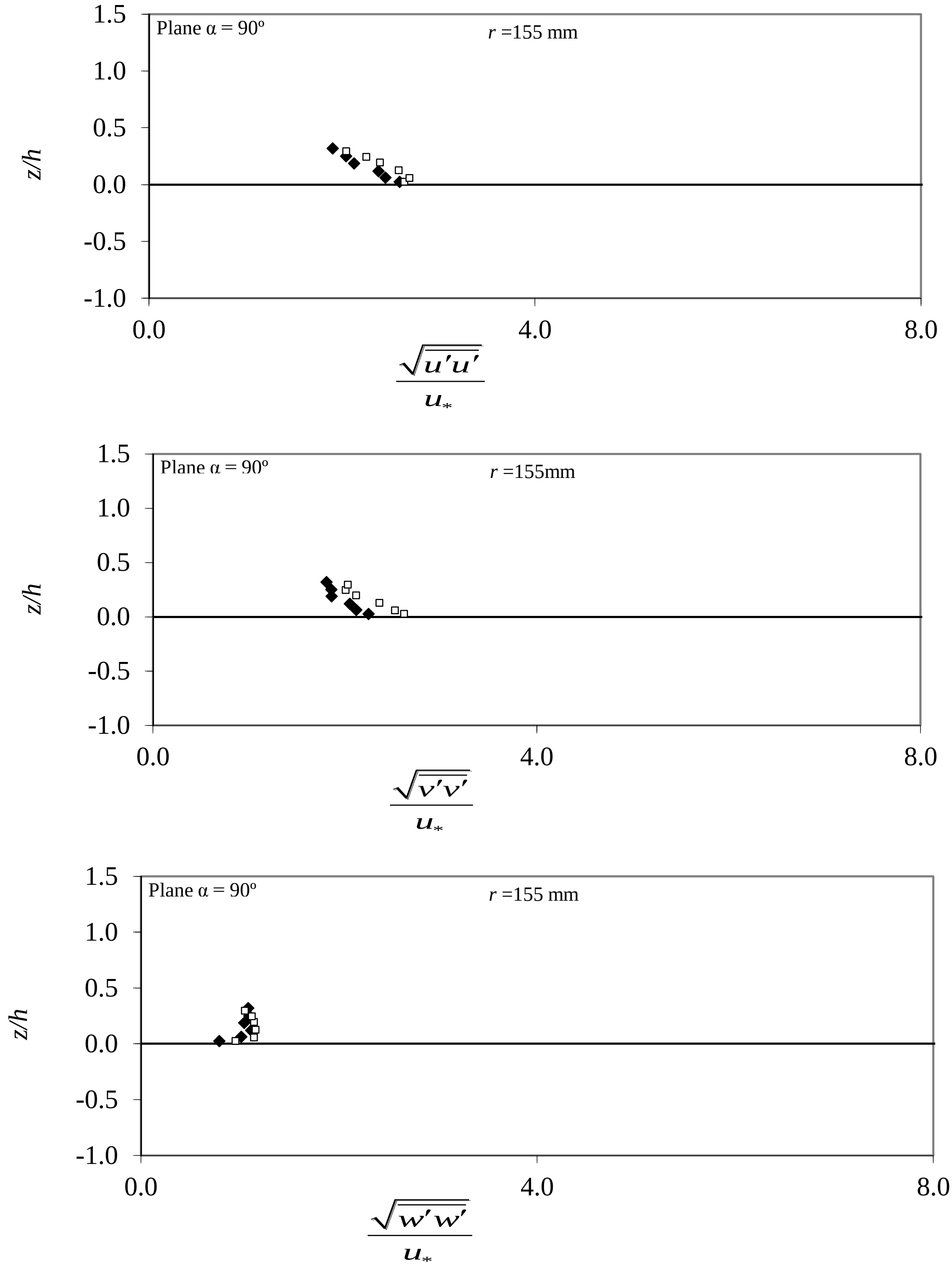

□: Isolated Pier, ♦: Effect of Second Pier at 3d Spacing

Fig 5.30 Effect of downstream pier on the velocity of upstream pier for comparison of normalised turbulence intensities (α = 90° and r = 155 mm)

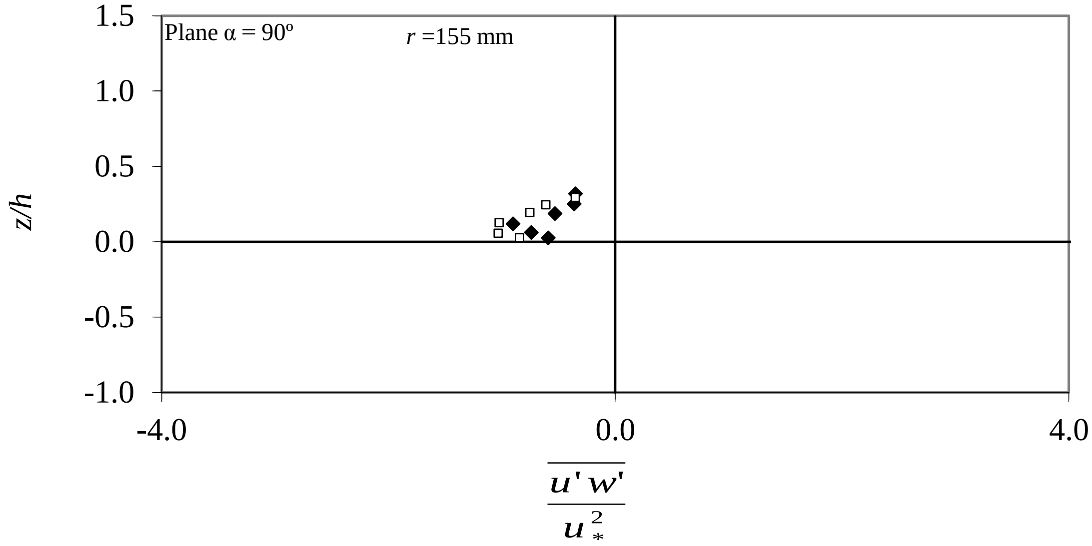

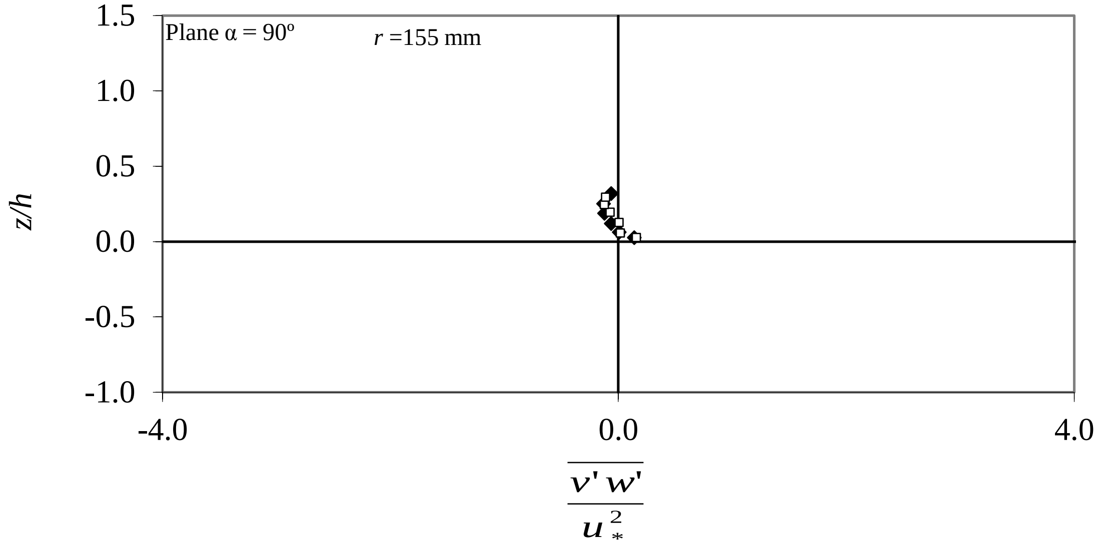

□: Isolated Pier, ♦: Effect of Second Pier at 3d Spacing

Fig 5.31 Effect of downstream pier on the velocity of upstream pier for comparison of normalised Reynolds's stresses (α = 90° and r = 155 mm)

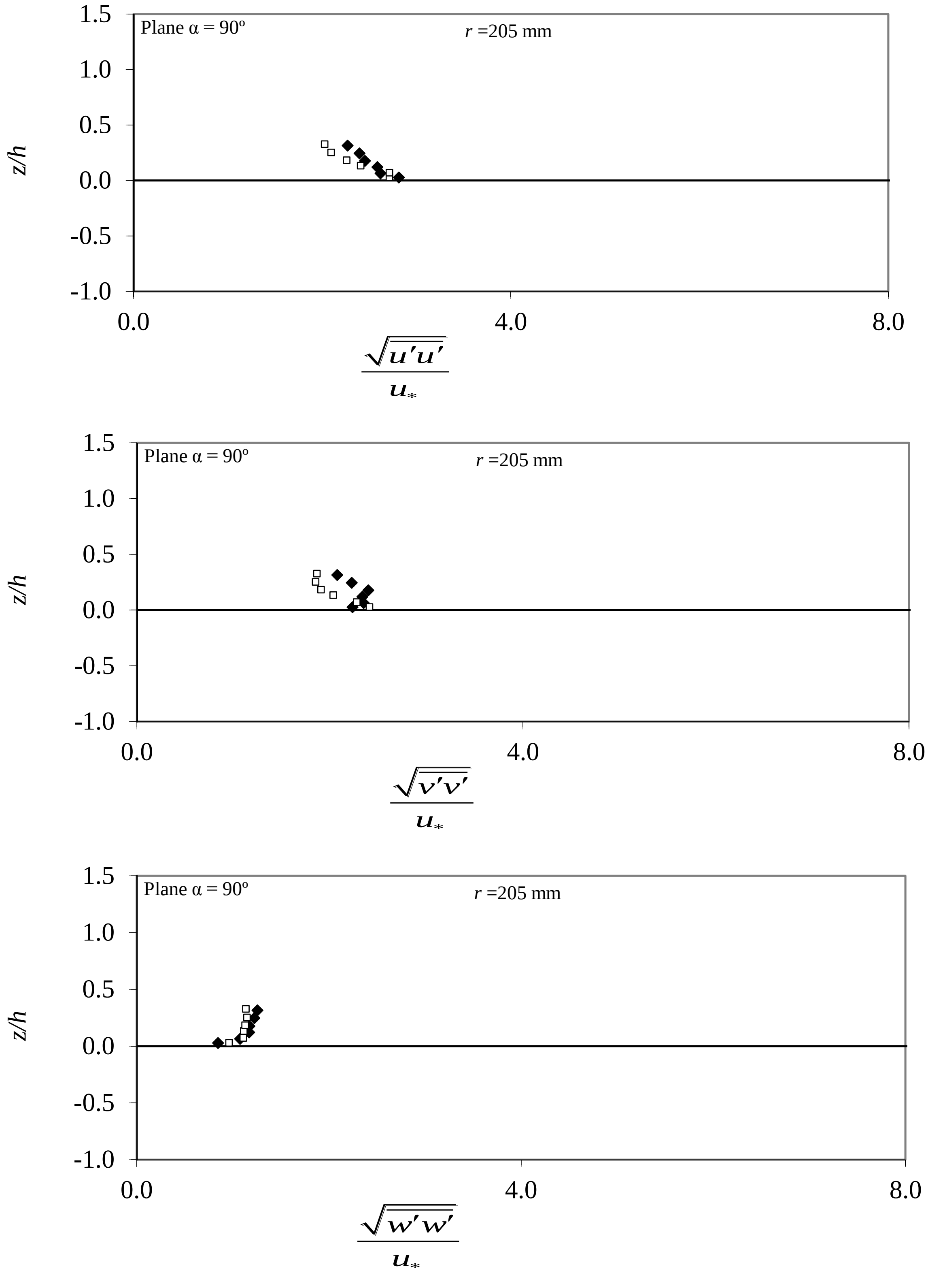

□: Isolated Pier, ♦: Effect of Second Pier at 3d Spacing

Fig 5.32 Effect of downstream pier on the velocity of upstream pier for comparison of normalised turbulence intensities (α = 90° and r = 205 mm)

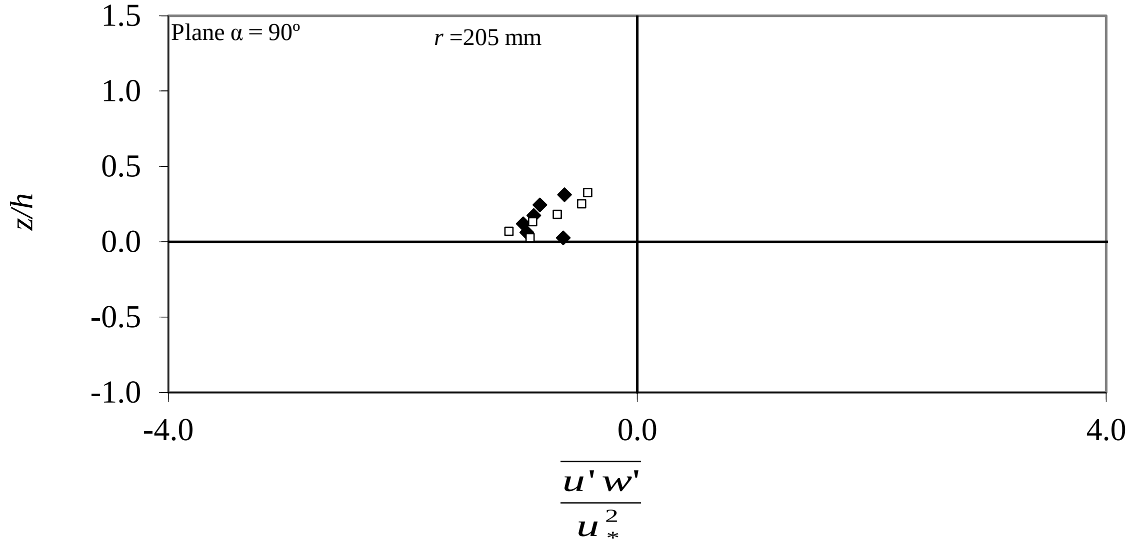

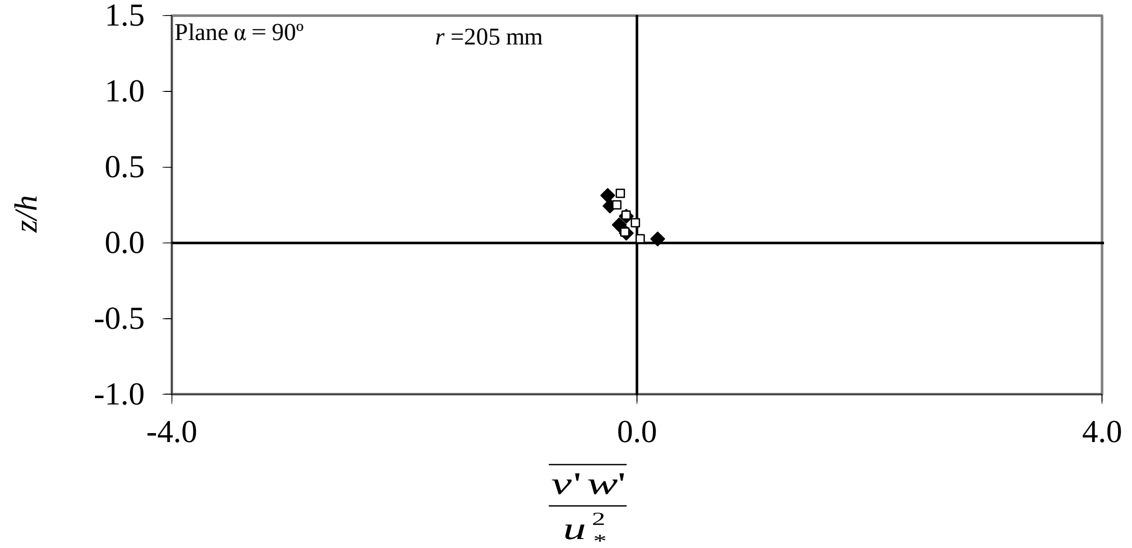

□: Isolated Pier, ♦: Effect of Second Pier at 3d Spacing

Fig 5.33 Effect of downstream pier on the velocity of upstream pier for comparison of normalised Reynolds's stresses (α = 90° and r = 205 mm)

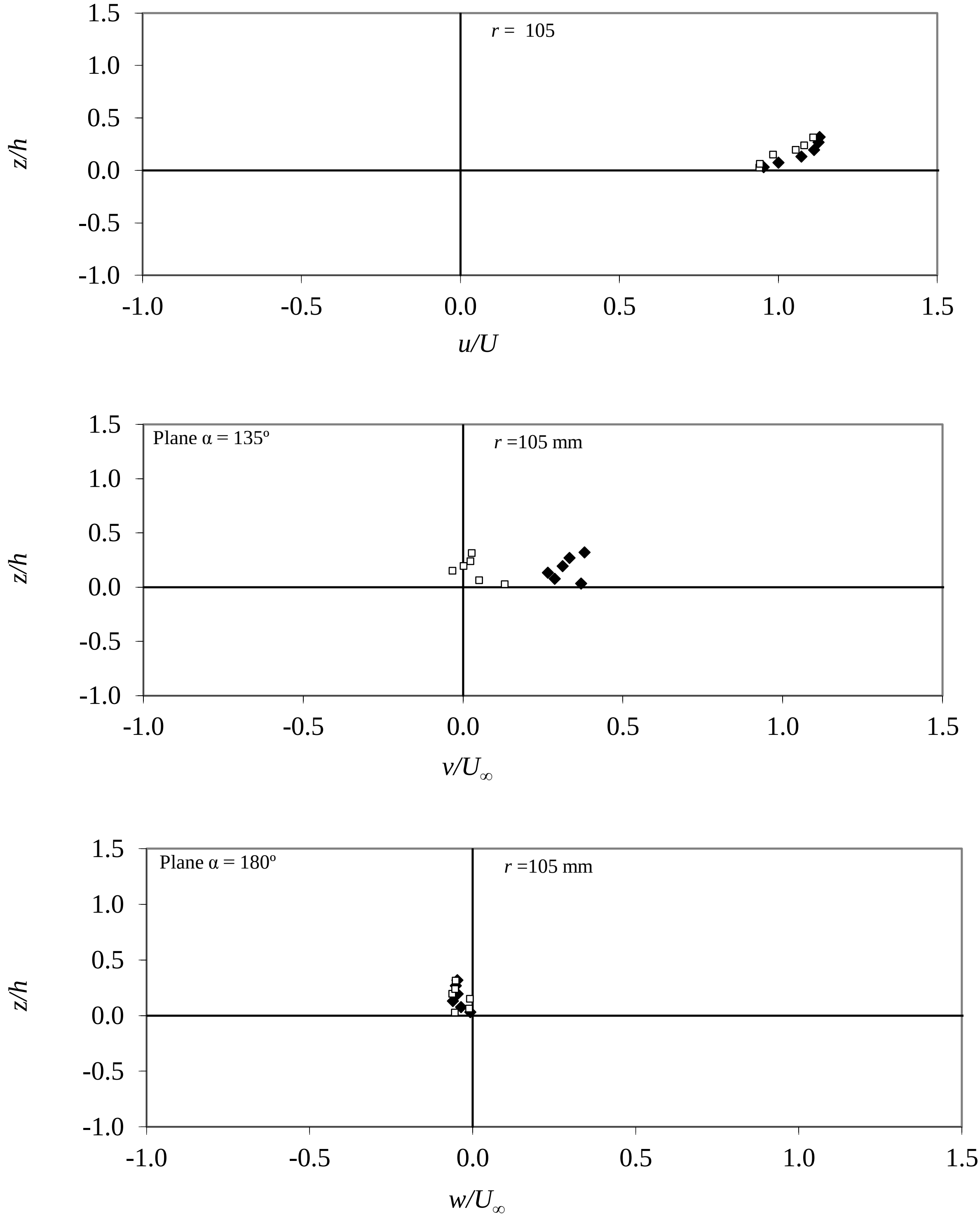

□: Isolated Pier, ♦: Effect of Second Pier at 3d Spacing

Fig 5.34 Effect of downstream pier on the velocity of upstream pier for comparison of normalised velocity components (α = 135° and r = 105 mm)

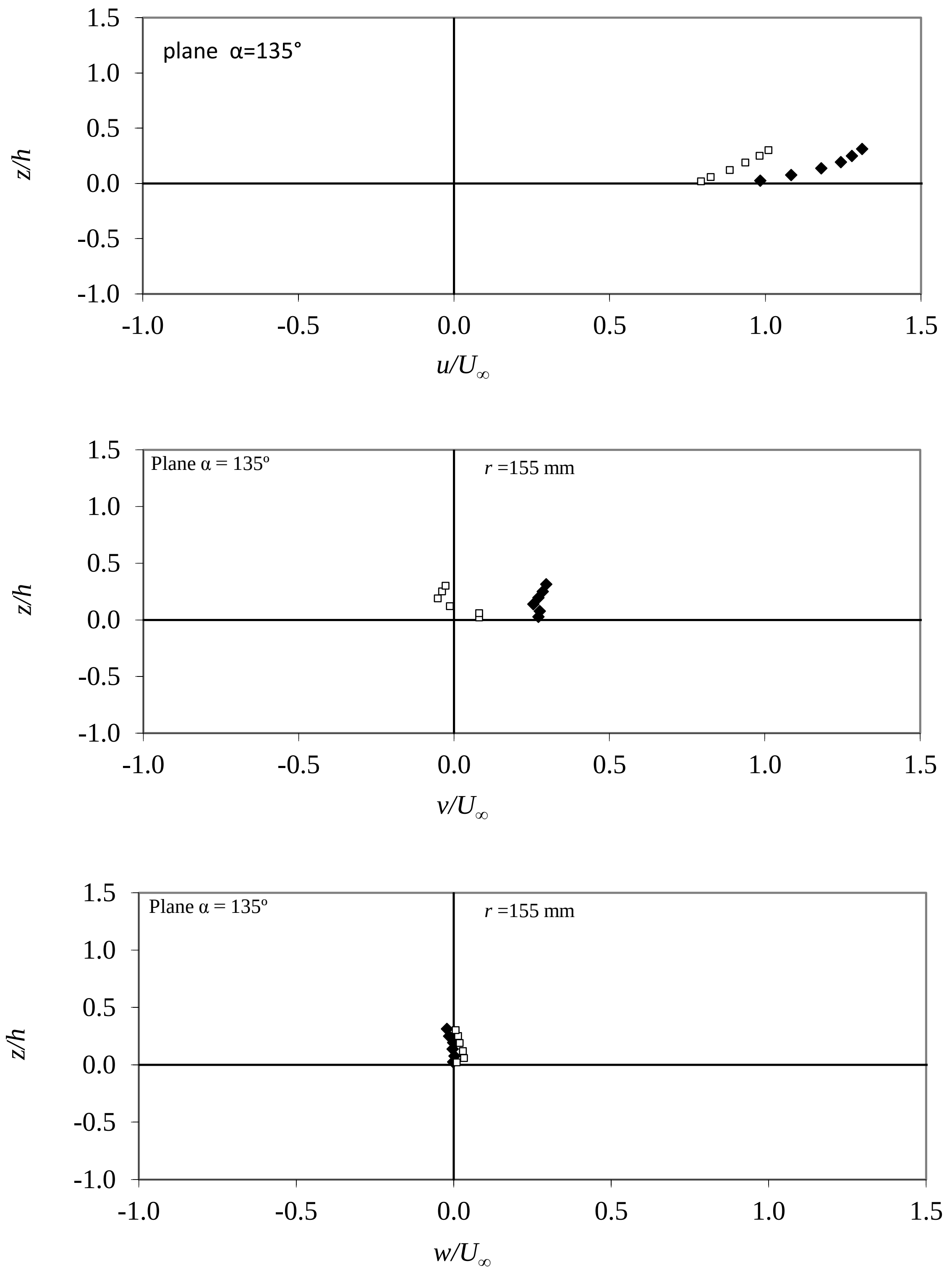

□: Isolated Pier, ♦: Effect of Second Pier at 3d Spacing

Fig 5.35 Effect of downstream pier on the velocity of upstream pier for comparison of normalised velocity components (α = 135° and r = 155 mm)

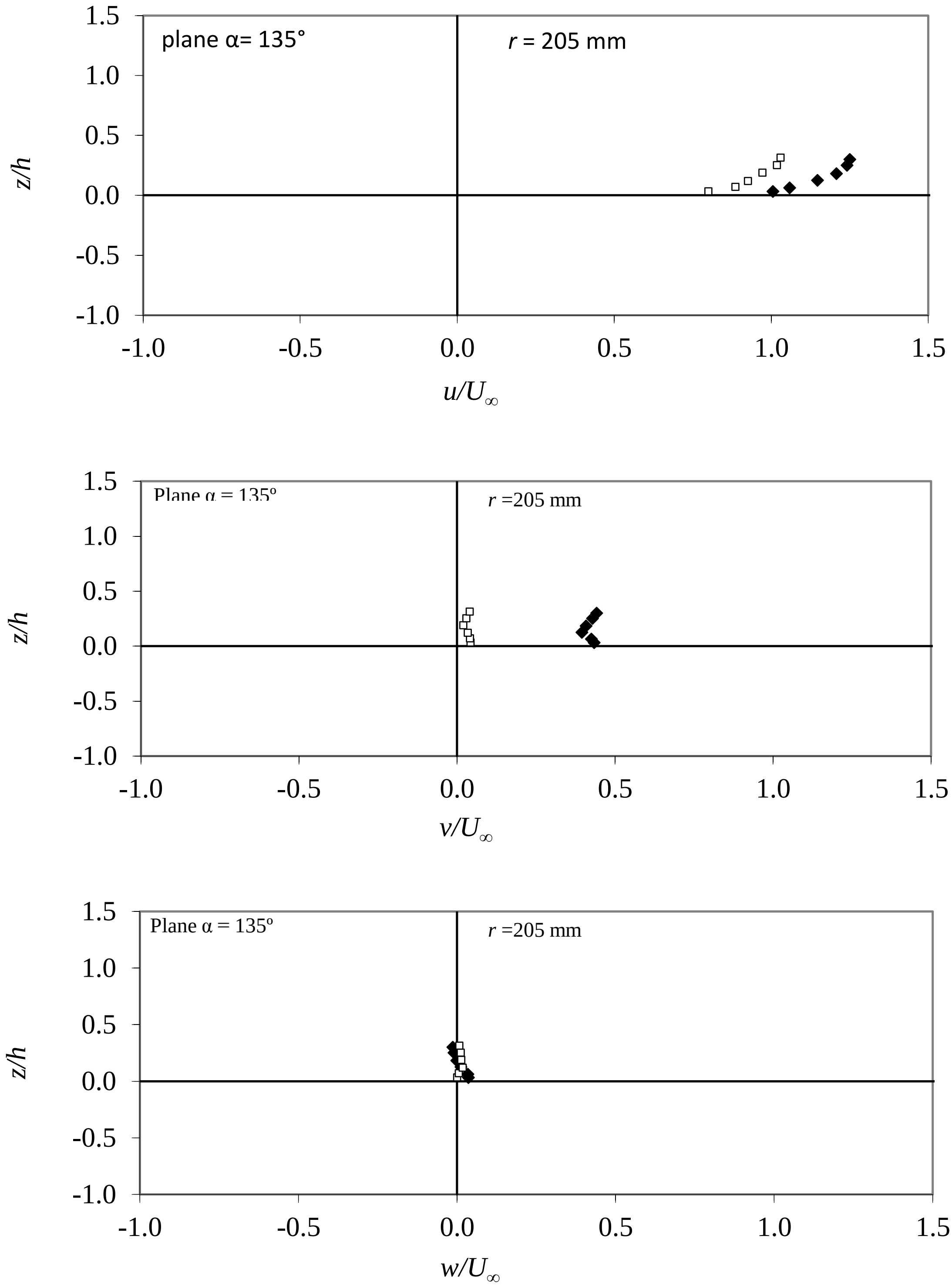

□: Isolated Pier, ♦: Effect of Second Pier at 3d Spacing

Fig 5.36 Effect of downstream pier on the velocity of upstream pier for comparison of normalised velocity components (α = 135° and r = 205 mm)

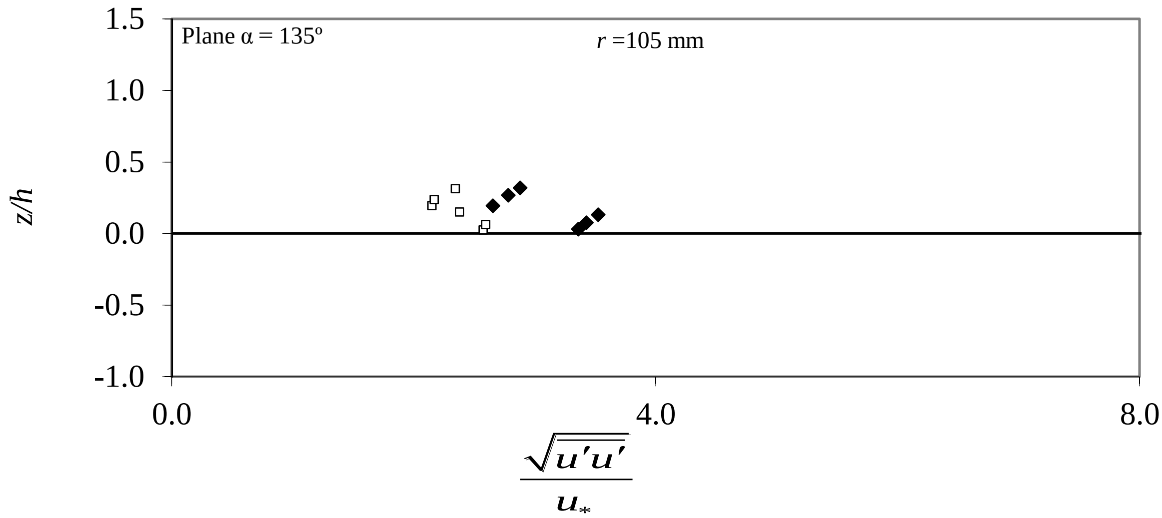

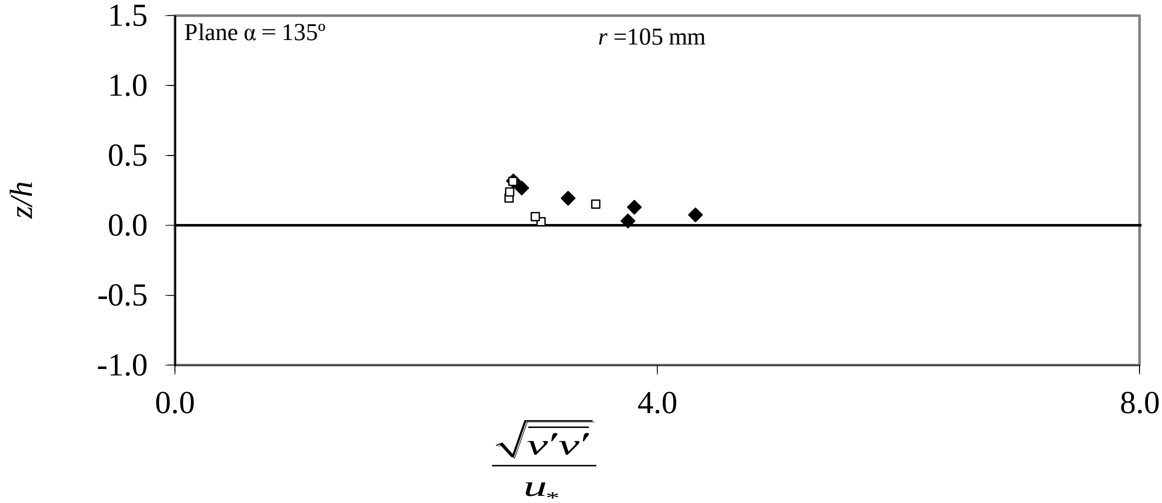

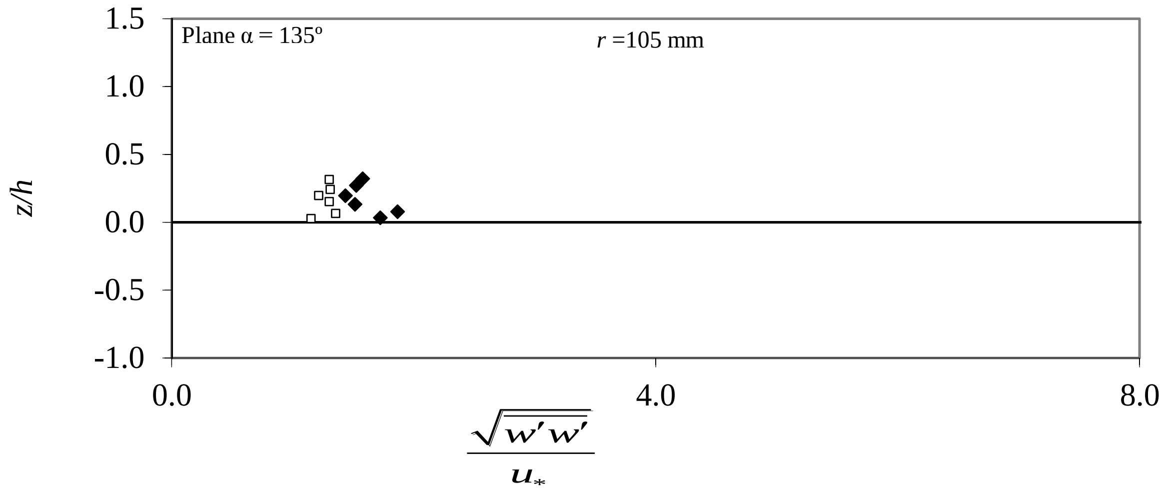

□: Isolated Pier, ♦: Effect of Second Pier at 3d Spacing

Fig 5.37 Effect of downstream pier on the velocity of upstream pier for comparison of normalised turbulence intensities (α = 135° and r = 105 mm)

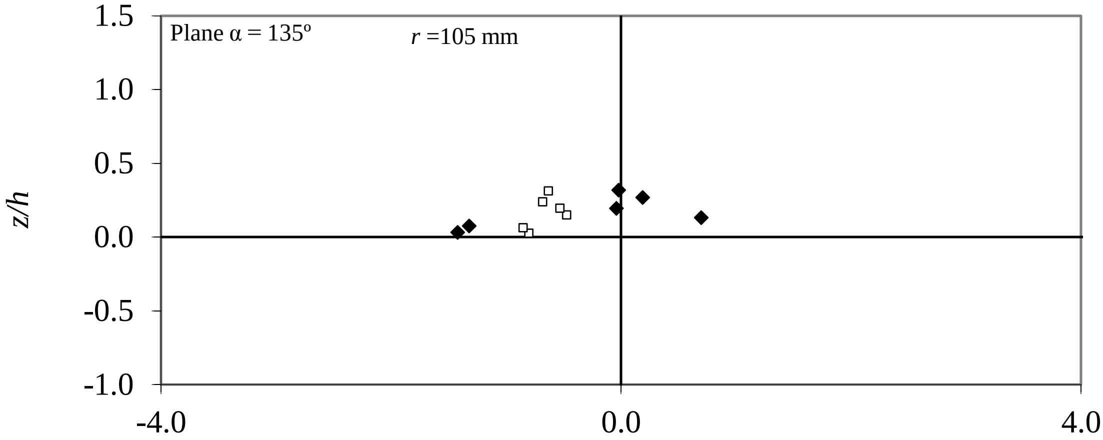

$$\frac{\overline{u'w'}}{u_*^2}$$

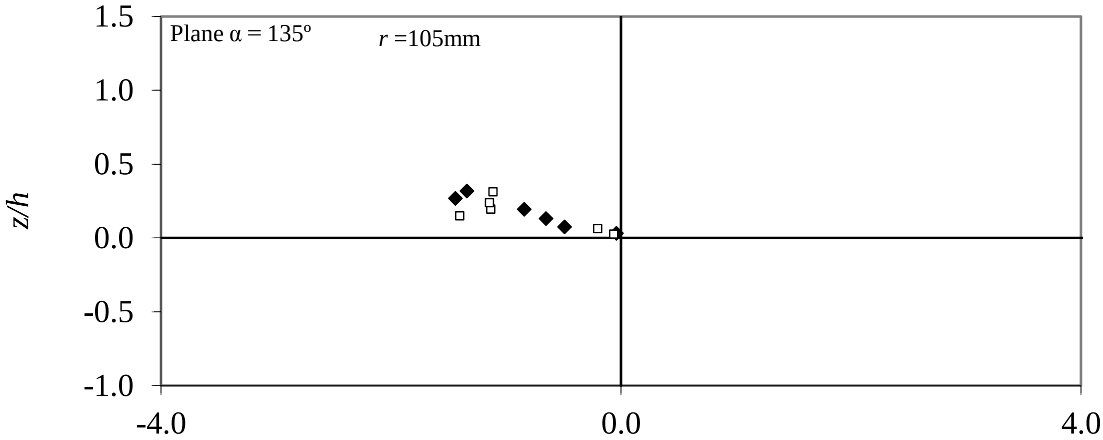

$$\frac{\overline{v'w'}}{u_*^2}$$

□: Isolated Pier, ♦: Effect of Second Pier at 3d Spacing

Fig 5.38 Effect of downstream pier on the velocity of upstream pier for comparison of normalised Reynolds's stresses (α = 135° and r = 105 mm)

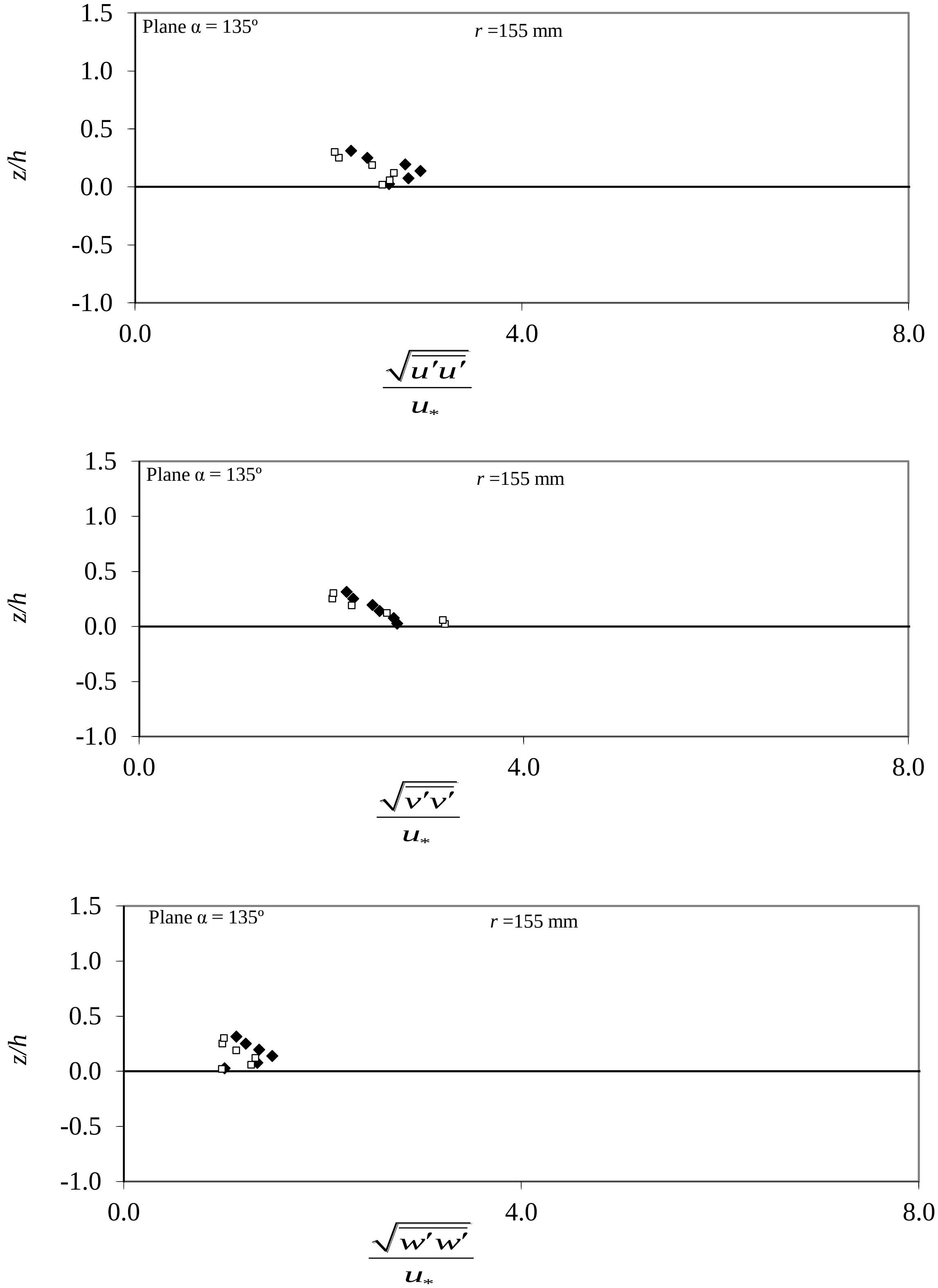

□: Isolated Pier, ♦: Effect of Second Pier at 3d Spacing

Fig 5.39 Effect of downstream pier on the velocity of upstream pier for comparison of normalised turbulence intensities (α = 135° and r = 155 mm)

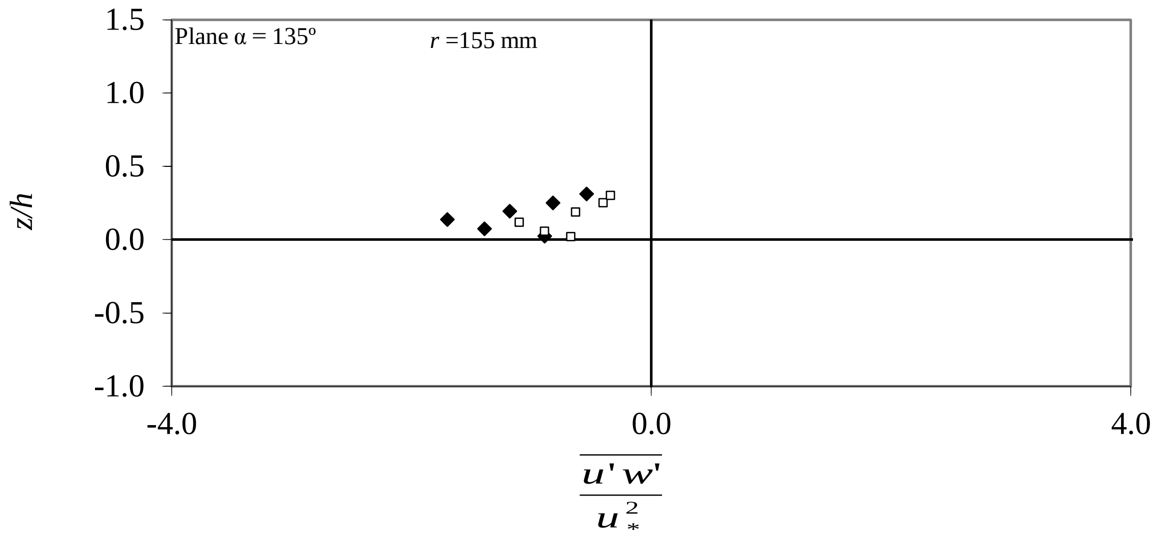

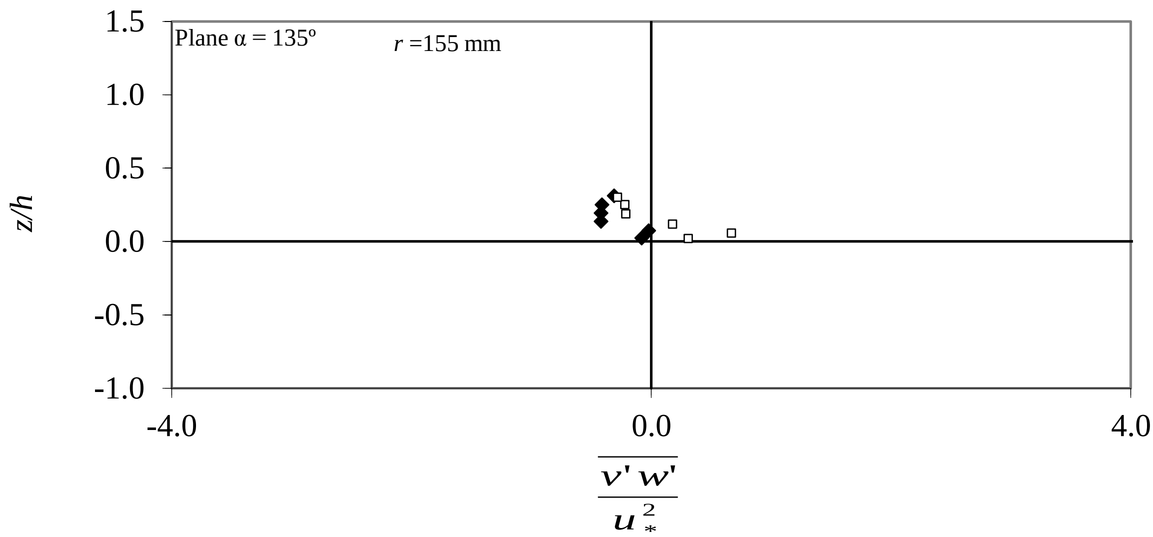

□: Isolated Pier, ♦: Effect of Second Pier at 3d Spacing

Fig 5.40 Effect of downstream pier on the velocity of upstream pier for comparison of normalised Reynolds's stresses (α = 135° and r = 155 mm)

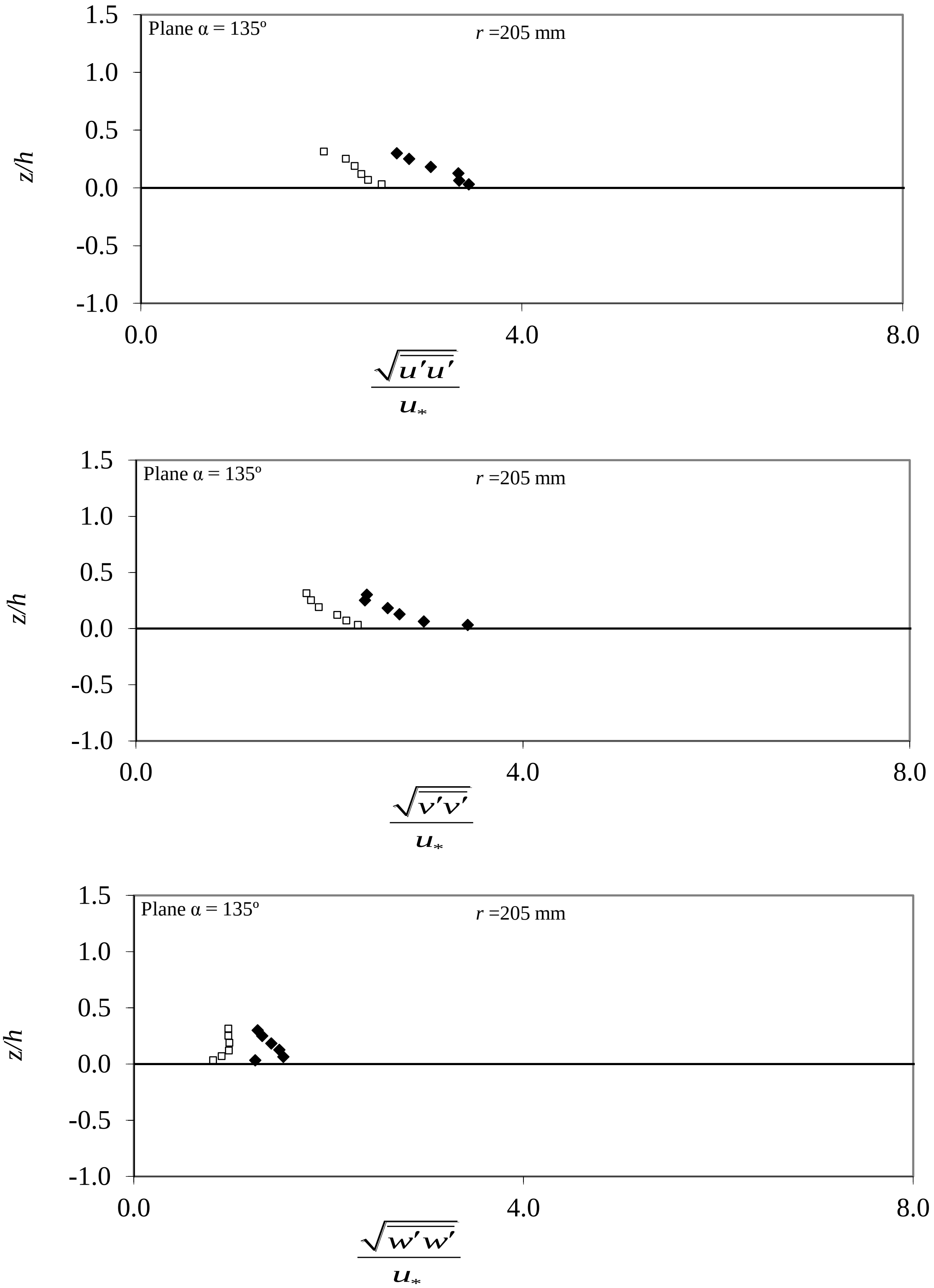

□: Isolated Pier, ♦: Effect of Second Pier at 3d Spacing

Fig 5.41 Effect of downstream pier on the velocity of upstream pier for comparison of normalised turbulence intensities (α = 135° and r = 205 mm)

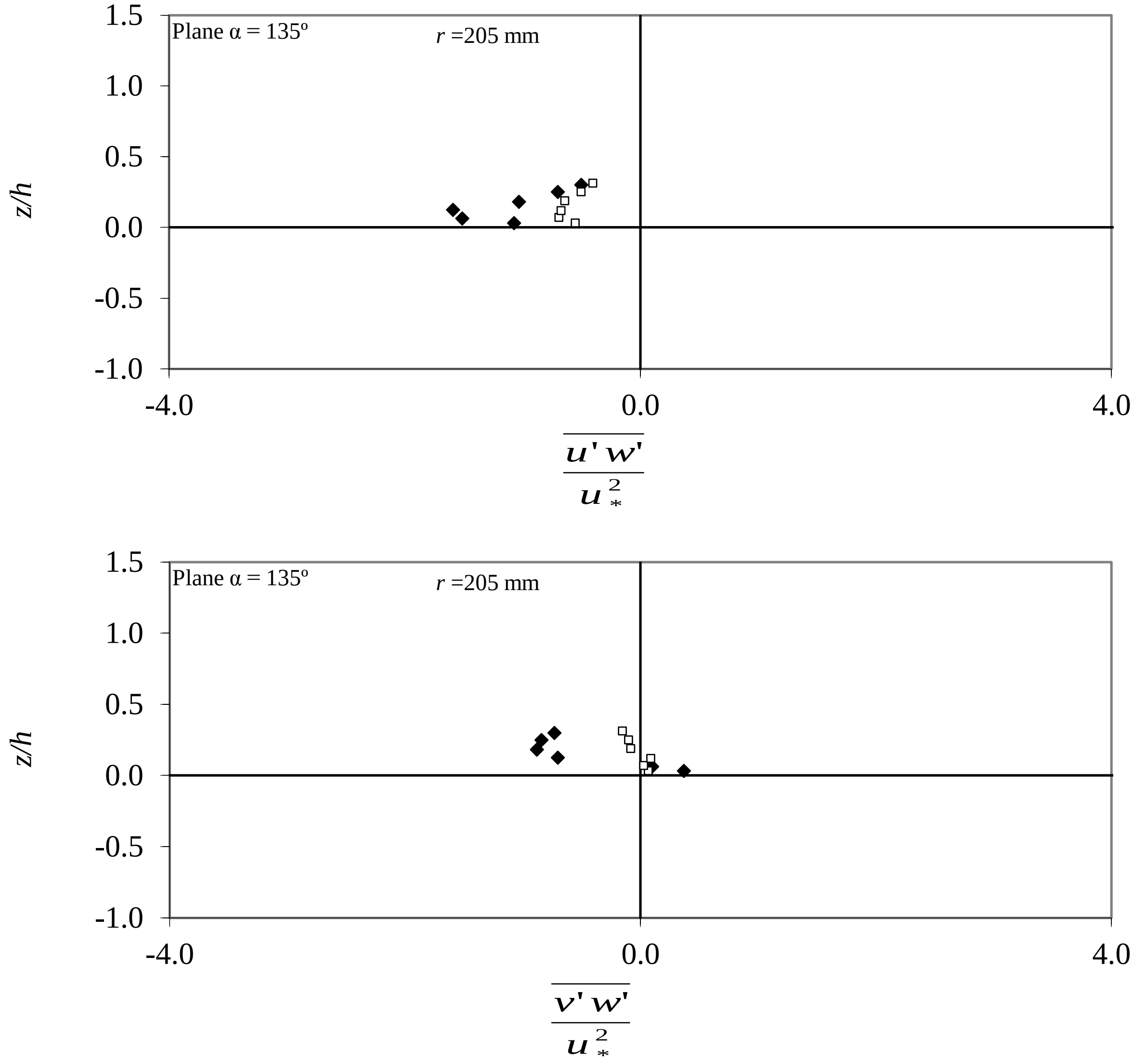

□: Isolated Pier, ♦: Effect of Second Pier at 3d Spacing

Fig 5.42 Effect of downstream pier on the velocity of upstream pier for comparison of normalised Reynolds's stresses (α = 135° and r = 205 mm)

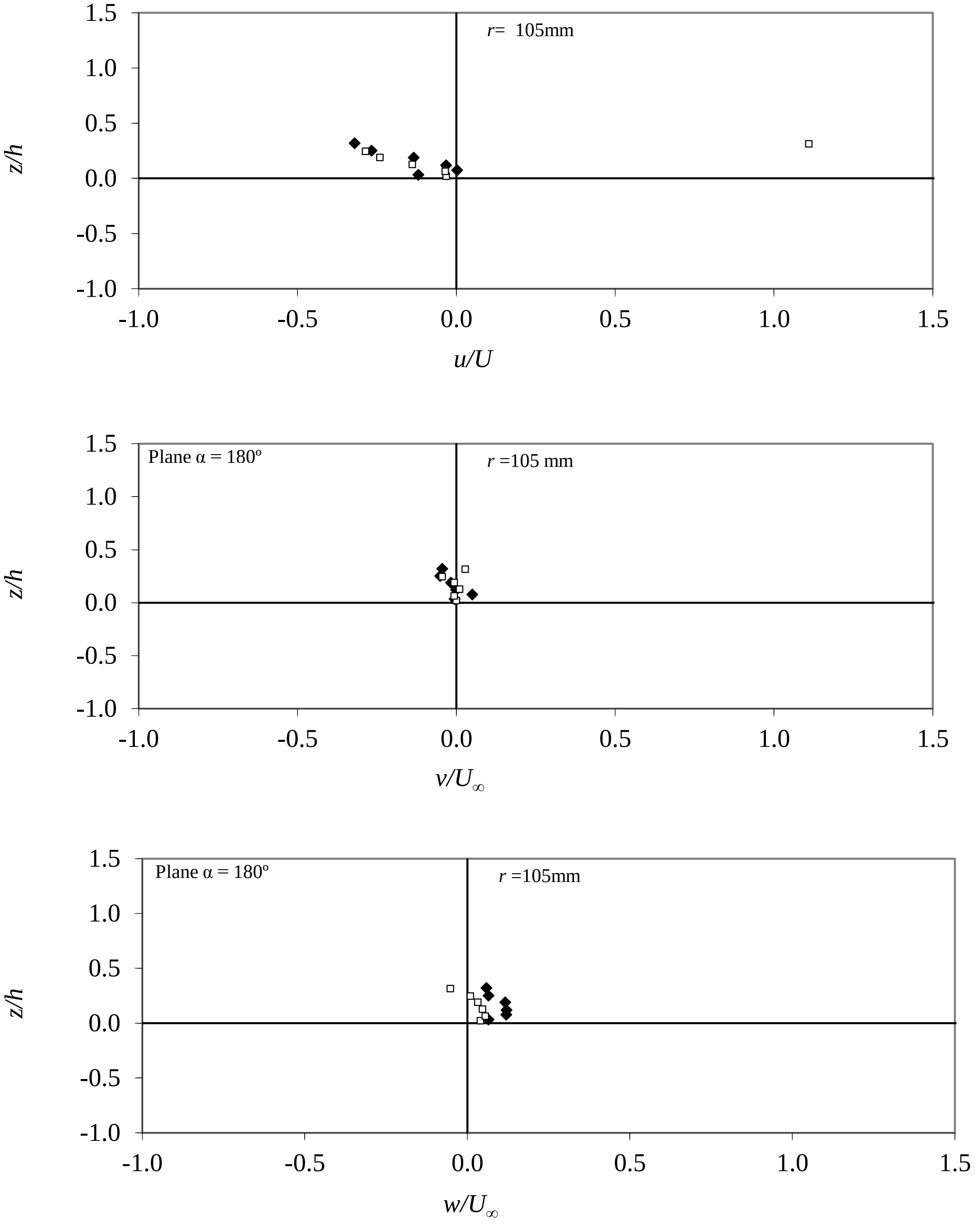

□: Isolated Pier, ♦: Effect of Second Pier at 3d Spacing

Fig 5.43 Effect of downstream pier on the velocity of upstream pier for comparison of normalised velocity components (α = 180° and r = 105 mm)

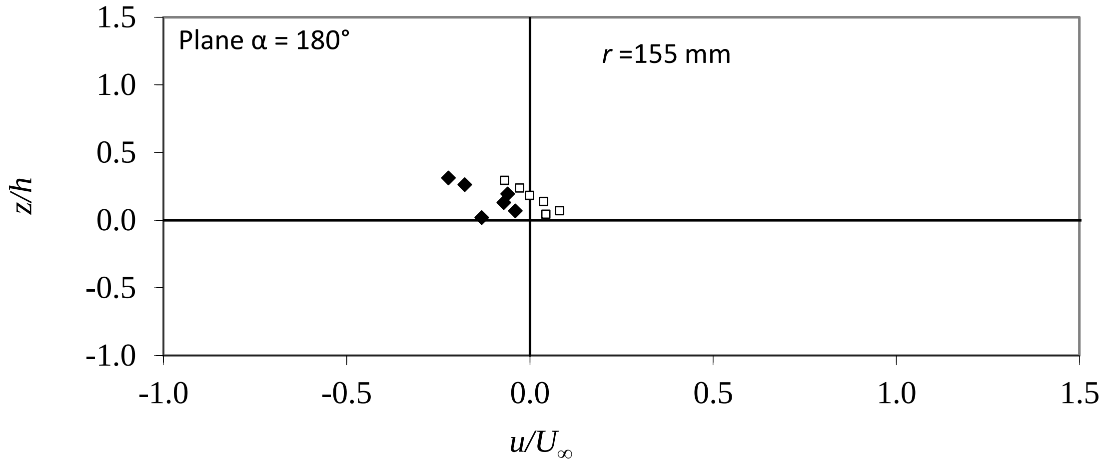

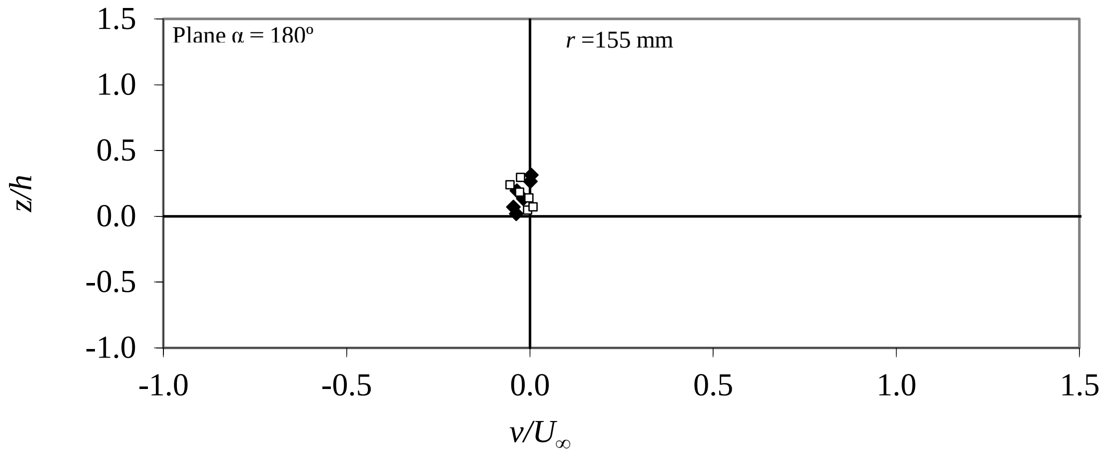

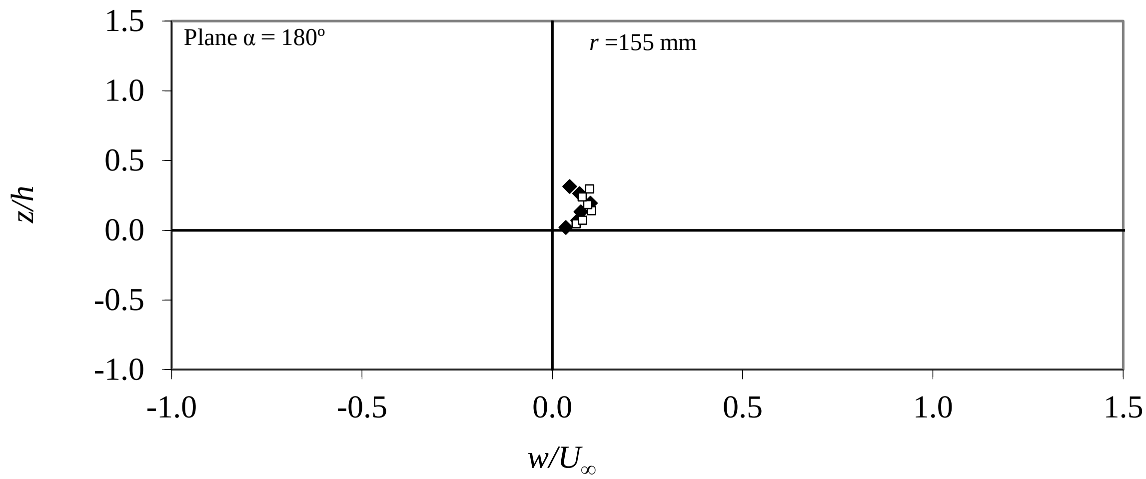

□: Isolated Pier, ♦: Effect of Second Pier at 3d Spacing

Fig 5.44 Effect of downstream pier on the velocity of upstream pier for comparison of normalised velocity components (α = 180° and r = 155 mm)

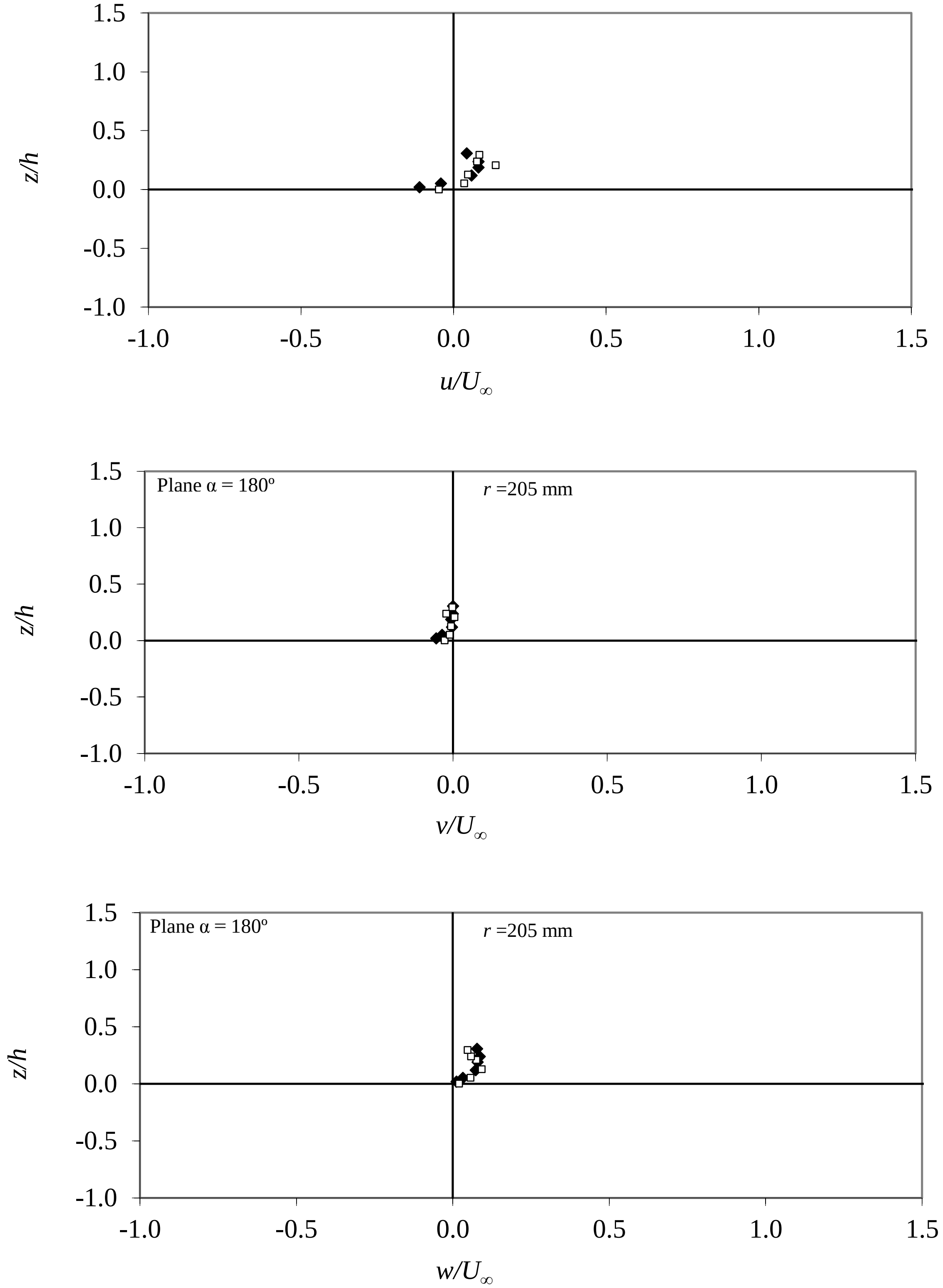

□: Isolated Pier, ♦: Effect of Second Pier at 3d Spacing

Fig 5.45 Effect of downstream pier on the velocity of upstream pier for comparison of normalised velocity components (α = 180° and r = 205 mm)

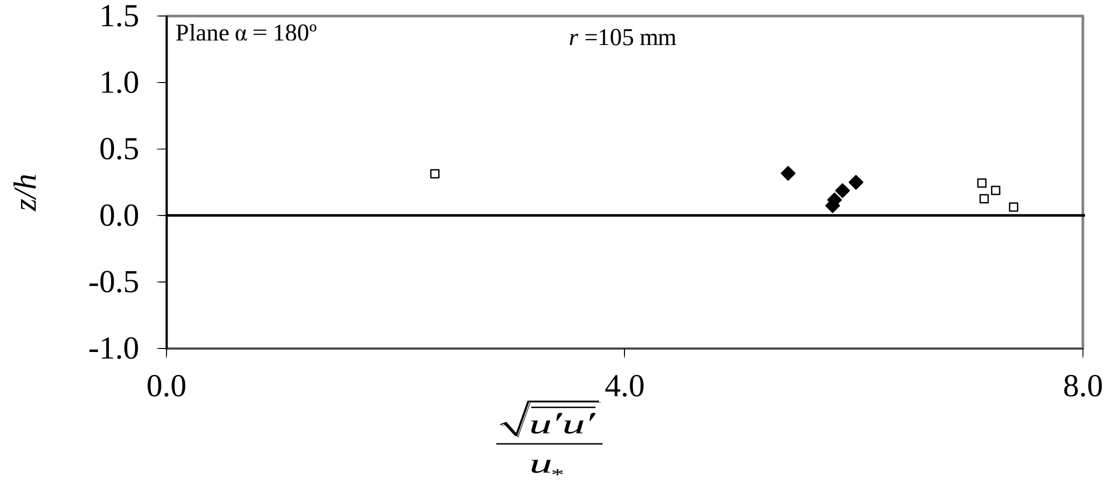

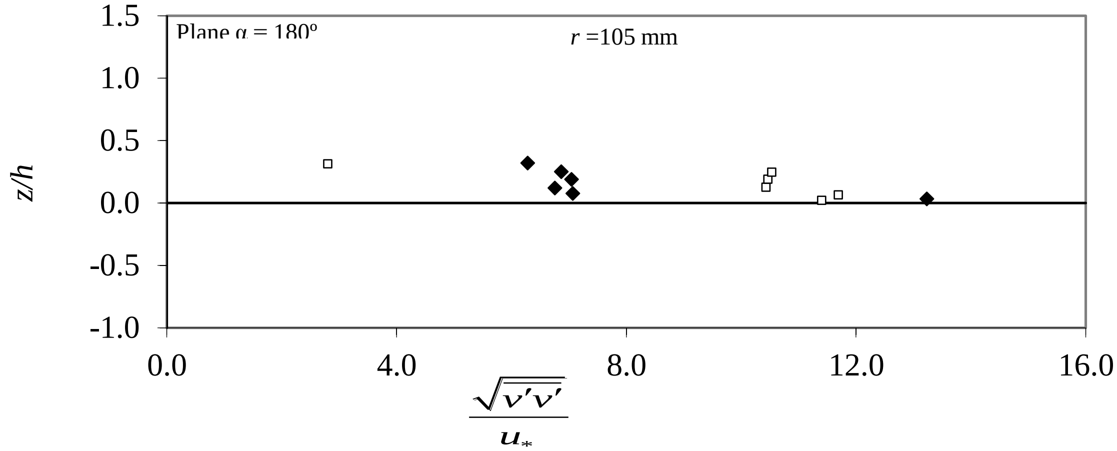

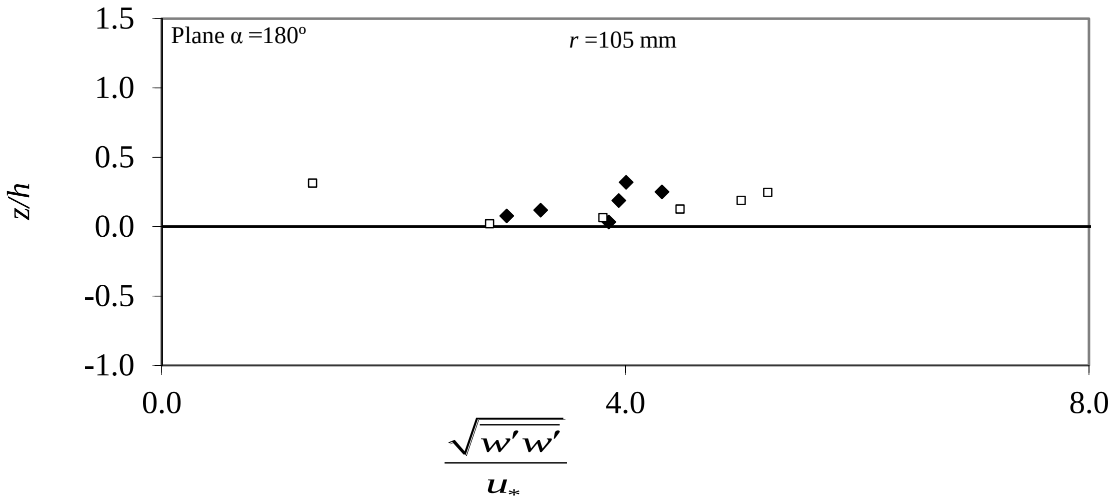

□: Isolated Pier, ♦: Effect of Second Pier at 3d Spacing

Fig 5.46 Effect of downstream pier on the velocity of upstream pier for comparison of normalised turbulence intensities (α = 180° and r = 105 mm)

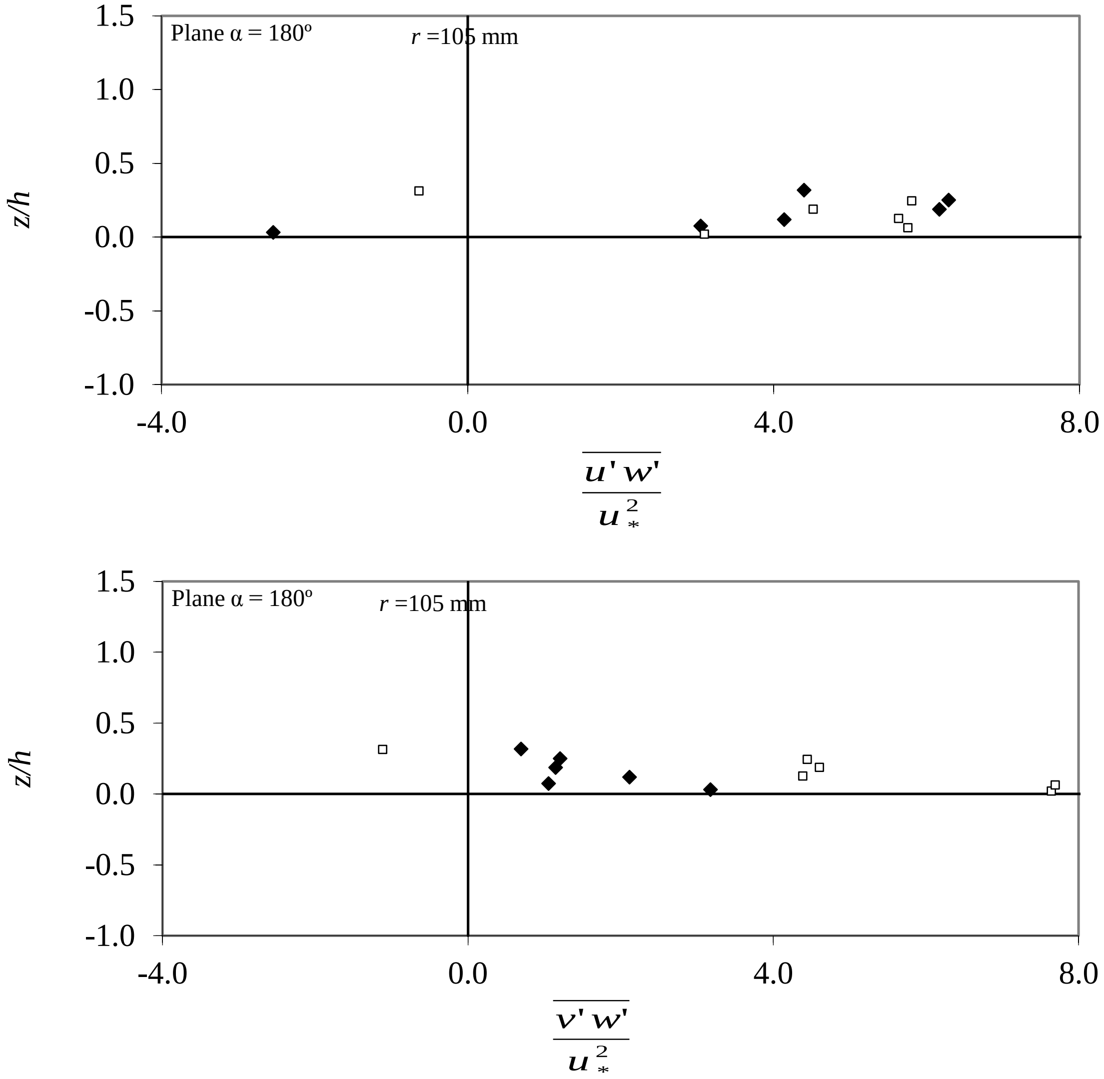

□: Isolated Pier, ♦: Effect of Second Pier at 3d Spacing

Fig 5.47 Effect of downstream pier on the velocity of upstream pier for comparison of normalised Reynolds's stresses (α = 180° and r = 105 mm)

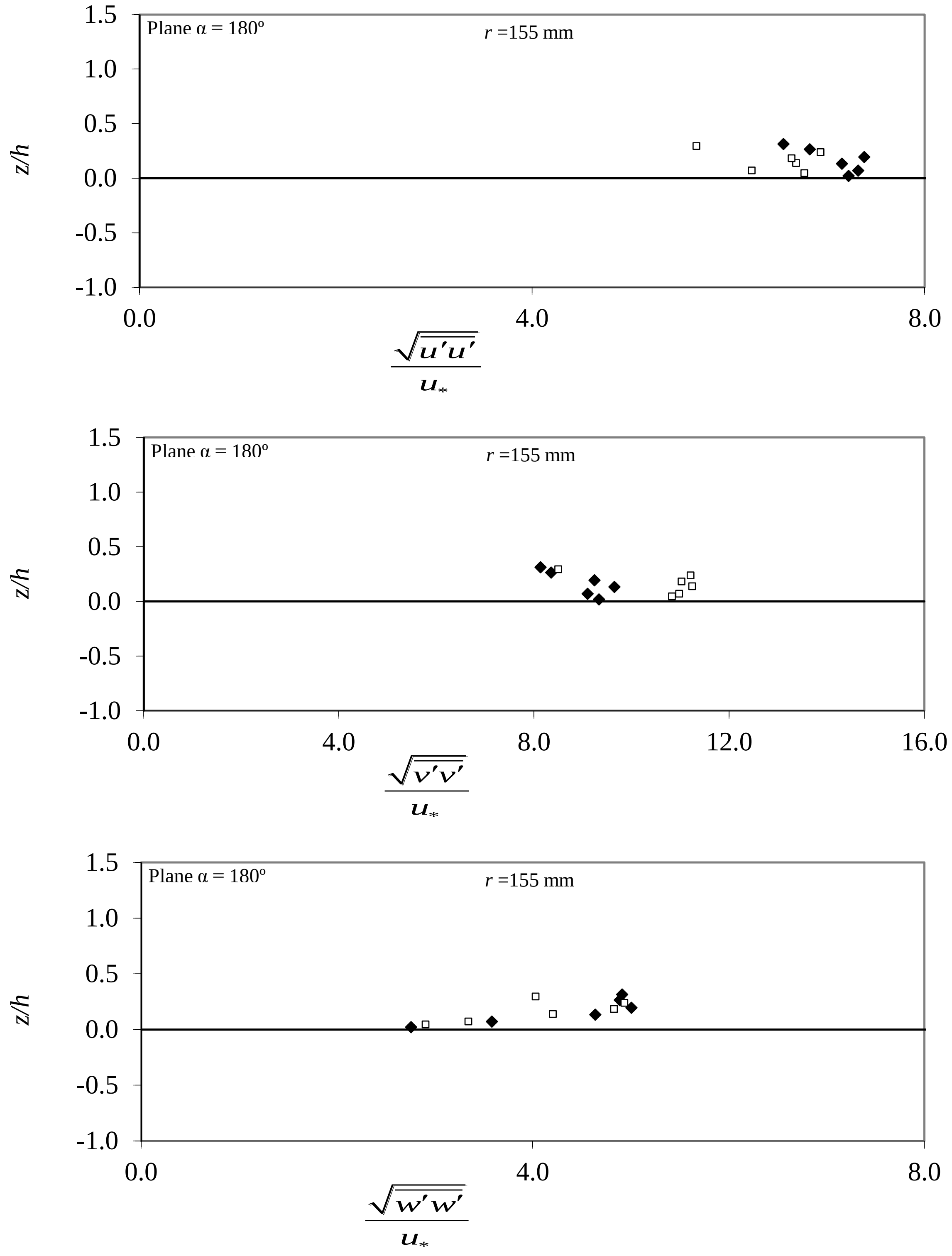

□: Isolated Pier, ♦: Effect of Second Pier at 3d Spacing

Fig 5.48 Effect of downstream pier on the velocity of upstream pier for comparison of normalised turbulence intensities (α = 180° and r = 155 mm)

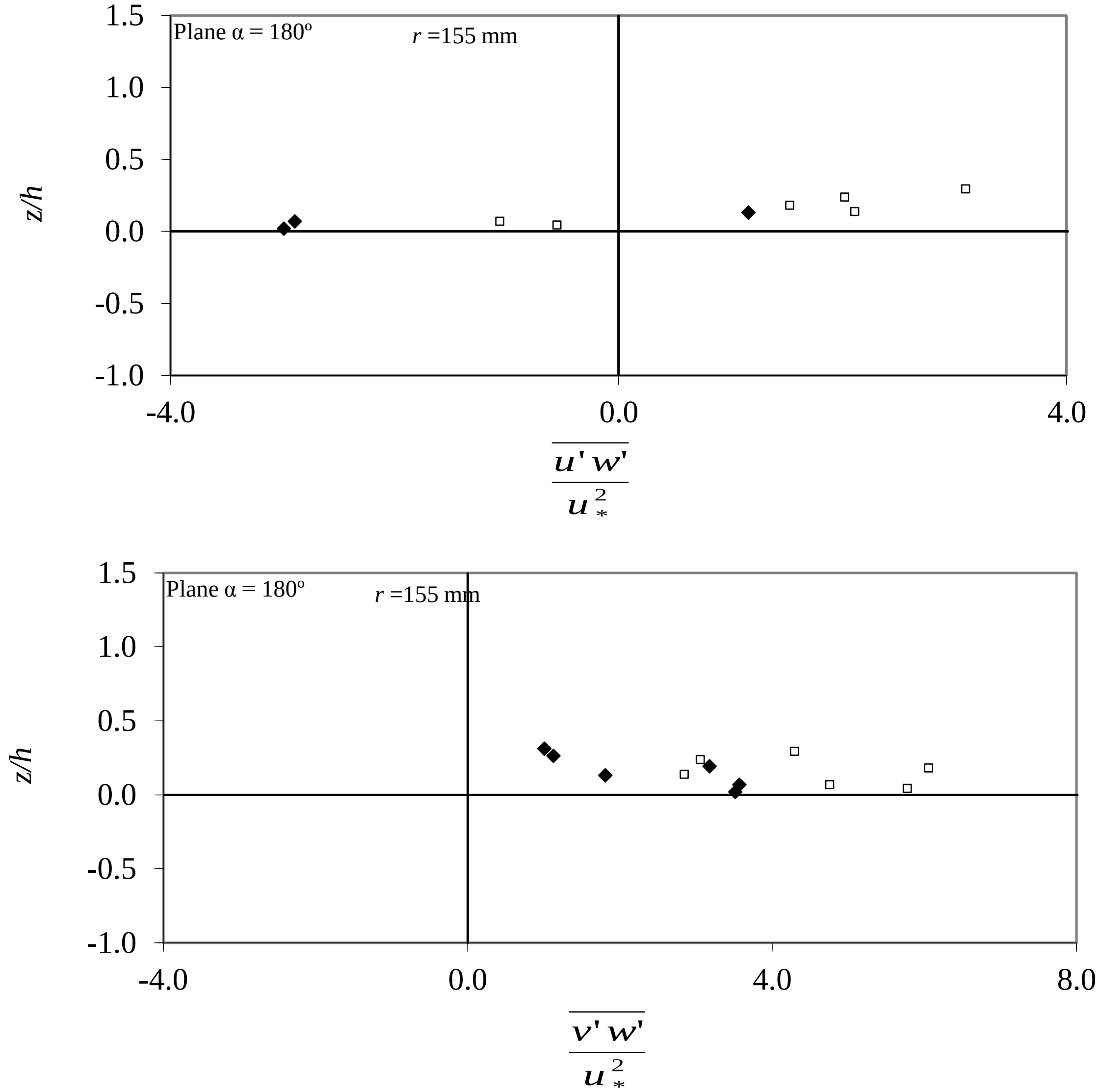

□: Isolated Pier, ♦: Effect of Second Pier at 3d Spacing

Fig 5.49 Effect of downstream pier on the velocity of upstream pier for comparison of normalised Reynolds's stresses (α = 180° and r = 155 mm)

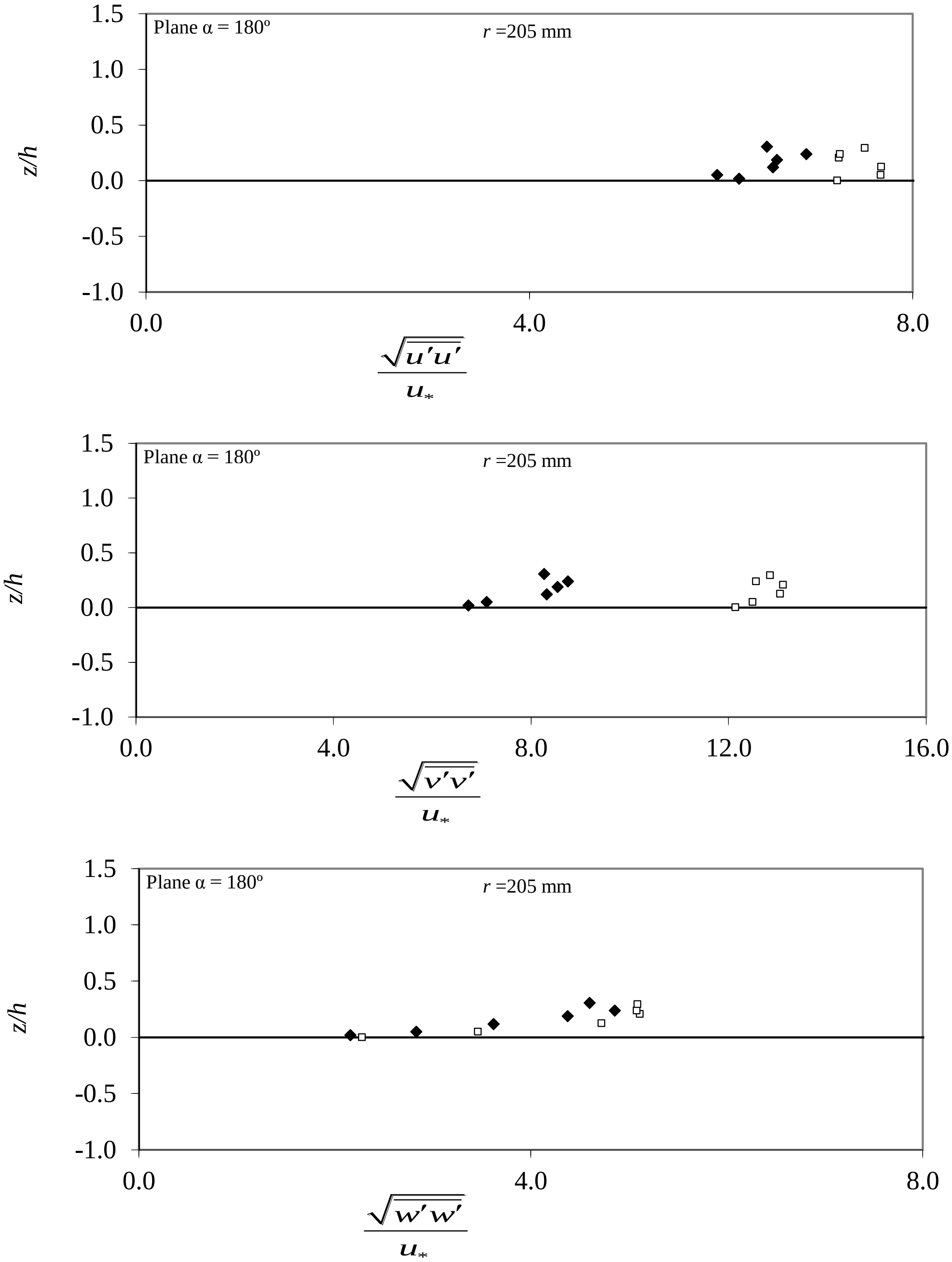

□: Isolated Pier, ♦: Effect of Second Pier at 3d Spacing

Fig 5.50 Effect of downstream pier on the velocity of upstream pier for comparison of normalised turbulence intensities (α = 180° and r = 205 mm)

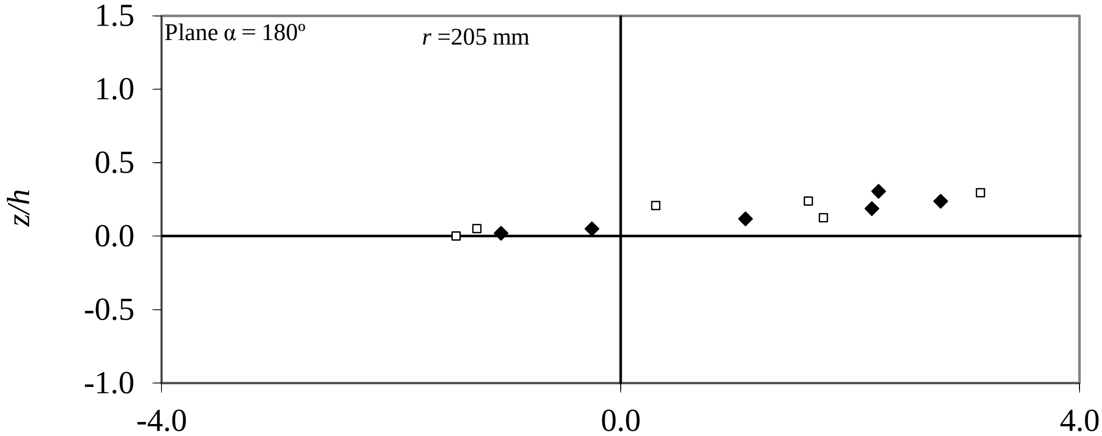

$$\frac{\overline{u'w'}}{u_*^2}$$

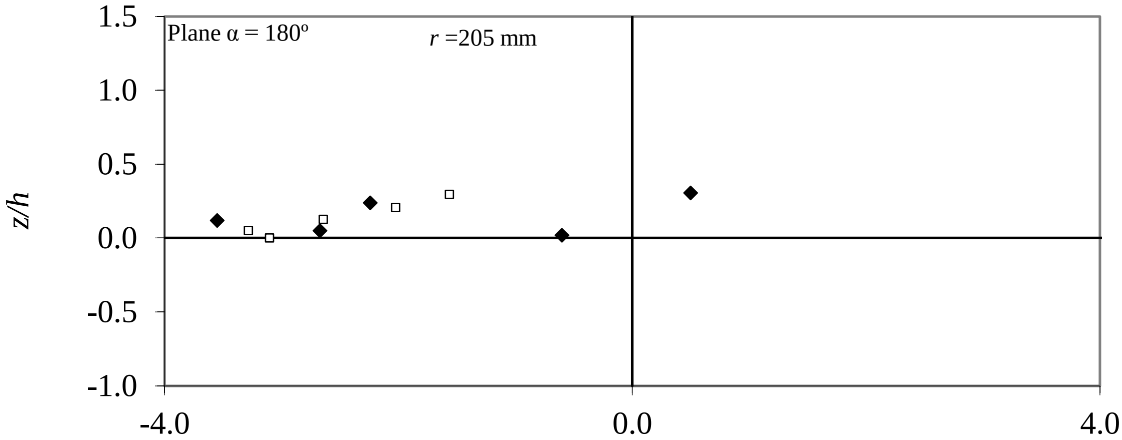

$$\frac{\overline{v'w'}}{u_*^2}$$

□: Isolated Pier, ♦: Effect of Second Pier at 3d Spacing

Fig 5.51 Effect of downstream pier on the velocity of upstream pier for comparison of normalised Reynolds's stresses (α = 180° and r = 205 mm)

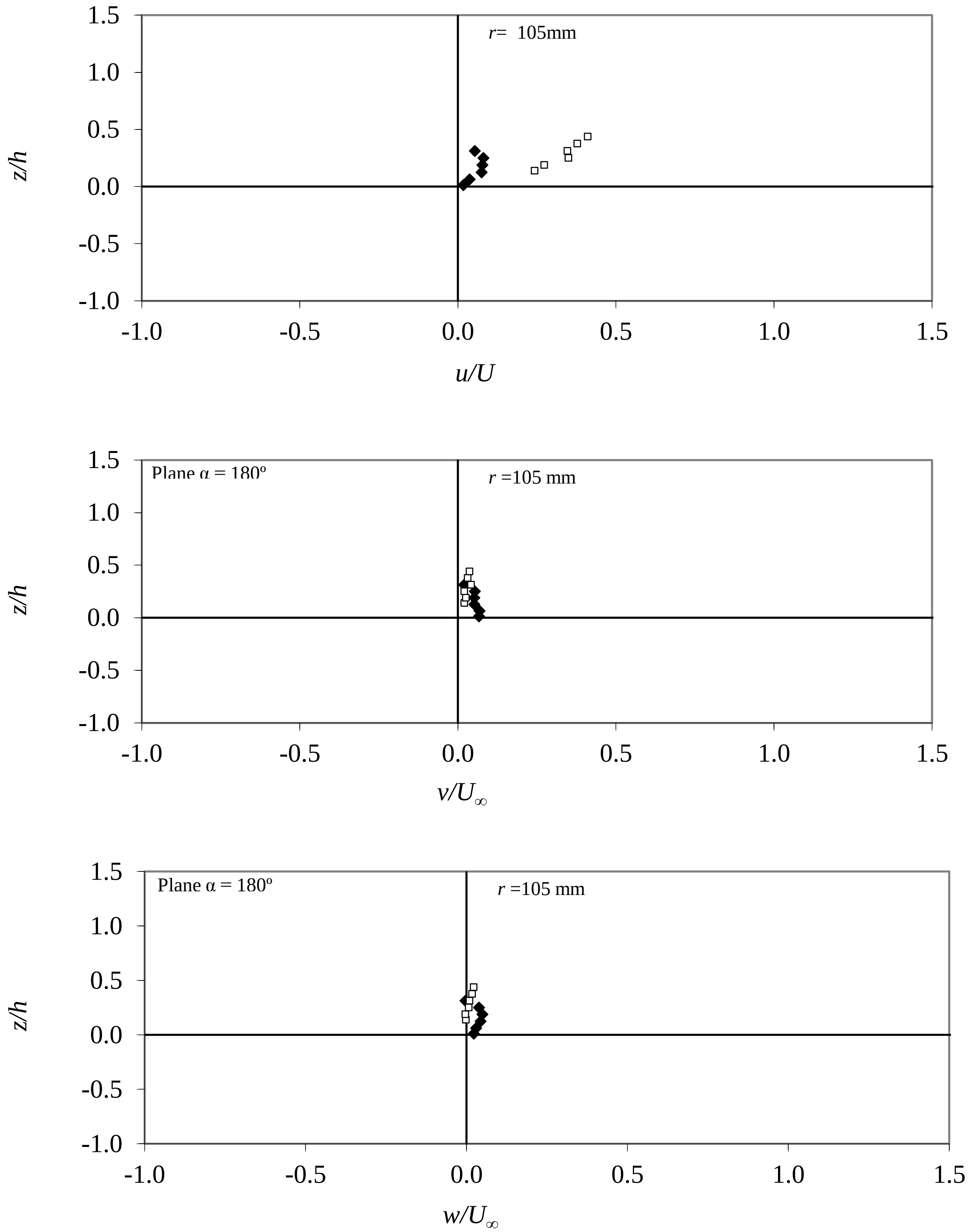

□: Isolated Pier, ♦: Effect of Second Pier at 3d Spacing

Fig 5.52 Effect of downstream pier on the velocity of upstream pier for comparison of normalised velocity components (α = 180° and r = 105 mm)

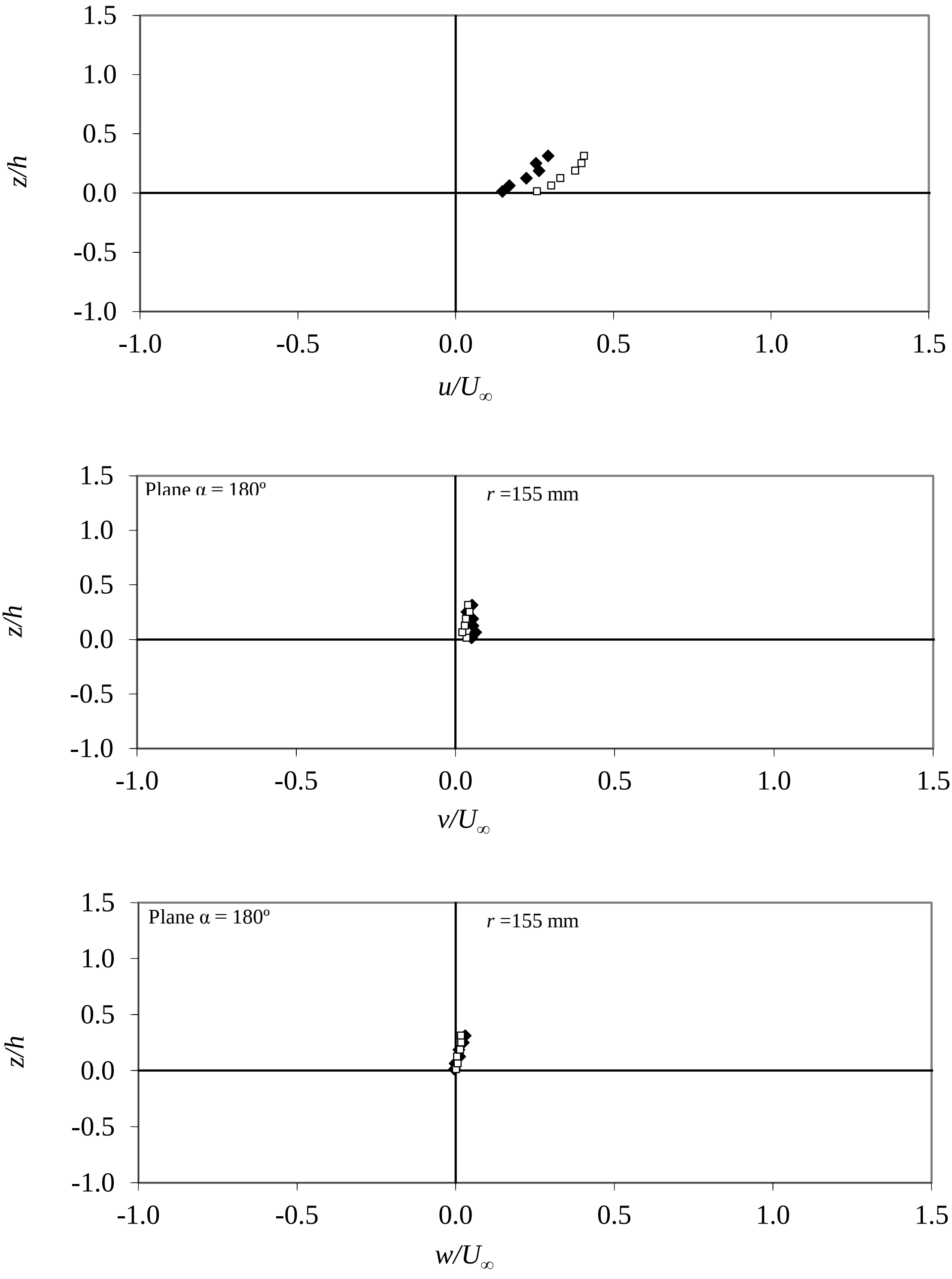

□: Isolated Pier, ♦: Effect of Second Pier at 3d Spacing

Fig 5.53 Effect of downstream pier on the velocity of upstream pier for comparison of normalised velocity components (α = 180° and r = 155 mm)

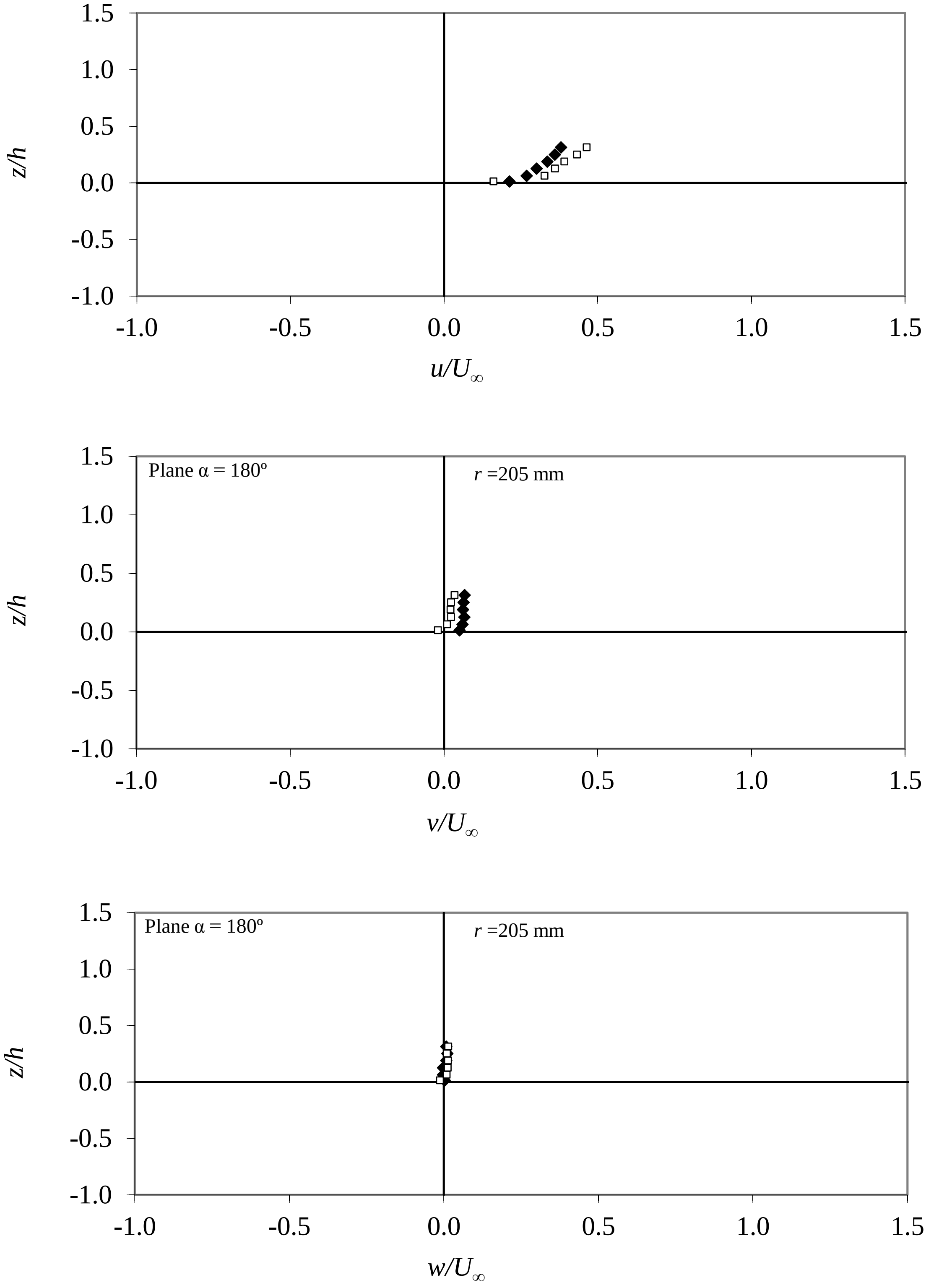

□: Isolated Pier, ♦: Effect of Second Pier at 3d Spacing

Fig 5.54 Effect of downstream pier on the velocity of upstream pier for comparison of normalised velocity components (α = 180° and r = 205 mm)

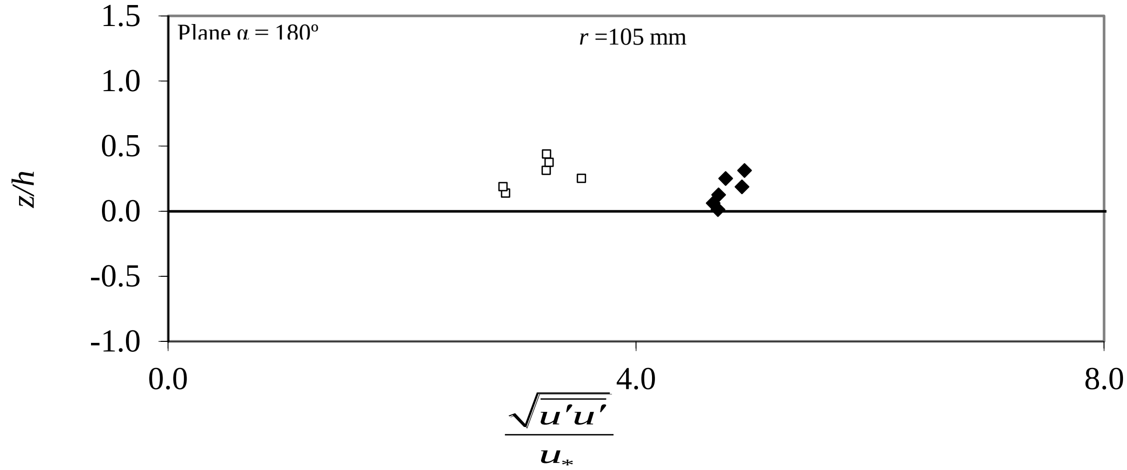

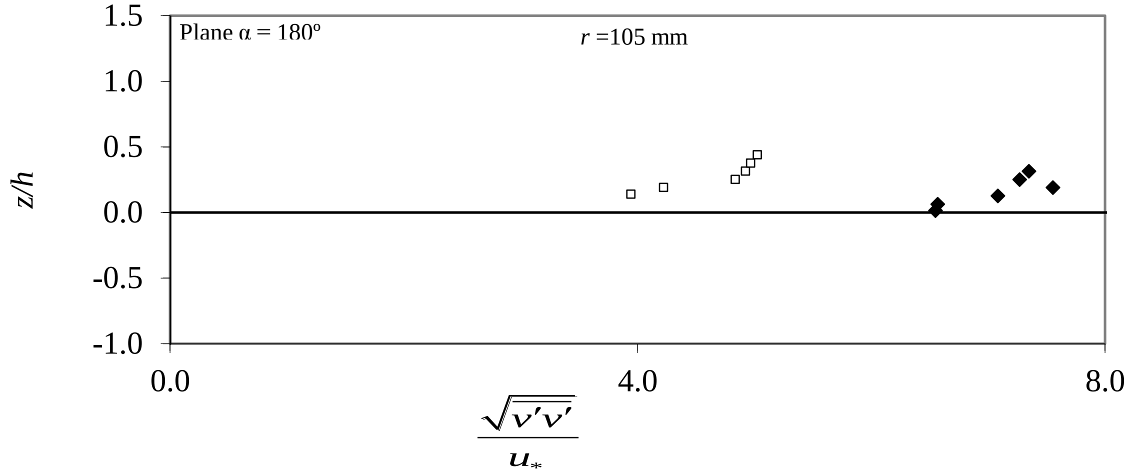

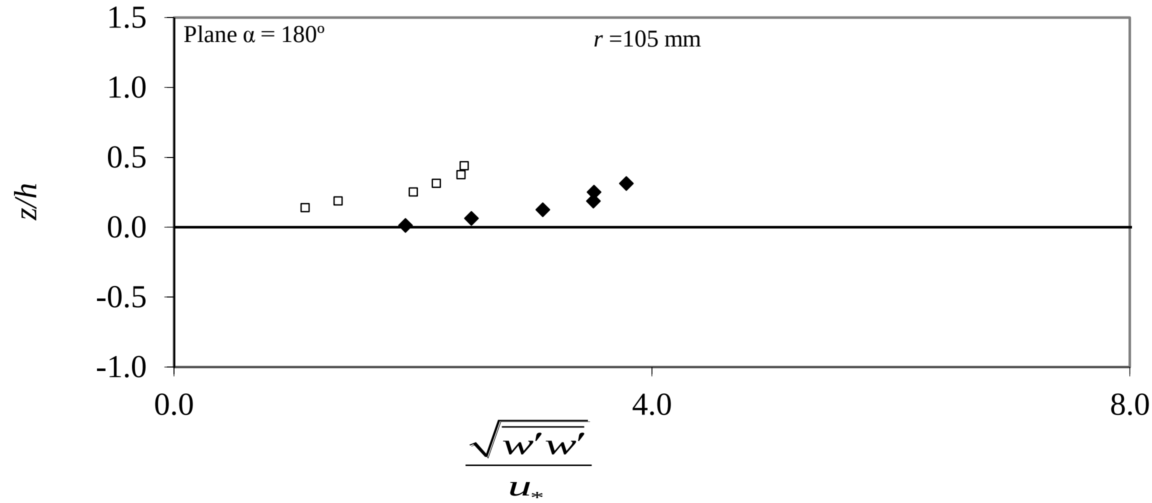

□: Isolated Pier, ♦: Effect of Second Pier at 3d Spacing

Fig 5.55 Effect of downstream pier on the velocity of upstream pier for comparison of normalised turbulence intensities (α = 180° and r = 105 mm)

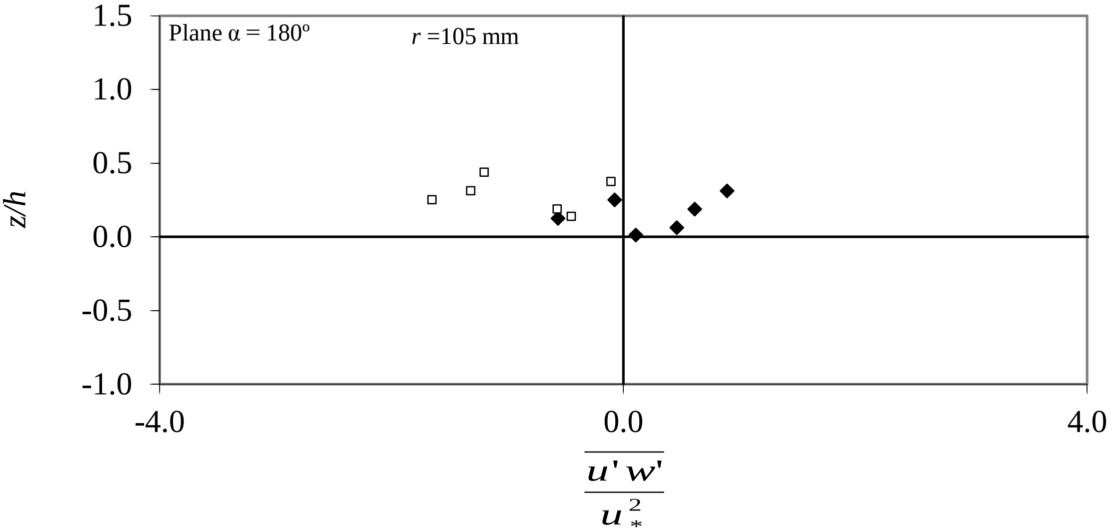

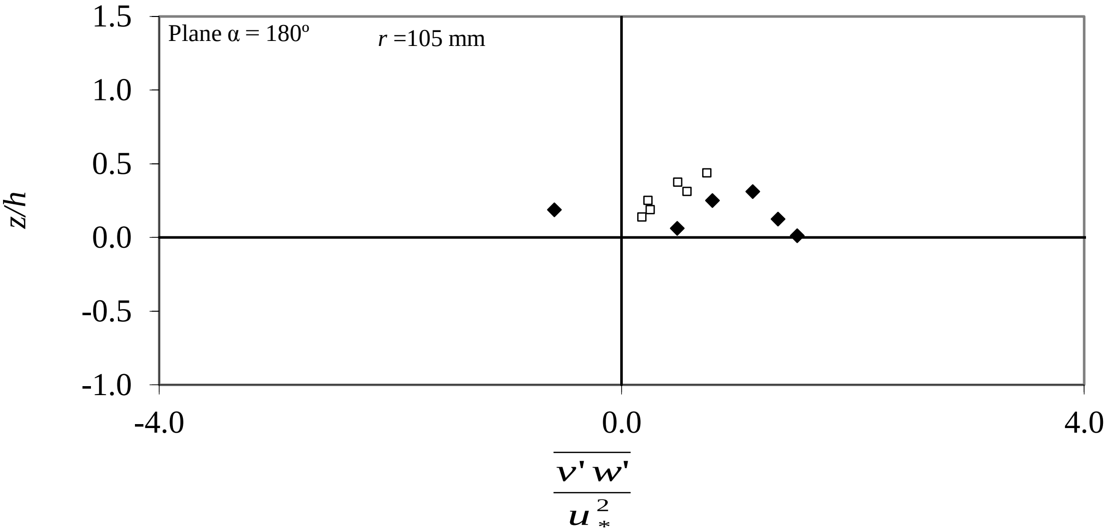

□: Isolated Pier, ♦: Effect of Second Pier at 3d Spacing

Fig 5.56 Effect of downstream pier on the velocity of upstream pier for comparison of normalised Reynolds's stresses (α = 180° and r = 105 mm)

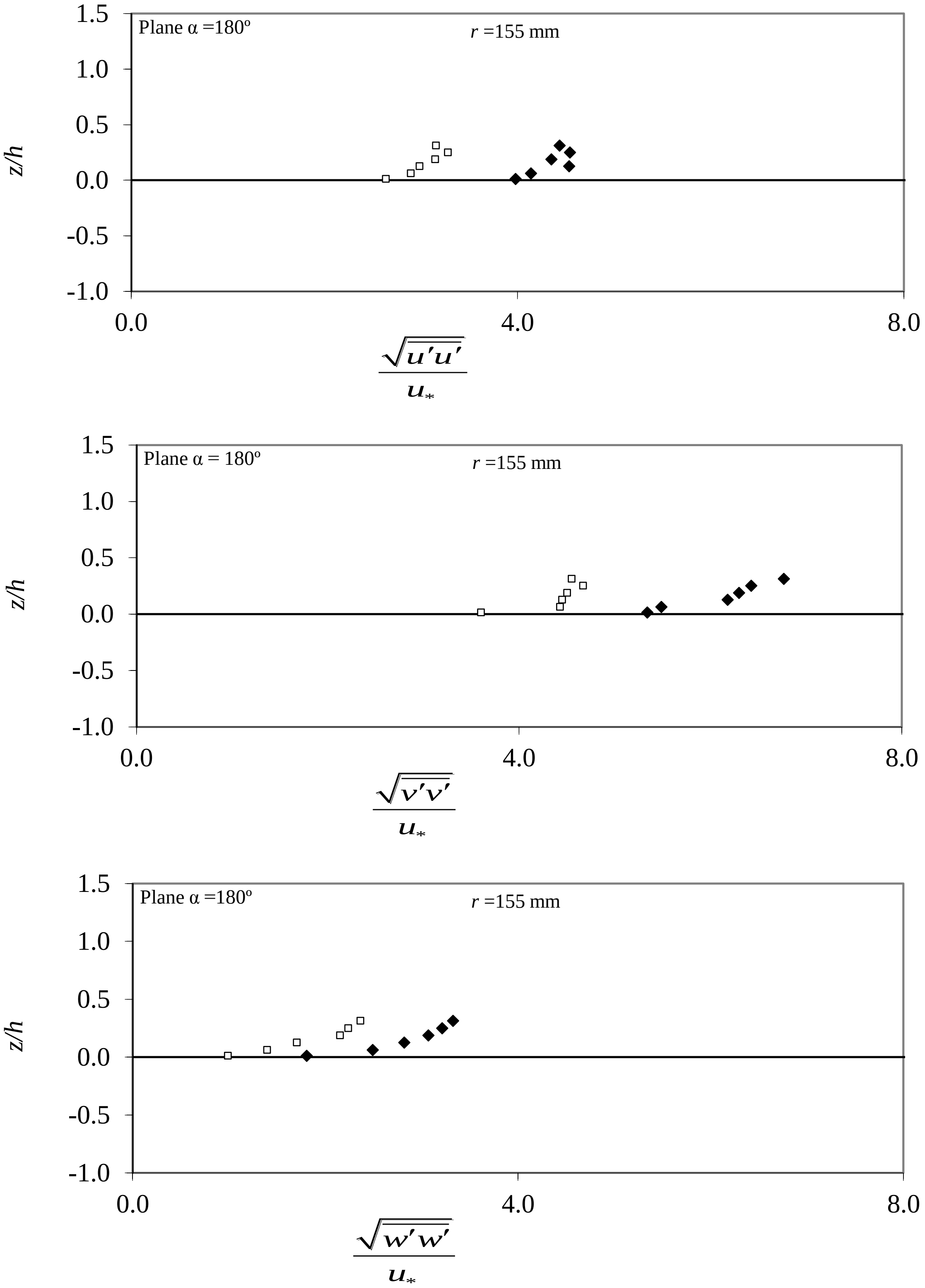

□: Isolated Pier, ♦: Effect of Second Pier at 3d Spacing

Fig 5.57 Effect of downstream pier on the velocity of upstream pier for comparison of normalised turbulence intensities (α = 180° and r = 155 mm)

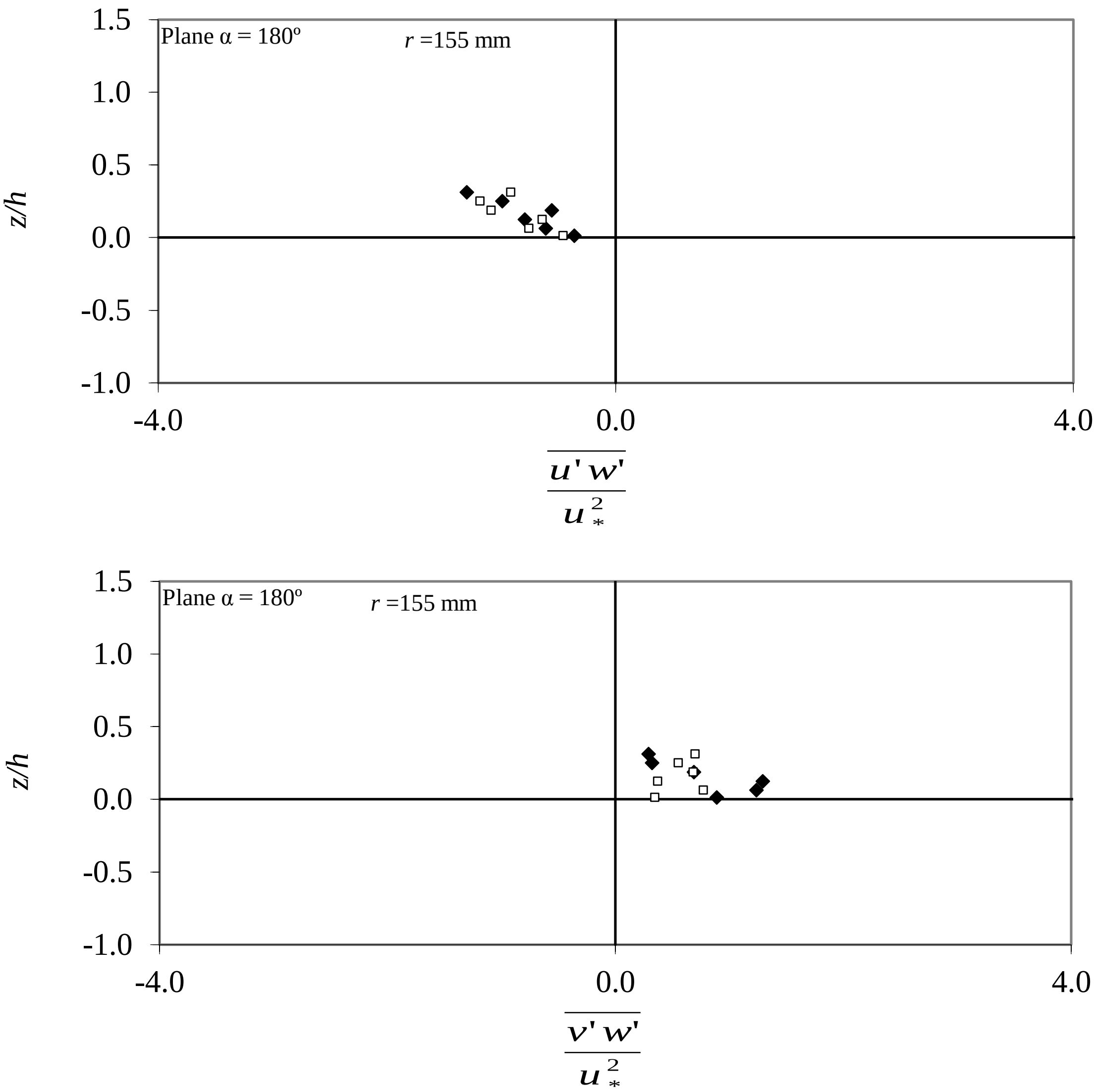

□: Isolated Pier, ♦: Effect of Second Pier at 3d Spacing

Fig 5.58 Effect of downstream pier on the velocity of upstream pier for comparison of normalised Reynolds's stresses (α = 180° and r = 155 mm)

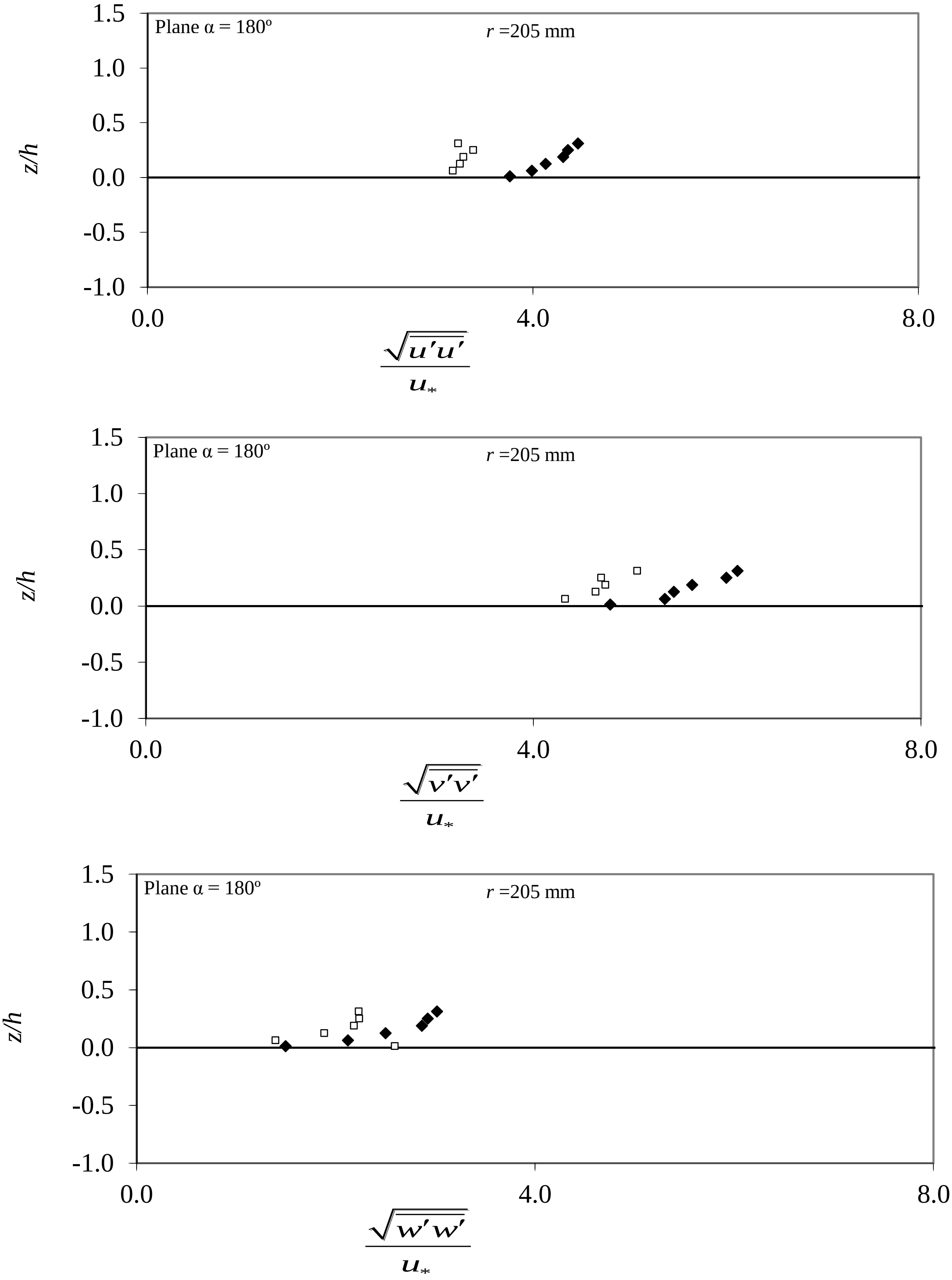

□: Isolated Pier, ♦: Effect of Second Pier at 3d Spacing

Fig 5.59 Effect of downstream pier on the velocity of upstream pier for comparison of normalised turbulence intensities (α = 180° and r = 205 mm)

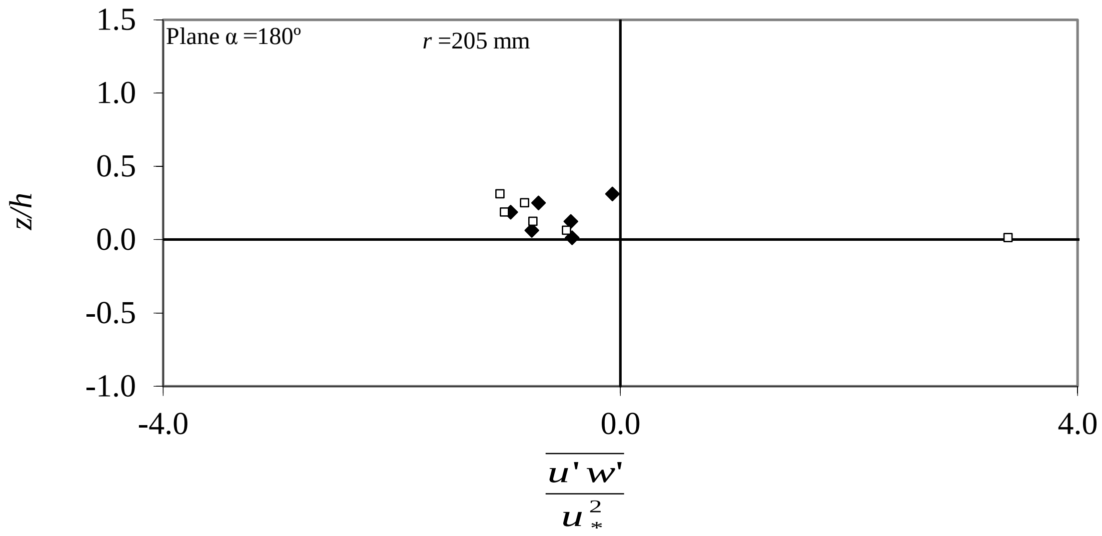

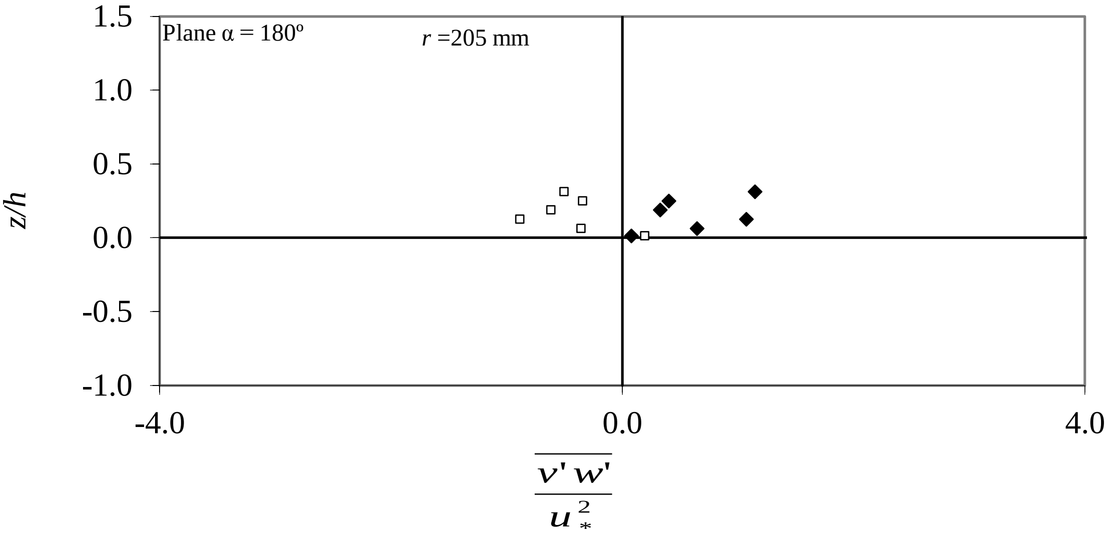

□: Isolated Pier, ♦: Effect of Second Pier at 3d Spacing

Fig 5.60 Effect of downstream pier on the velocity of upstream pier for comparison of normalised Reynolds's stresses (α = 180° and r = 205 mm)